Comparison of UniBonn and IGS08 Antenna Type Means

Wim Aerts and Michael Moore

December 6, 2013

1 Scope of the Comparison

This document reports on the differences observed between the antenna type means as obtained from Holger Milz of the University of Bonn (UniBonn) and the type means in the `igs08.atx` file (of week 1755).

The aim was to get an idea of the (dis)agreement of a type mean as obtained from different calibration facilities. This would give an indication of the difference in positioning that could be expected when using a type mean from one calibration center instead of from another.

The antenna types for which type means were provided by UniBonn are listed in Table 1. As there was no type calibration available in the `igs08_1755.atx` file for the TRM57971.00_TZGD, nor for the TRM59800.00_TCWD, obviously, the UniBonn calibrations for those antennas were not included in the study. The `igs08_1755.atx` furthermore only contains a G01 and G02 calibration, and no R01 nor R02 calibration for the TRM41249.00_NONE. Hence for this antenna, only the UniBonn calibrations on G01 and G02 are discussed in this report.

Table 1: Antenna Type Means provided by UniBonn.

Antenna type	radome	# Ant.	in `igs08_1755.atx`	remark
JAV_RINGANT_G3T	NONE	24	✓	
LEIAR25.R3	LEIT	47	✓	
LEIAR25.R4	LEIT	42	✓	
LEIAT504GG	NONE	4	✓	
LEIAX1202GG	NONE	4	✓	
NAX3G+C	NONE	10	✓	
TPSCR.G3	TPSH	19	✓	
TRM41249.00	NONE	21	✓	no R01, R02 in `igs08_1755.atx`
TRM55971.00	NONE	6	✓	
TRM55971.00	TZGD	31	✓	
TRM57971.00	NONE	8	✓	
TRM57971.00	TZGD	14	✗	
TRM59800.00	NONE	19	✓	
TRM59800.00	SCIS	19	✓	
TRM59800.00	TCWD	18	✗	

2 Disclaimers

As the authors only compared type means from UniBonn with the type means as included in the `igs08_1755.atx` file, many frequencies (such as G05) in the UniBonn calibration were *not* considered! Neither was their quality checked in any way!

Only differences between type means were studied. The authors did *not* judge the quality of the type means of both calibration facilities. A deviation of the UniBonn type mean from the type mean in the `igs08_1755.atx` file, which is indeed currently seen as "the reference", does not necessarily indicate that the type mean calculated by UniBonn is at fault. Discrepancies can occur for a number of reasons, a.o.:

- variation between antennas: as the type means compared here are not derived from the same set of individual antennas, differences can be expected

- systematic calibration errors: as the robot and anechoic chamber calibration methods use a different approach, the systematic errors in the measurements differ (e.g. because of different near field multi path environment), which shows up in the type means

The question whether it would be a good idea or not to combine type means of Geo++ and UniBonn was not investigated directly. Results from the comparisons, however, do argue against combination of Geo++ calibration on certain frequencies with UniBonn calibration on other frequencies, as this would introduce different systematic errors on different frequencies in a type mean antenna model. The seed for this concern is the resemblance of the type mean differences over all antennas of the same class on some frequencies. The set of plots, e.g. in Figures 32(e), 36(e) and 40(e); or the set of Figures 28(e), 46(e) and 50(e); clearly show that different antennas show very similar (and pronounced) elevation dependent differences between the Geo++ and UniBonn type mean.

3 Methodology

The type means from both calibration facilities were compared and differenced using two different and independent methods. Results from both methods are included in Section 6 and were found to be in full agreement, as the reader can judge for him- or herself.

3.1 Method 1: antexfun (applied by Wim Aerts)

The difference between the type means from the different `.atx` files was calculated using the `antexfun.m` code. This octave code reads out the Phase Centre Offset (PCO) and Phase Centre Variation (PCV) of a certain antenna type from the `.atx` files and combines both into an overall Phase Centre Correction (PCC) (=PCO+PCV).

At each frequency, the PCC of both files is shifted to align both calibrations. Two types of shifts were performed. One shift makes sure the value for zenith of both calibrations is zero. The other shift makes sure the mean value of both calibrations is the same. The latter shift assures that the histogram of the differences is centered around 0.

Calibration differences are then calculated on these shifted PCCs. No elevation dependent weighting is applied.

3.2 Method 2: antdpcv (applied by Michael Moore)

Software written by Geo++, mainly `ant2ant`, `atx2ant` and `antdpcv` were used to read in the `.atx` files, convert the PCCs so that both type means had no PCO bias, and difference their PCVs. The results were then plotted and analyzed in scripts written in python.

4 Results

4.1 Dependence on Used Method

Comparison of the type means with the method of Section 3.2 or using the method of Section 3.1 using the shift that aligns zenith of both calibrations, gives identical results.

Comparison of the type means with the method of Section 3.1 using the shift that aligns the mean of both calibrations mostly results in better agreement (smaller difference) between both type means. Except for the NAX3G+C_NONE on G02 and R02.

4.2 Summary of Differences per Antenna

The differences for all relevant antennas from Table 1 between the type calibrations of both sources, under the shift that aligns the zenith value of the calibrations, are summarized in Table 2. Table 3 reports the differences when the shift to align the mean values of the calibrations was applied.

The latter shift does not suffer from the possibility that some measurement error on zenith might get amplified and colours the result. Except for the NAX3G+C_NONE on G02 and R02, and the TRM55971.00_TZGD on R02, indeed, the "mean" shift results in better agreement between both type means than the "zenith" shift.

Both tables contain the percentage of $5° \times 5°$ azimuth and elevation bins for which the difference between two calibrations is smaller than 1 mm as well as the difference range (minimum and maximum of the difference over all azimuth and elevation angles).

From the tables, one gets an idea of the agreement between the type means for each of the antennas:

- **JAV_RINGANT_G3T NONE** Good agreement on G01, R01. Poor agreement for the South East quadrant on G02, and the Eastern hemisphere on R02. There is a significant increase in standard deviation (due to a considerable azimuthal dependence) for G02 and R02.
- **LEIAR25.R3 LEIT** Good agreement on G01 and R01, fair agreement for G02, poor agreement for R02.
- **LEIAR25.R4 LEIT** Good agreement on all frequencies. Some disagreement at low elevations for G02.
- **LEIAT504GG NONE** Excellent agreement on G01, good agreement on R01, poor agreement on G02 and R02.
- **LEIAX1202GG NONE** Excellent agreement on G01, R01. Fair agreement on G02, R02.
- **NAX3G+C NONE** Fair agreement on G01, R01. No agreement at all on G02, R02. Possibly here the near field effects of the positioning system show up in the results. The antenna does not have a large ground plane (such as a choke ring) to shield it from its surroundings.
- **TPSCR.G3 TPSH** Good agreement on G01. Poor agreement on G02, R01, R02. At least less correspondence than expected, when looking at both calibrations, which are fairly symmetrical and do not show much azimuthal variation.
- **TRM41249.00 NONE** Good agreement on G01, fair agreement on G02. No calibrations for R01 and R02 in `igs08_1755.atx`.
- **TRM55971.00 NONE** Excellent agreement on G01, good agreement on G02, R01, R02
- **TRM55971.00 TZGD** Excellent agreement on G01, G02, R01, poor agreement on R02. The larger difference on R02 is yet unexplained.
- **TRM57971.00 NONE** Excellent agreement on G01, G02 , good agreement on R01, R02.
- **TRM57971.00 TZGD** No comparison performed, not in `igs08_1755.atx`.
- **TRM59800.00 NONE** Excellent agreement on G01 and R01, poor agreement on G02 and R02. Maybe a larger near field effect of the antenna positioning system for the lower frequencies? But definitely less pronounced than in the case of the NAX3G+C_NONE.
- **TRM59800.00 SCIS** Excellent agreement on G01 and R01, poor agreement on G02 and R02. In accordance with the results for the TRM59800.00_NONE.
- **TRM59800.00 TCWD** No comparison performed, not in `igs08_1755.atx`.

type	radome	G01			G02			R01			R02		
		< 1mm	max	min	< 1mm	max	min	< 1mm	max	min	< 1mm	max	min
JAV_RINGANT_G3T	NONE	93%	0.98	-1.92	62%	3.56	-2.52	94%	1.12	-1.79	39%	7.28	-0.68
LEIAR25.R3	LEIT	72%	3.70	-0.05	83%	1.33	-3.49	79%	3.83	-0.18	60%	3.30	-0.27
LEIAR25.R4	LEIT	92%	0.64	-1.36	74%	0.70	-4.42	92%	0.31	-1.53	70%	0.83	-3.44
LEIAT504GG	NONE	97%	1.66	-0.72	35%	2.91	-0.11	80%	1.83	-0.63	20%	4.44	0.00
LEIAX1202GG	NONE	94%	1.53	-1.24	66%	0.36	-3.11	82%	1.95	-0.51	74%	2.08	-3.12
NAX3G+C	NONE	75%	2.57	-1.03	28%	1.29	-8.79	57%	3.39	-0.52	27%	0.52	-7.40
TPSCR.G3	TPSH	74%	0.74	-2.43	34%	3.86	-1.23	29%	0.06	-4.91	33%	3.80	-1.18
TRM41249.00	NONE	57%	1.97	0.00	85%	1.61	-2.98	-	-	-	-	-	-
TRM55971.00	NONE	81%	2.03	-0.12	89%	1.53	-2.73	76%	2.87	-0.27	75%	3.21	-0.46
TRM55971.00	TZGD	100%	0.53	-1.08	89%	1.07	-3.26	98%	1.38	-0.89	58%	4.32	-0.29
TRM57971.00	NONE	95%	1.92	-1.05	85%	1.56	-3.36	84%	2.24	-1.34	77%	2.17	-2.55
TRM57971.00	TZGD	-	-	-	-	-	-	-	-	-	-	-	-
TRM59800.00	NONE	91%	1.43	-1.28	39%	2.65	-0.85	91%	1.66	-1.24	21%	4.40	0.00
TRM59800.00	SCIS	95%	2.57	-1.06	36%	3.79	-1.64	90%	2.59	-1.22	28%	4.95	0.00
TRM59800.00	TCWD	-	-	-	-	-	-	-	-	-	-	-	-

Table 2: Summary of the differences between UniBonn and IGS antenna type mean calibrations after shift to align zenith. 100-80 79-70 69-34 33-0

		G01			G02			R01			R02		
type	radome	< 1mm	max	min	< 1mm	max	min	< 1mm	max	min	< 1mm	max	min
JAV_RINGANT_G3T	NONE	93%	1.14	-1.76	76%	2.82	-3.26	94%	1.21	-1.70	39%	5.48	-2.48
LEIAR25.R3	LEIT	90%	2.96	-0.80	82%	1.59	-3.23	92%	3.18	-0.84	73%	2.40	-1.17
LEIAR25.R4	LEIT	98%	0.84	-1.16	85%	1.38	-3.74	98%	0.63	-1.22	85%	1.52	-2.75
LEIAT504GG	NONE	98%	1.47	-0.91	72%	1.59	-1.42	98%	1.53	-0.93	52%	2.35	-2.09
LEIAX1202GG	NONE	94%	1.51	-1.25	86%	1.11	-2.36	96%	1.54	-0.92	82%	2.56	-2.64
NAX3G+C	NONE	80%	2.11	-1.49	26%	3.86	-6.22	81%	2.52	-1.39	24%	3.05	-4.88
TPSCR.G3	TPSH	94%	1.34	-1.84	57%	2.37	-2.71	52%	1.76	-3.22	54%	2.30	-2.68
TRM41249.00	NONE	99%	1.21	-0.75	81%	1.76	-2.82	-	-	-	-	-	-
TRM55971.00	NONE	97%	1.52	-0.63	89%	1.59	-2.68	90%	2.35	-0.79	89%	2.81	-0.86
TRM55971.00	TZGD	100%	1.00	-0.60	87%	1.32	-3.01	97%	1.55	-0.72	47%	3.34	-1.27
TRM57971.00	NONE	95%	2.03	-0.95	83%	1.64	-3.28	92%	2.52	-1.05	83%	1.89	-2.83
TRM57971.00	TZGD	-	-	-	-	-	-	-	-	-	-	-	-
TRM59800.00	NONE	95%	1.63	-1.08	62%	1.43	-2.06	95%	1.84	-1.06	53%	2.48	-1.92
TRM59800.00	SCIS	94%	2.67	-0.95	45%	2.31	-3.13	93%	2.80	-1.00	41%	2.92	-2.03
TRM59800.00	TCWD	-	-	-	-	-	-	-	-	-	-	-	-

Table 3: Summary of the differences between UniBonn and IGS antenna type mean calibrations after shift to align mean. 100-80 79-70 69-34 33-0

5 Recommendations

The findings in Section 4.2 lead to the following recommendations:

- **NAX3G+C NONE** Seen the lack of correspondence, it might be good to recheck the type mean generation. Maybe some error was made during this process.
- **TPSCR.G3 TPSH** Because of the correspondence that is much less than expected for a choke ring antenna type, it might be good to recheck the type mean generation. Maybe some error was made during this process.
- **JAV_RINGANT_G3T NONE**, **LEIAT504GG NONE**, **TRM55971.00 TZGD**, **TRM59800.00 NONE**, and **TRM59800.00 SCIS** should be used with caution. Large differences at some frequencies might indicate quality problems with either one or both of the provided type mean antenna models for these frequencies.
- **LEIAR25.R3 LEIT** is expected to be accurate as both calibration facilities provide models that are fairly close. Using either one of both antenna models will not change the calculated position by too much (for most applications).
- **LEIAR25.R4 LEIT**, **LEIAX1202GG NONE**, **TRM41249.00 NONE**, **TRM55971.00 NONE**, and **TRM57971.00 NONE** are expected to be accurate as both calibration facilities provide models that are very close. Using either one of both antenna models will not change the calculated position by too much (for most applications).
- **TRM57971.00 TZGD** and **TRM59800.00 TCWD** are not in `igs08_1755.atx`. No recommendations can be given.

UniBonn includes calibrations for all known GNSS frequencies. Even if a certain antenna does not support the frequency. For the **TRM41249.00 NONE** for example, a model for G05 is provided, although this antenna is not designed to receive G05 (which indeed results in a rather noisy PCC for G05 in the UniBonn `.atx` file). A decision should be taken on whether it makes sense to include a frequency in an antenna type mean model if the antenna does not support it.

6 Detailed Results

The following pages contain plots that quantify and illustrate the differences between the type mean calibrations as obtained form UniBonn and as from the `igs08_1755.atx` file.

All graphs were obtained by the shift to align zenith of both antenna type mean models. The shift that aligns the mean of both calibrations results in similar figures, only offset by a certain value. This value is different for a different antenna and a different frequency, but constant over all azimuth and elevation angles in the model for a certain frequency of a certain antenna.

Each page holds the graphs for a single frequency of one of the antenna types. The same graph types re-appear in the same order on each page:

a) Polar skyplot indicating the angle bins which differ by more than 1 mm and more than 2 mm as obtained by the `antdpcv` method.

b) Same as item a) but as obtained by the `antexfun` method.

c) Polar skyplot (left) and Cartesian representation (right) of the differences as obtained by the `antexfun` method. Both share the same color scale.

d) Difference ranges for each elevation bin as obtained by the `antdpcv` method. The error bars indicate the standard deviation, the solid lines show the mean, max and min values for that elevation range.

e) An overlay of the differences as a function of elevation for all different azimuth angles as obtained by the `antexfun` method.

f) Histogram of the differences as obtained by the `antdpvc` method.

g) Histogram of the differences as obtained by the `antexfun` method.

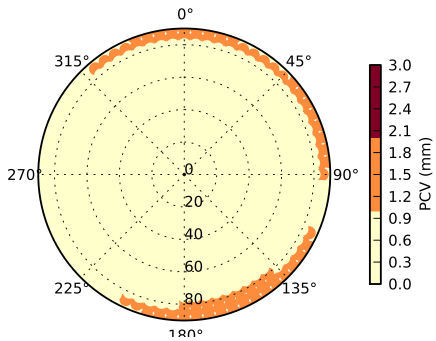

(a) staircase skyplot (antdpcv)

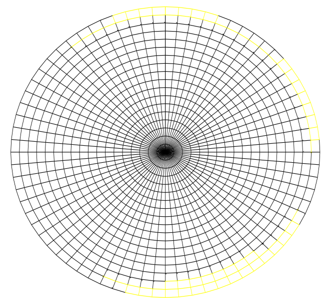

(b) staircase skyplot (antexfun)

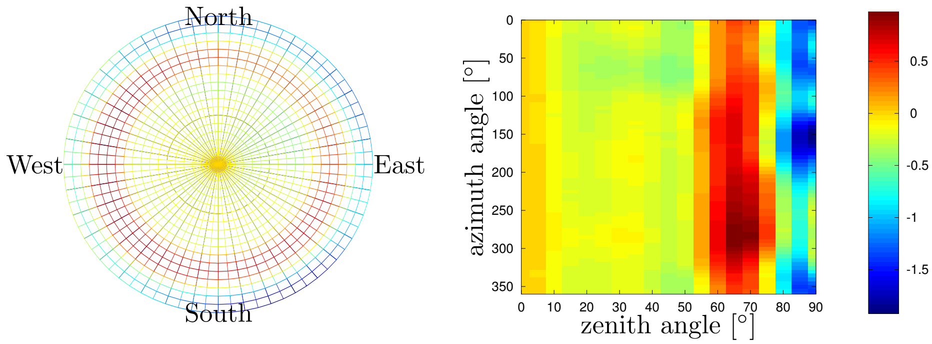

(c) polar (l) and cartesian (r) skyplot (antexfun)

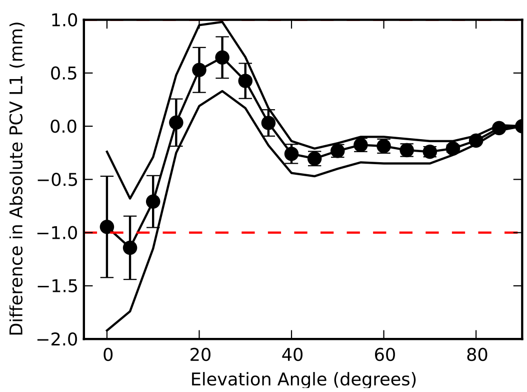

(d) elevation dependent difference ranges (antdpcv)

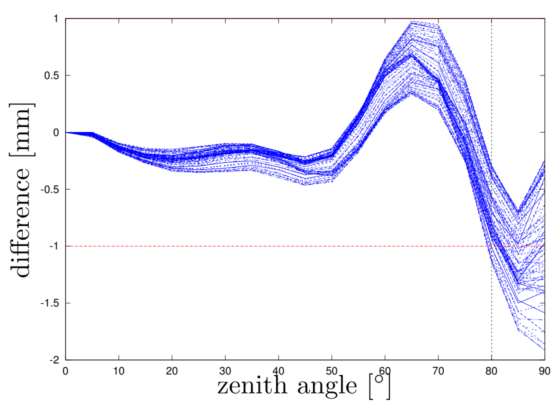

(e) overlay for all azimuth angles (antexfun)

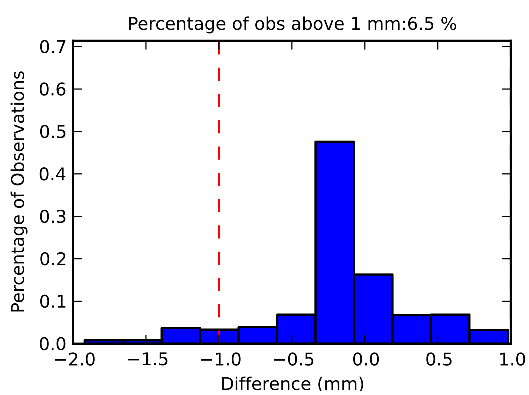

(f) histogram (antdpcv)

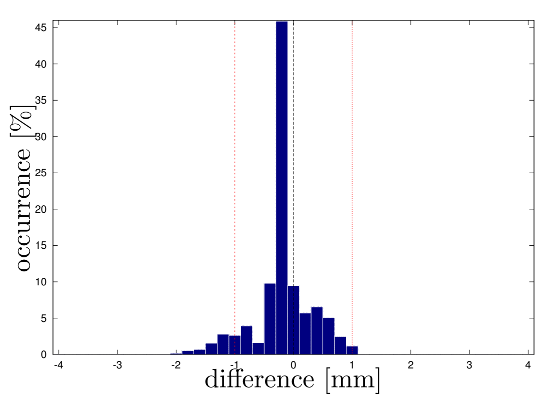

(g) histogram (antexfun)

Figure 1: Calibration differences for *JAV_RINGANT_G3T_NONE* on G01.

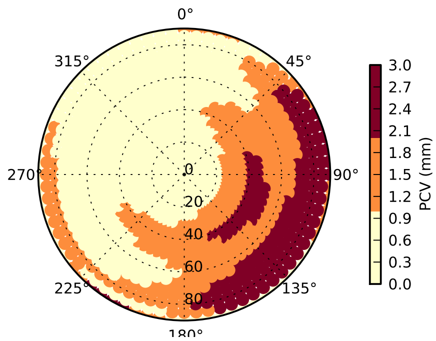

(a) staircase skyplot (antdpcv)

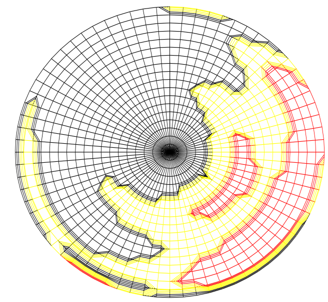

(b) staircase skyplot (antexfun)

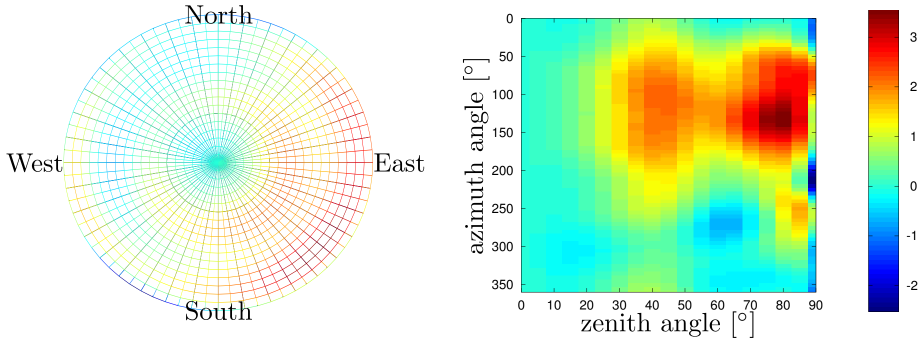

(c) polar (l) and cartesian (r) skyplot (antexfun)

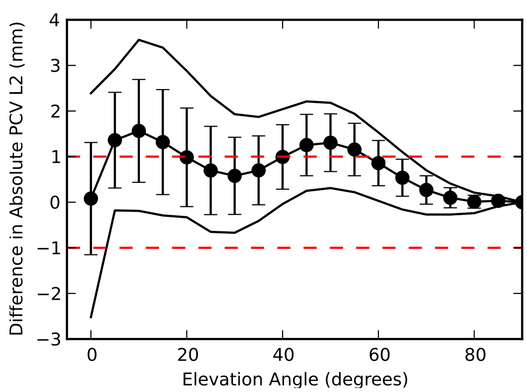

(d) elevation dependent difference ranges (antdpcv)

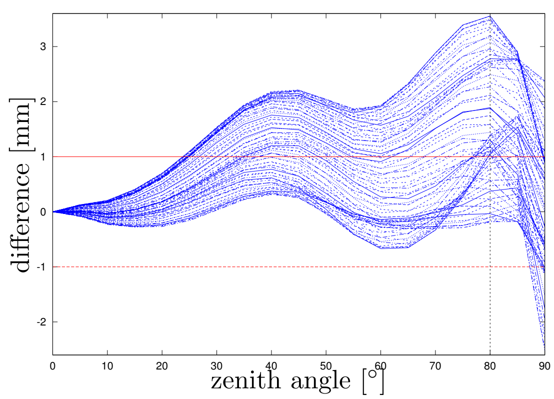

(e) overlay for all azimuth angles (antexfun)

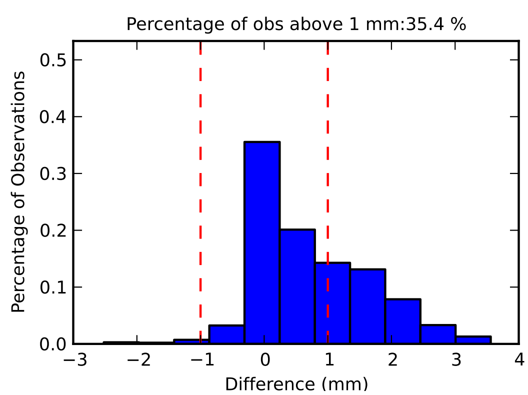

(f) histogram (antdpcv)

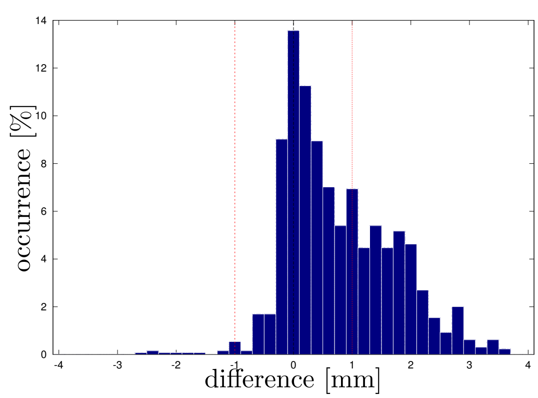

(g) histogram (antexfun)

Figure 2: Calibration differences for $JAV\_RINGANT\_G3T\_NONE$ on G02.

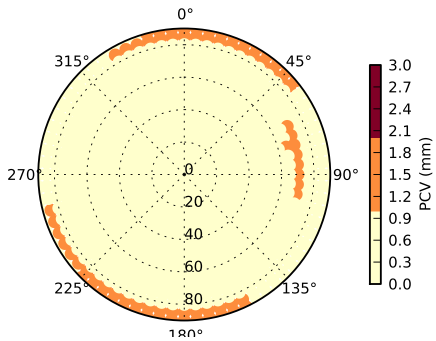

(a) staircase skyplot (antdpcv)

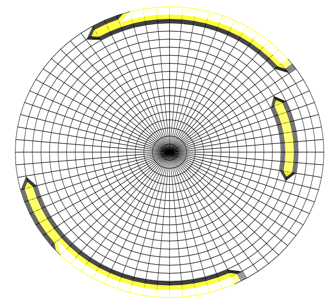

(b) staircase skyplot (antexfun)

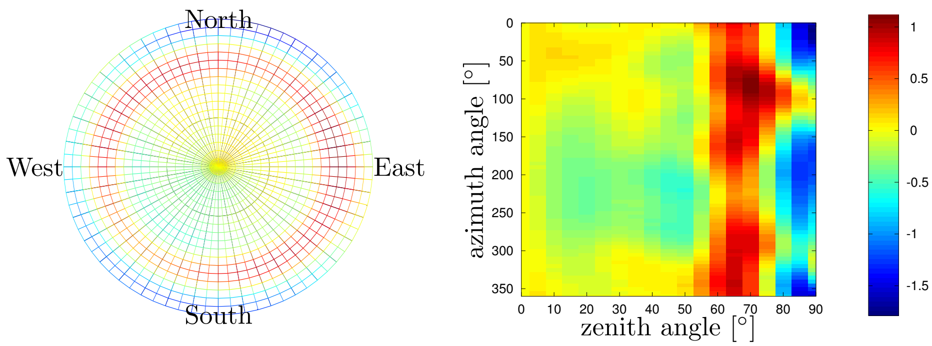

(c) polar (l) and cartesian (r) skyplot (antexfun)

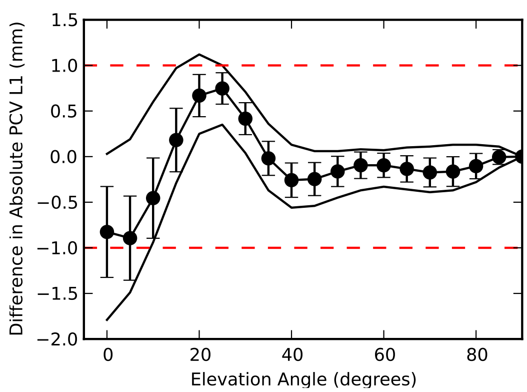

(d) elevation dependent difference ranges (antdpcv)

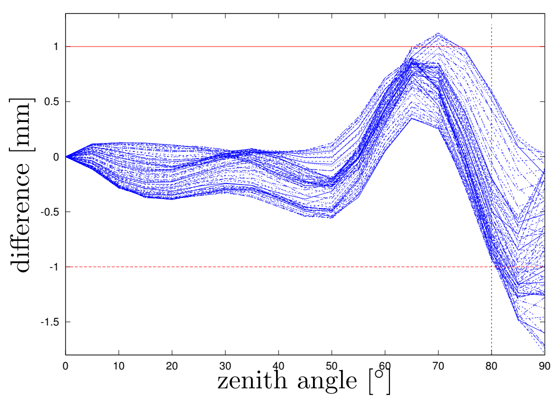

(e) overlay for all azimuth angles (antexfun)

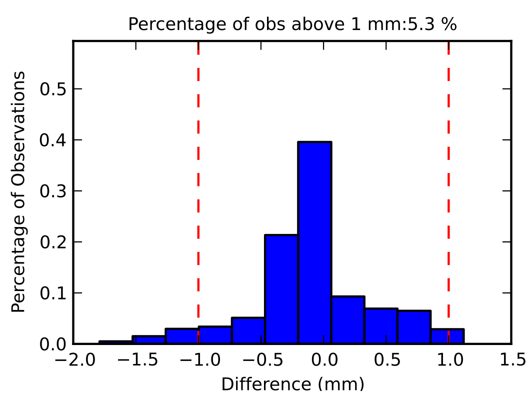

(f) histogram (antdpcv)

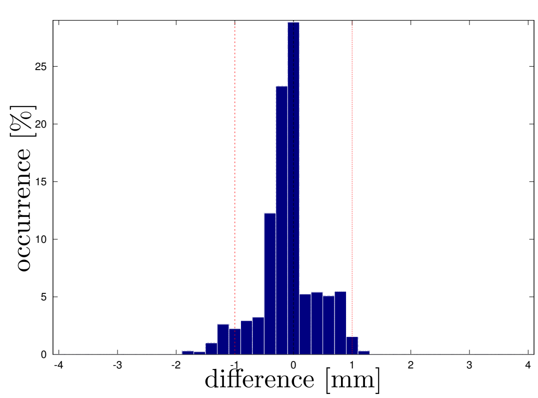

(g) histogram (antexfun)

Figure 3: Calibration differences for $JAV\_RINGANT\_G3T\_NONE$ on R01.

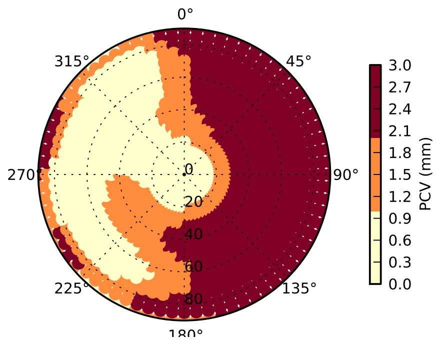

(a) staircase skyplot (antdpcv)

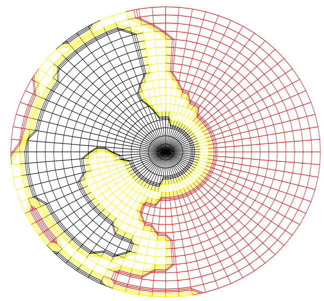

(b) staircase skyplot (antexfun)

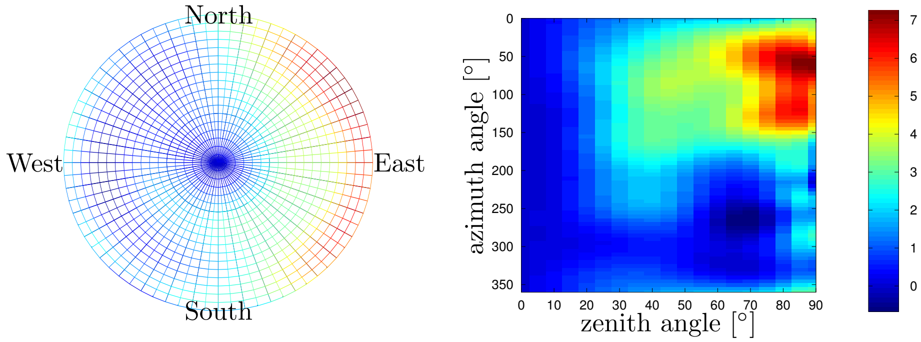

(c) polar (l) and cartesian (r) skyplot (antexfun)

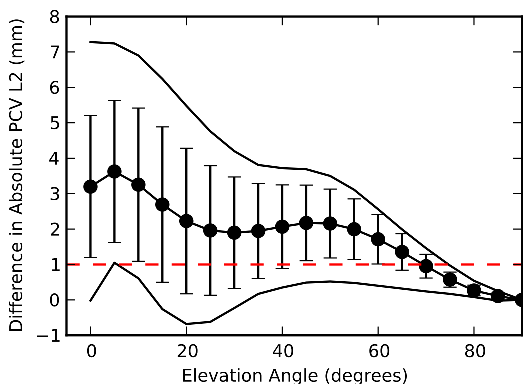

(d) elevation dependent difference ranges (antdpcv)

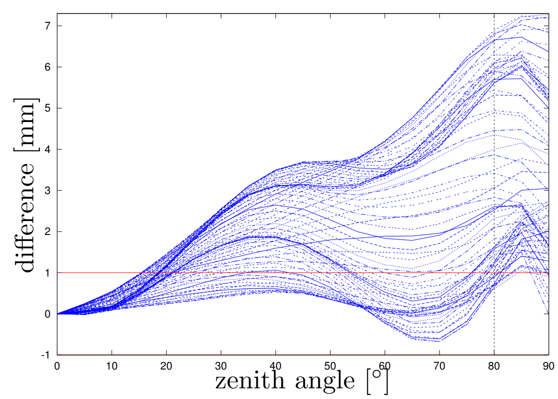

(e) overlay for all azimuth angles (antexfun)

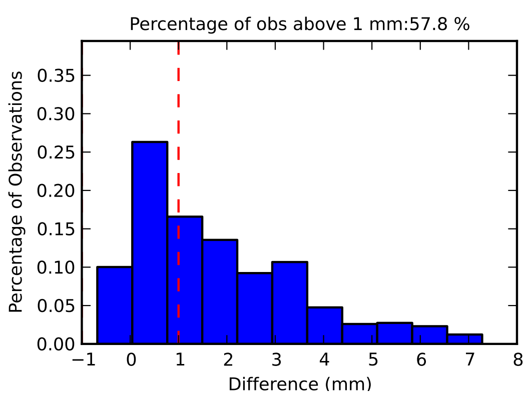

(f) histogram (antdpcv)

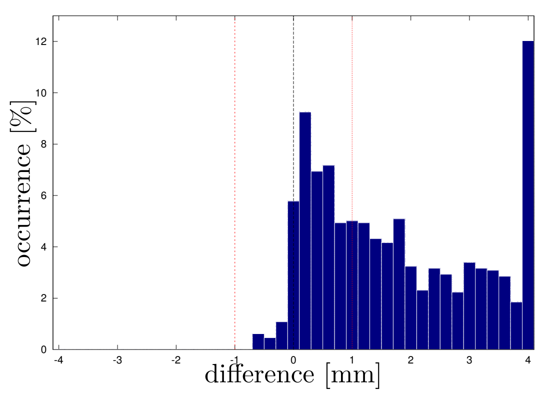

(g) histogram (antexfun)

Figure 4: Calibration differences for *JAV_RINGANT_G3T_NONE* on R02.

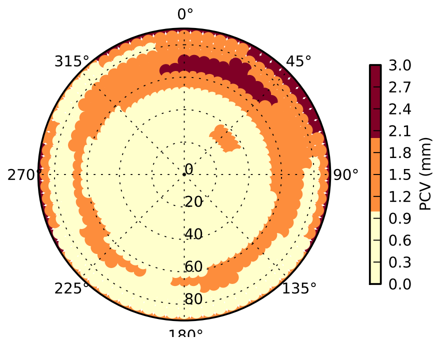

(a) staircase skyplot (antdpcv)

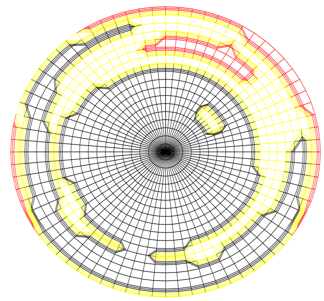

(b) staircase skyplot (antexfun)

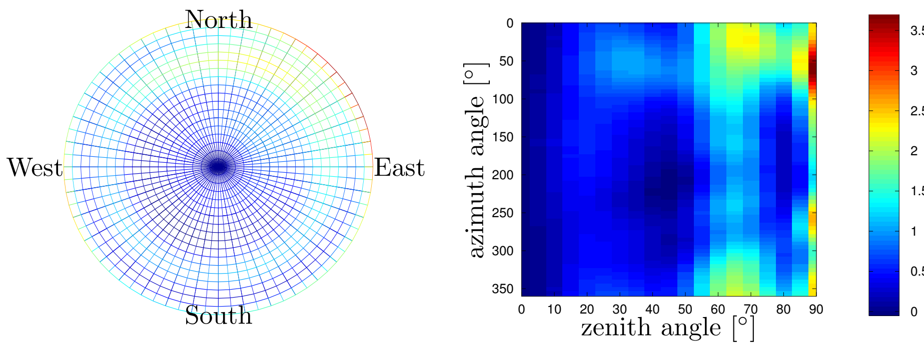

(c) polar (l) and cartesian (r) skyplot (antexfun)

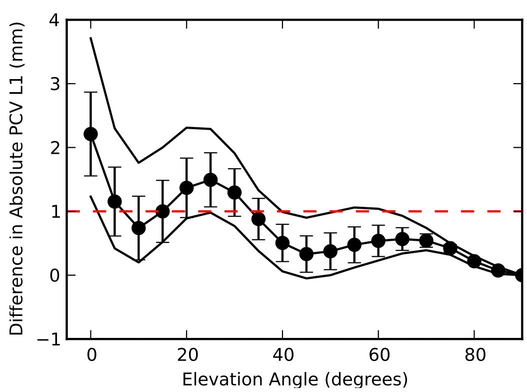

(d) elevation dependent difference ranges (antdpcv)

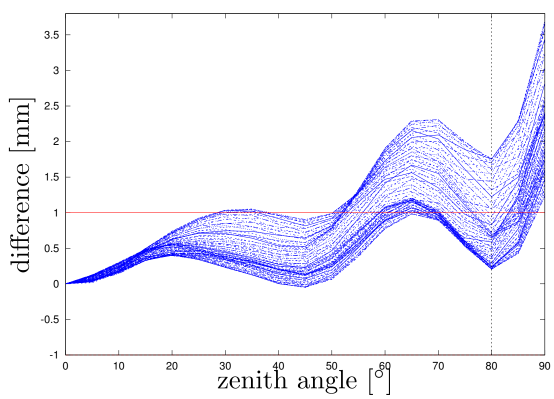

(e) overlay for all azimuth angles (antexfun)

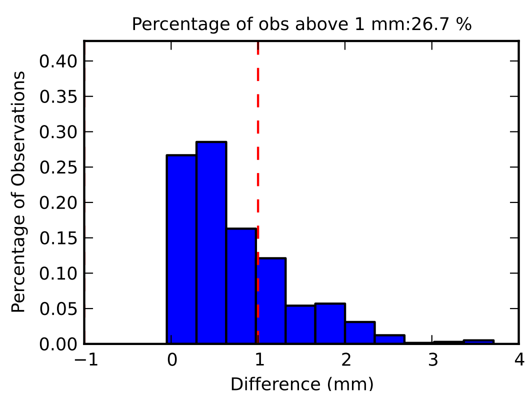

(f) histogram (antdpcv)

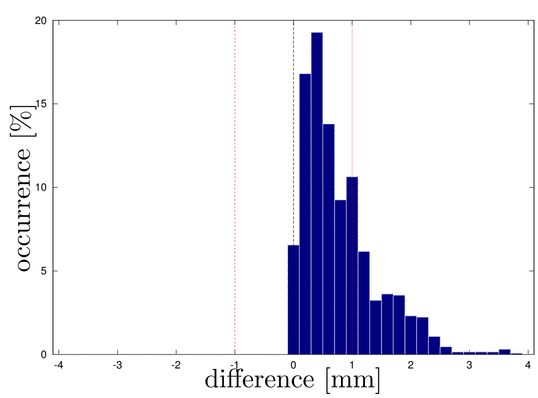

(g) histogram (antexfun)

Figure 5: Calibration differences for $LEIAR25.R3\_\_\_\_\_\_LEIT$ on G01.

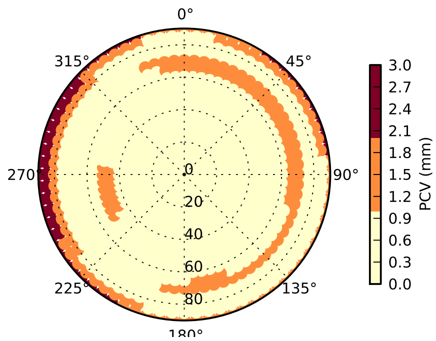

(a) staircase skyplot (antdpcv)

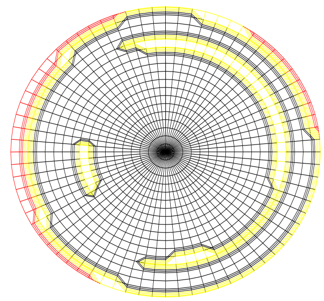

(b) staircase skyplot (antexfun)

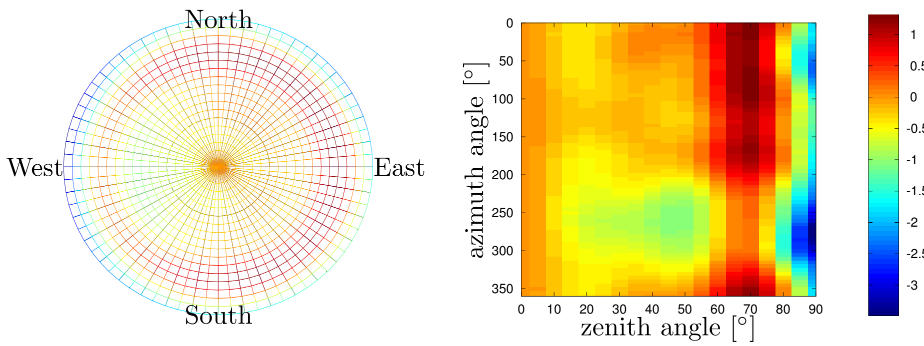

(c) polar (l) and cartesian (r) skyplot (antexfun)

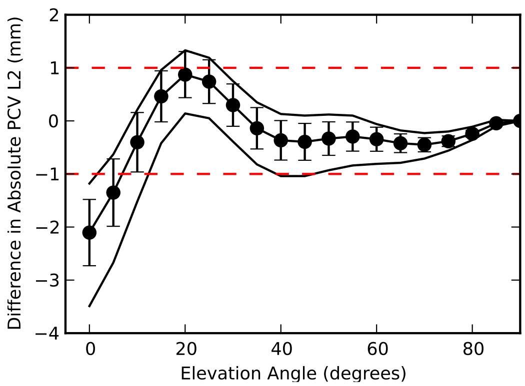

(d) elevation dependent difference ranges (antdpcv)

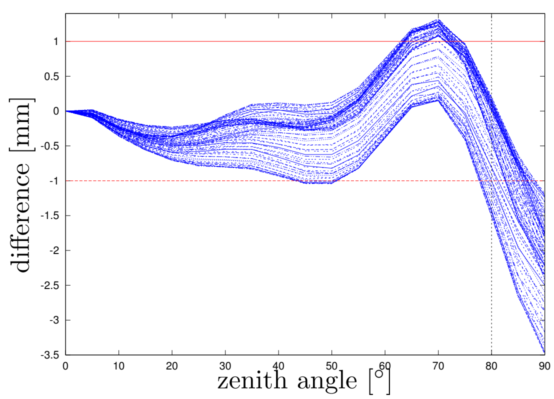

(e) overlay for all azimuth angles (antexfun)

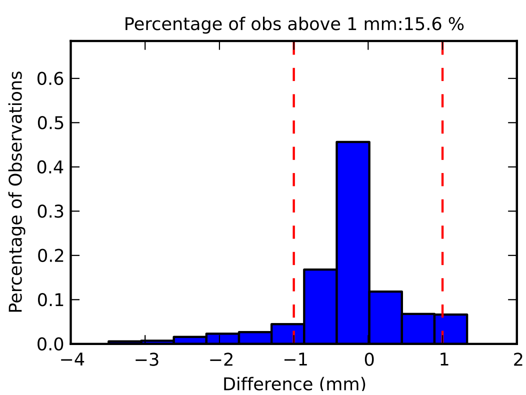

(f) histogram (antdpcv)

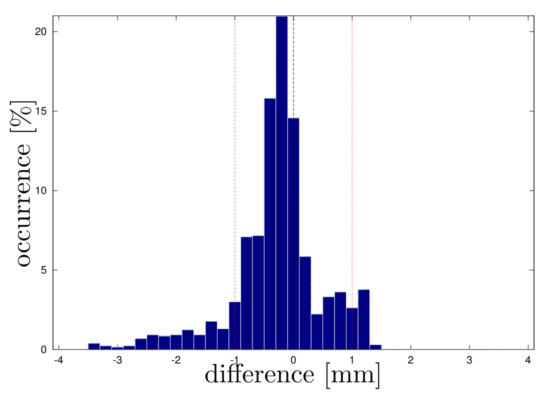

(g) histogram (antexfun)

Figure 6: Calibration differences for $LEIAR25.R3\_\_\_\_\_\_LEIT$ on G02.

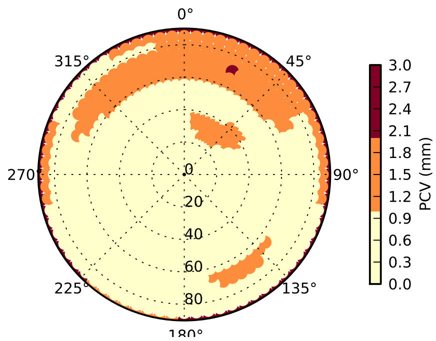

(a) staircase skyplot (antdpcv)

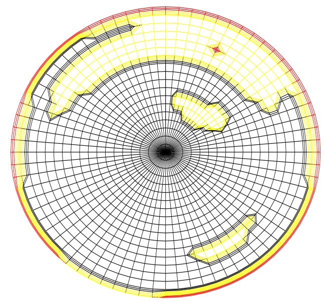

(b) staircase skyplot (antexfun)

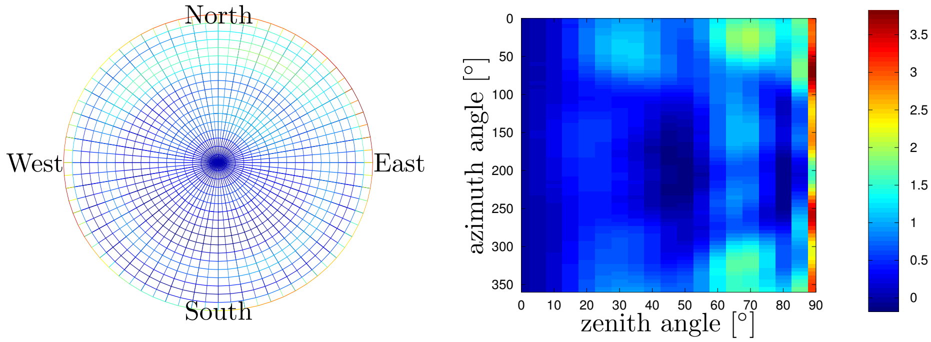

(c) polar (l) and cartesian (r) skyplot (antexfun)

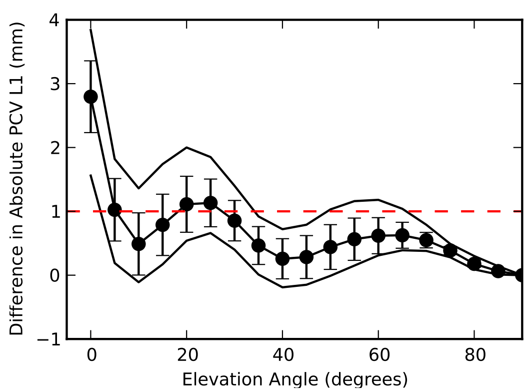

(d) elevation dependent difference ranges (antdpcv)

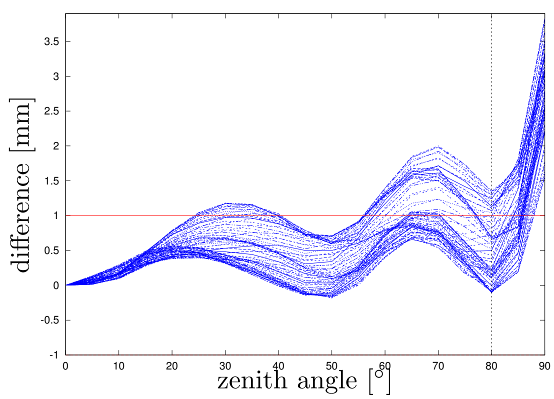

(e) overlay for all azimuth angles (antexfun)

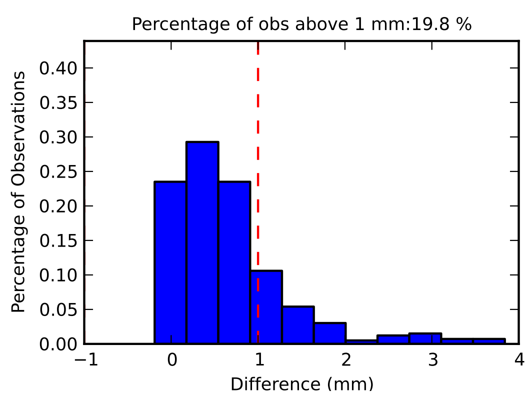

(f) histogram (antdpcv)

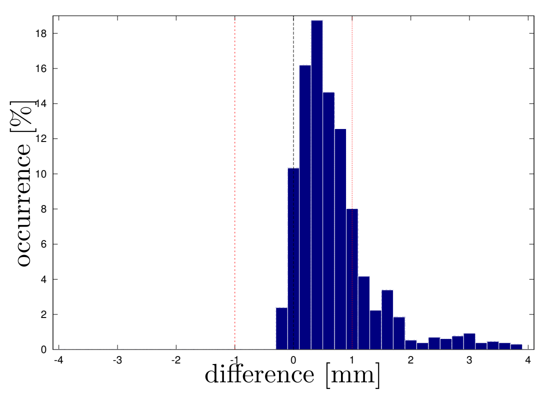

(g) histogram (antexfun)

Figure 7: Calibration differences for $LEIAR25.R3\_\_\_\_\_\_LEIT$ on R01.

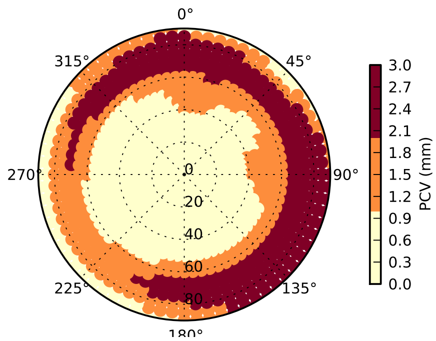

(a) staircase skyplot (antdpcv)

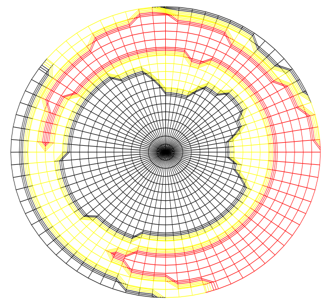

(b) staircase skyplot (antexfun)

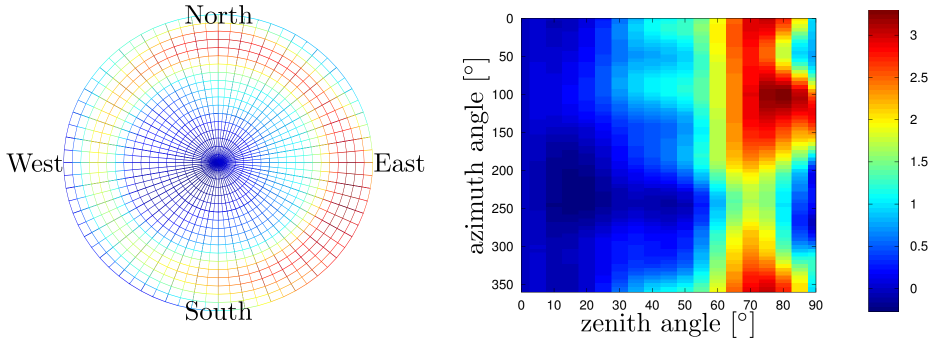

(c) polar (l) and cartesian (r) skyplot (antexfun)

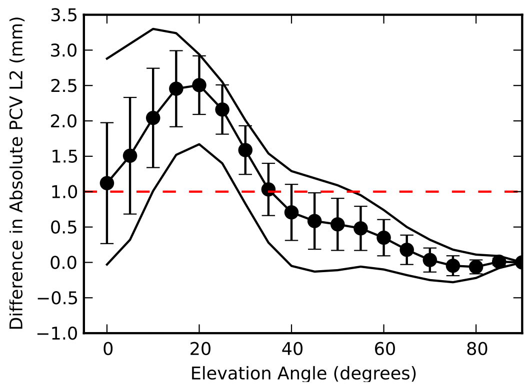

(d) elevation dependent difference ranges (antdpcv)

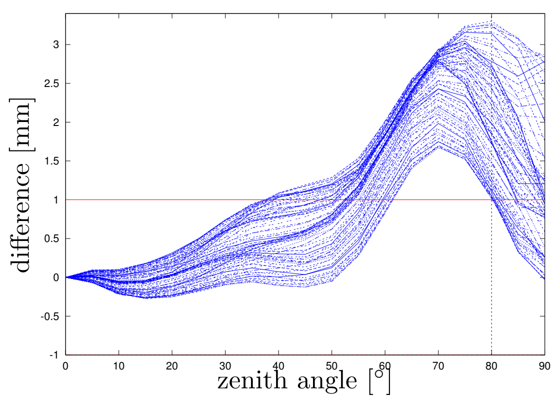

(e) overlay for all azimuth angles (antexfun)

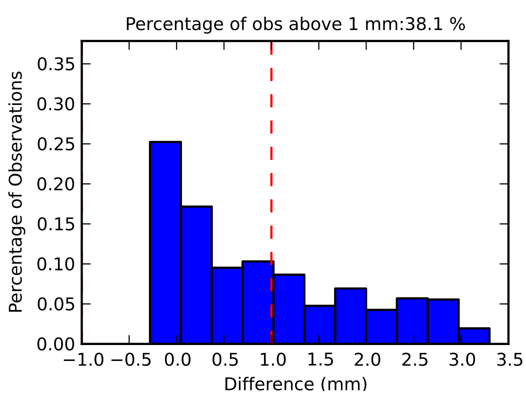

(f) histogram (antdpcv)

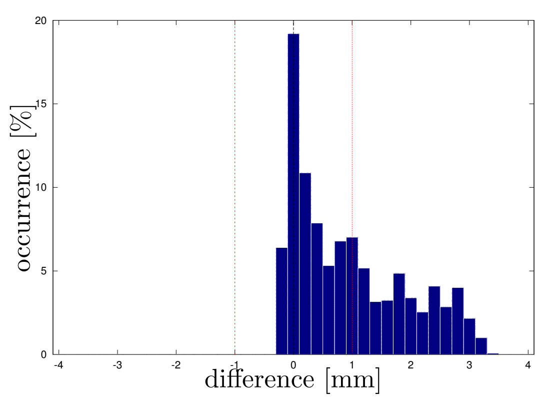

(g) histogram (antexfun)

Figure 8: Calibration differences for $LEIAR25.R3\_\_\_\_\_\_LEIT$ on R02.

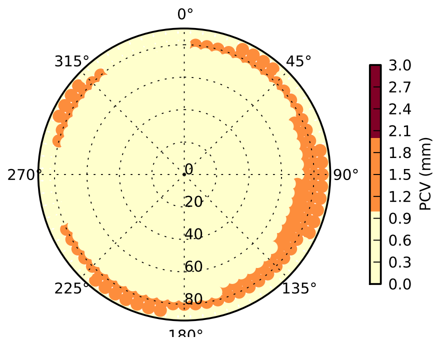

(a) staircase skyplot (antdpcv)

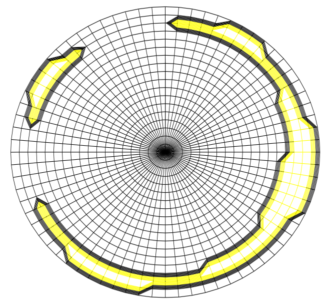

(b) staircase skyplot (antexfun)

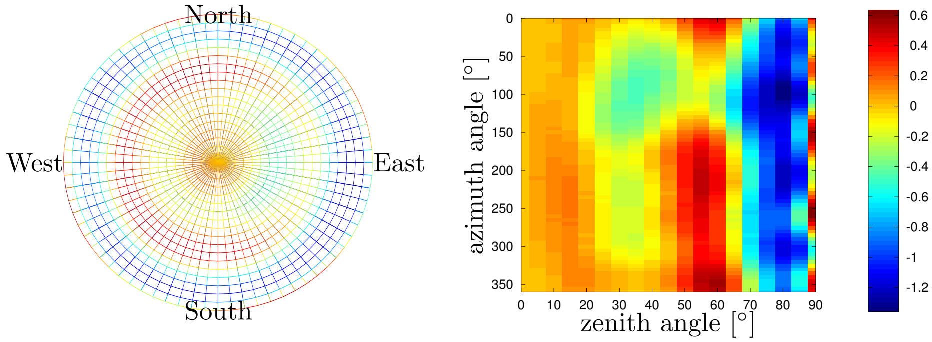

(c) polar (l) and cartesian (r) skyplot (antexfun)

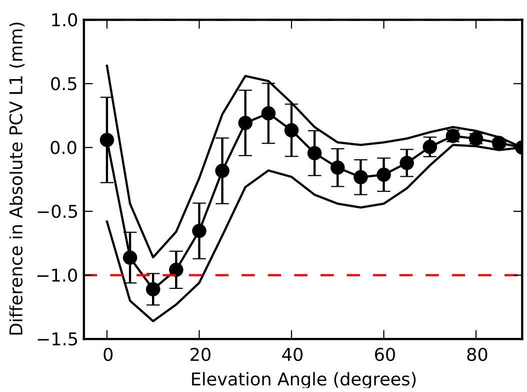

(d) elevation dependent difference ranges (antdpcv)

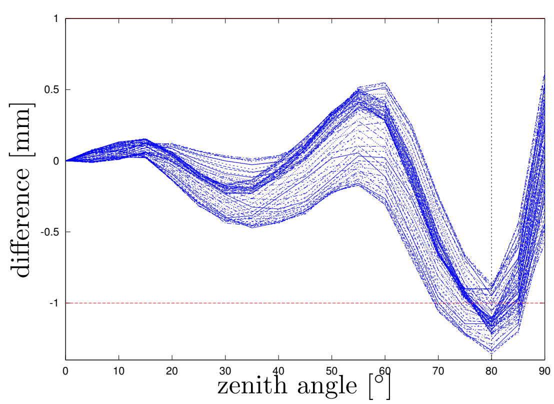

(e) overlay for all azimuth angles (antexfun)

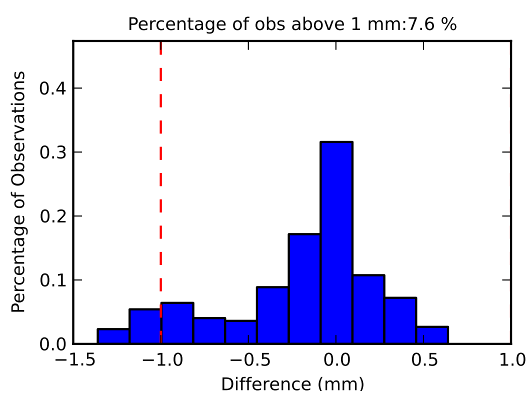

(f) histogram (antdpcv)

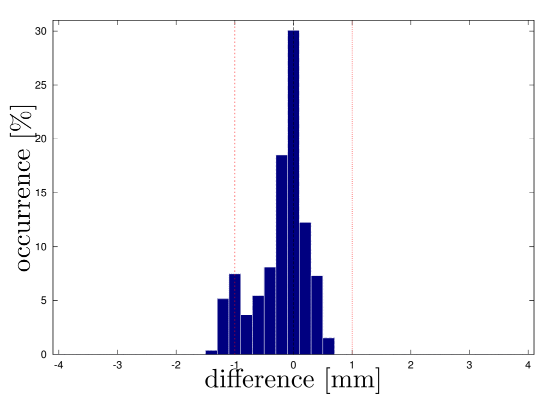

(g) histogram (antexfun)

Figure 9: Calibration differences for $LEIAR25.R4\_\_\_\_\_\_LEIT$ on G01.

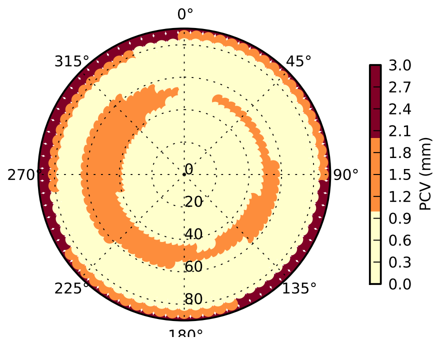

(a) staircase skyplot (antdpcv)

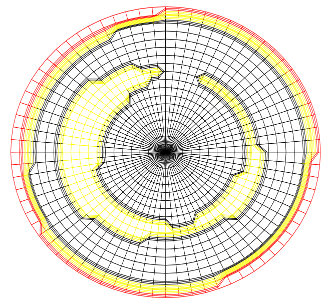

(b) staircase skyplot (antexfun)

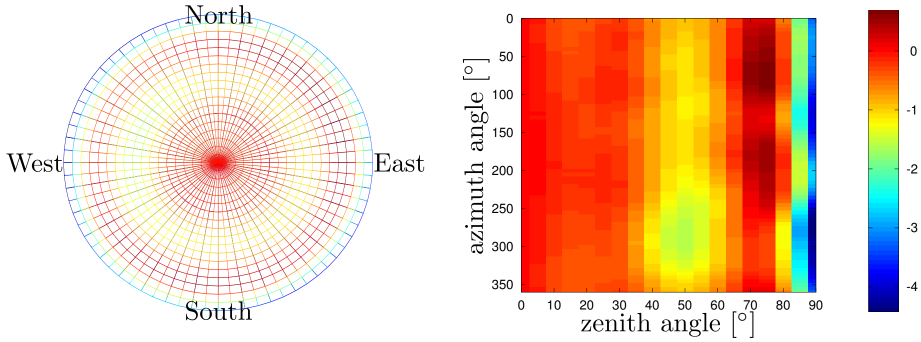

(c) polar (l) and cartesian (r) skyplot (antexfun)

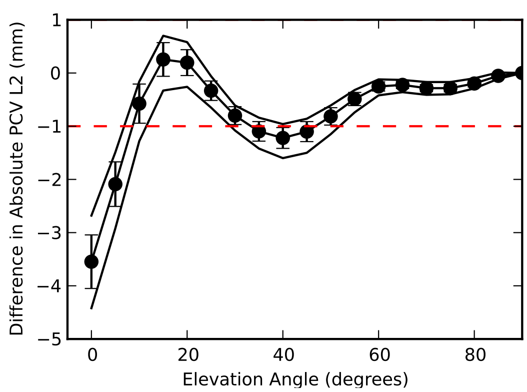

(d) elevation dependent difference ranges (antdpcv)

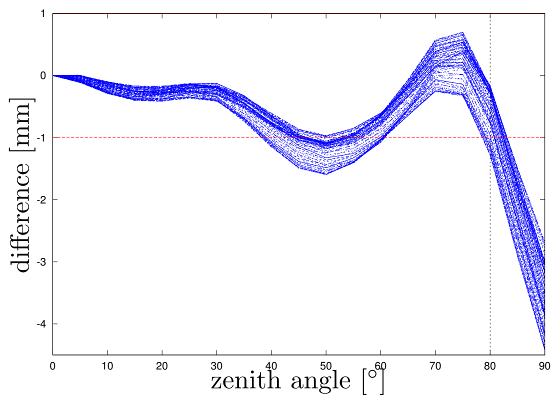

(e) overlay for all azimuth angles (antexfun)

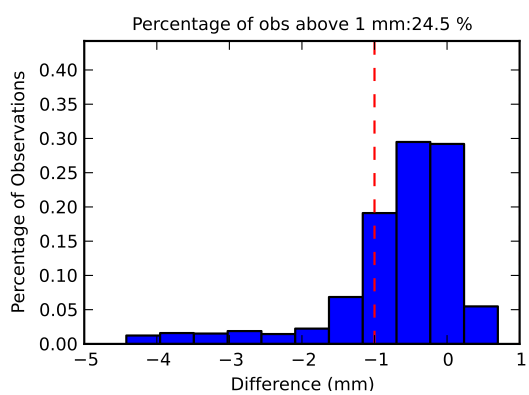

(f) histogram (antdpcv)

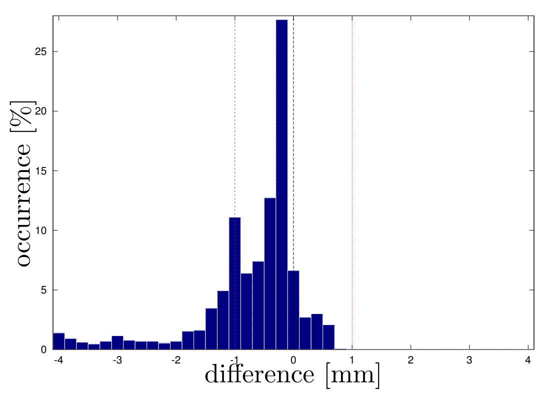

(g) histogram (antexfun)

Figure 10: Calibration differences for $LEIAR25.R4\_\_\_\_\_\_LEIT$ on G02.

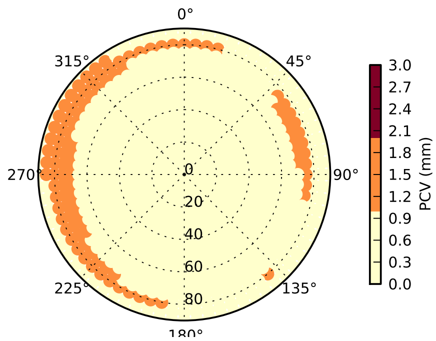

(a) staircase skyplot (antdpcv)

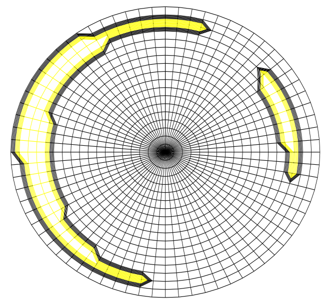

(b) staircase skyplot (antexfun)

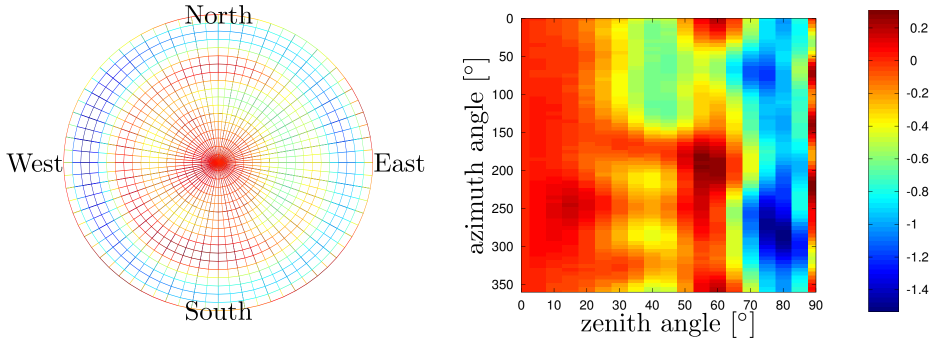

(c) polar (l) and cartesian (r) skyplot (antexfun)

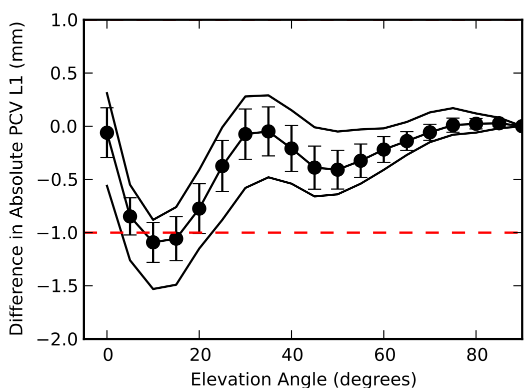

(d) elevation dependent difference ranges (antdpcv)

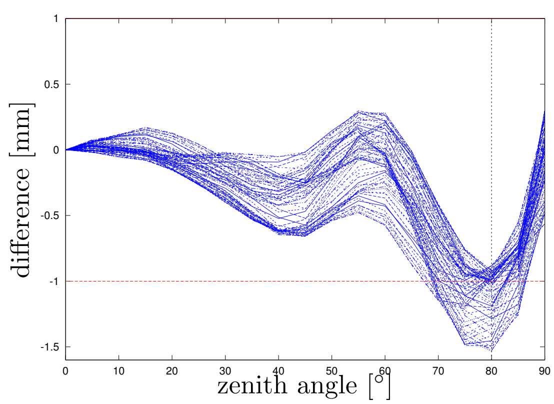

(e) overlay for all azimuth angles (antexfun)

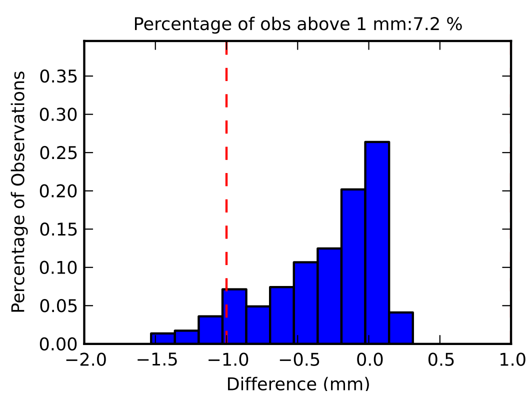

(f) histogram (antdpcv)

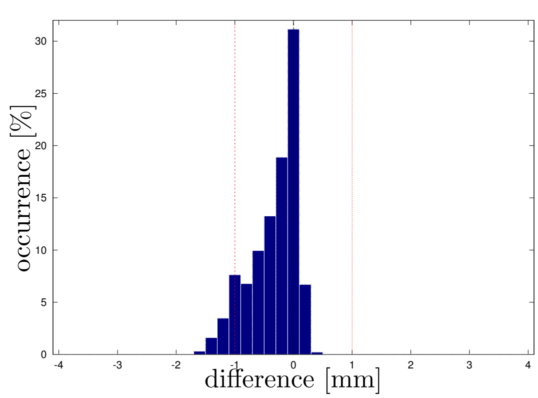

(g) histogram (antexfun)

Figure 11: Calibration differences for $LEIAR25.R4\_\_\_\_\_\_LEIT$ on R01.

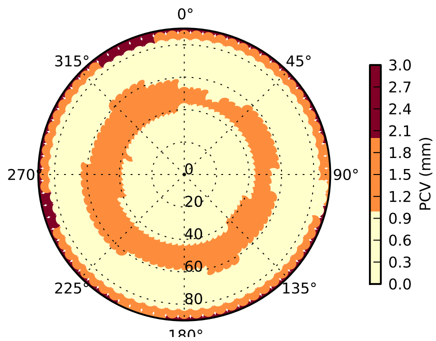

(a) staircase skyplot (antdpcv)

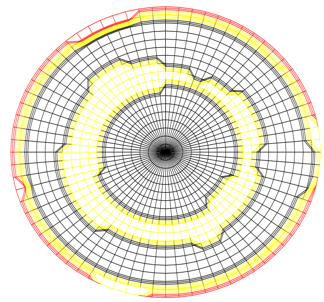

(b) staircase skyplot (antexfun)

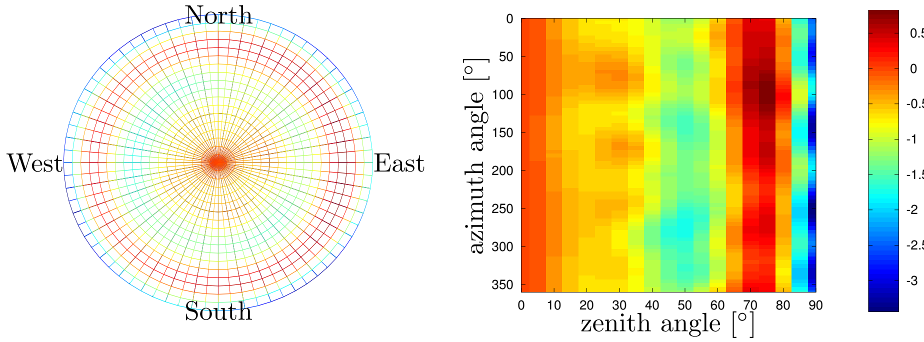

(c) polar (l) and cartesian (r) skyplot (antexfun)

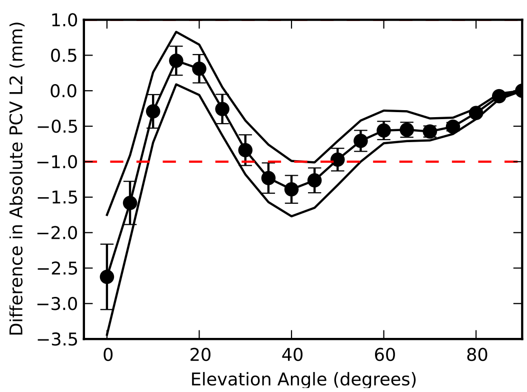

(d) elevation dependent difference ranges (antdpcv)

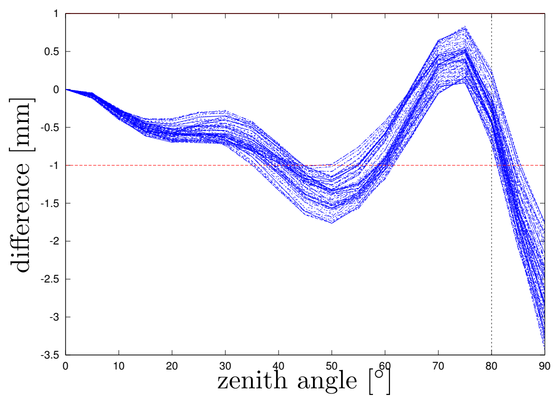

(e) overlay for all azimuth angles (antexfun)

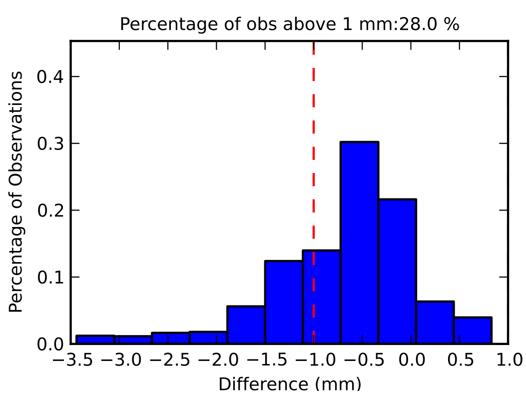

(f) histogram (antdpcv)

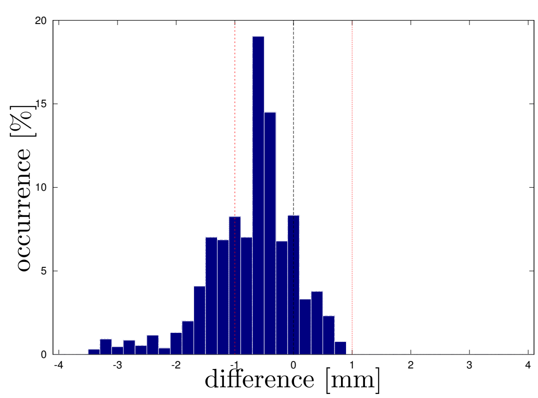

(g) histogram (antexfun)

Figure 12: Calibration differences for $LEIAR25.R4\_\_\_\_\_\_LEIT$ on R02.

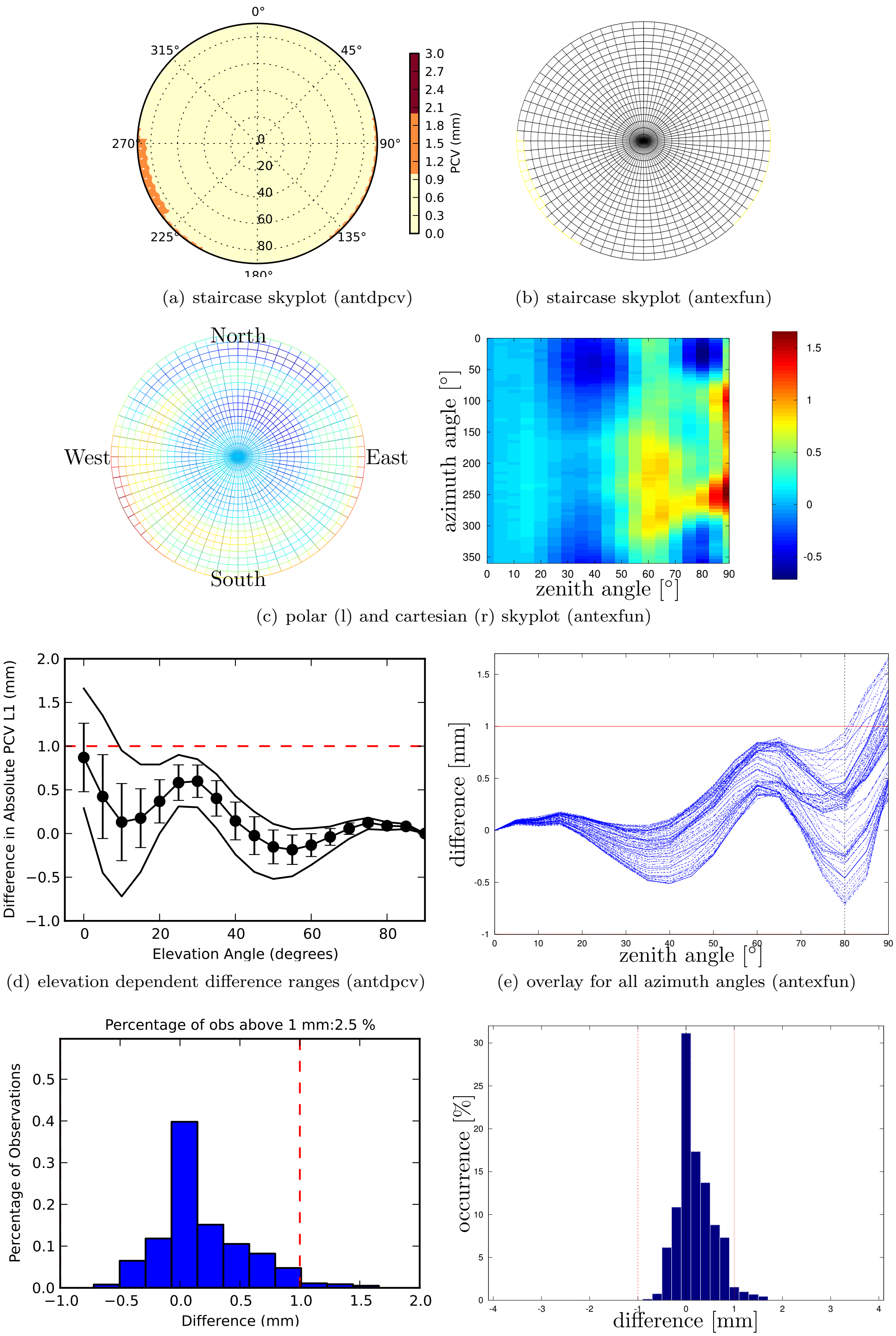

(a) staircase skyplot (antdpcv)

(b) staircase skyplot (antexfun)

(c) polar (l) and cartesian (r) skyplot (antexfun)

(d) elevation dependent difference ranges (antdpcv)

(e) overlay for all azimuth angles (antexfun)

(f) histogram (antdpcv)

(g) histogram (antexfun)

Figure 13: Calibration differences for $LEIAT504GG\_\_\_\_\_\_NONE$ on G01.

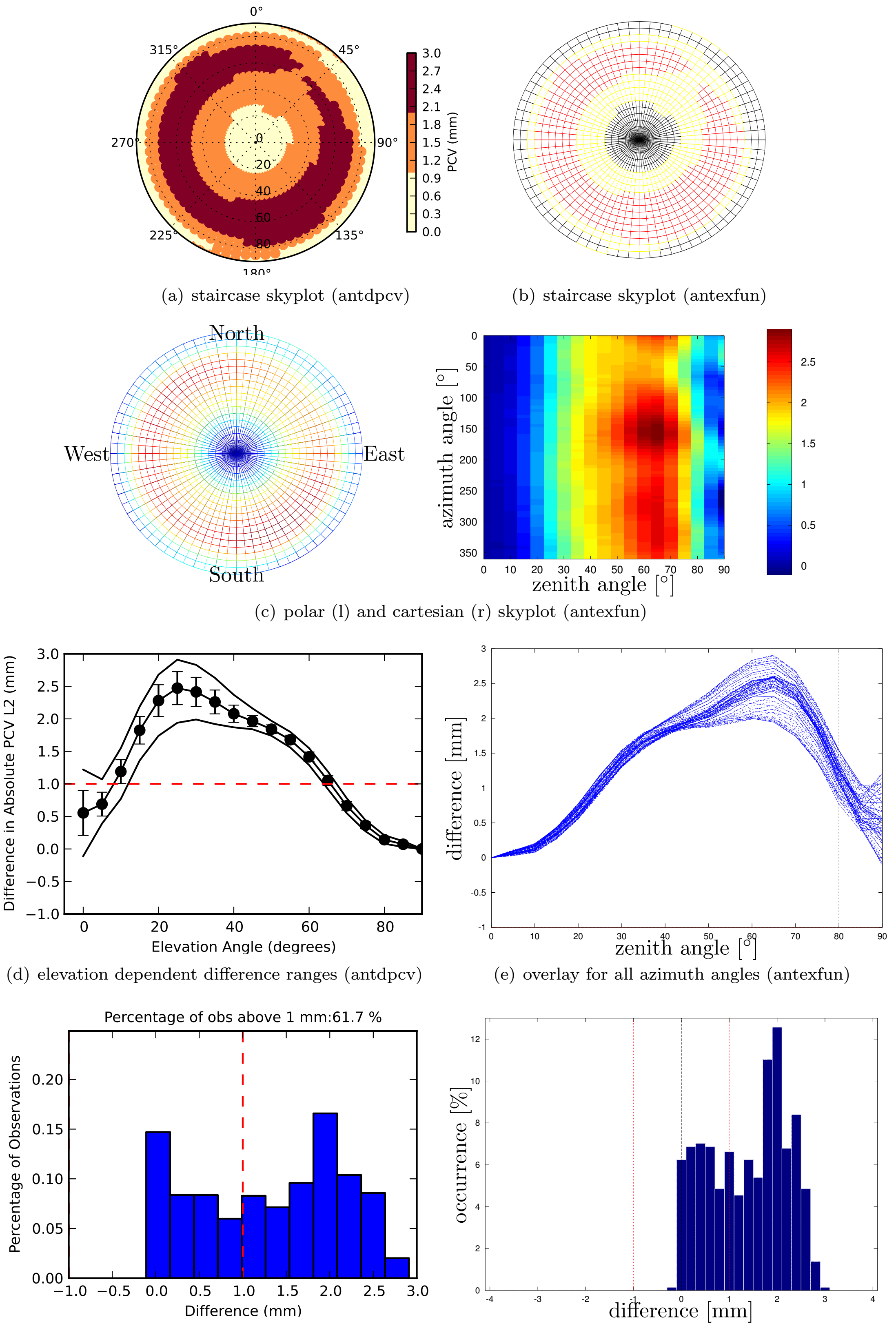

(a) staircase skyplot (antdpcv)

(b) staircase skyplot (antexfun)

(c) polar (l) and cartesian (r) skyplot (antexfun)

(d) elevation dependent difference ranges (antdpcv)

(e) overlay for all azimuth angles (antexfun)

(f) histogram (antdpcv)

(g) histogram (antexfun)

Figure 14: Calibration differences for $LEIAT504GG\_\_\_\_\_\_NONE$ on G02.

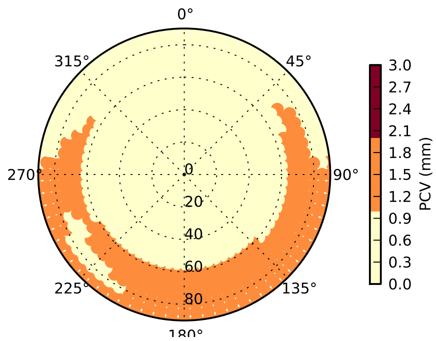

(a) staircase skyplot (antdpcv)

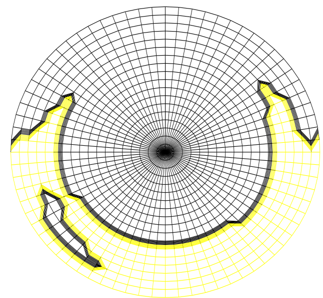

(b) staircase skyplot (antexfun)

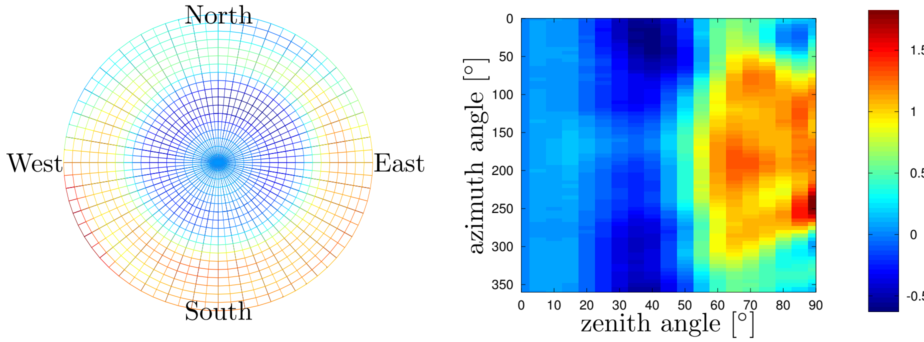

(c) polar (l) and cartesian (r) skyplot (antexfun)

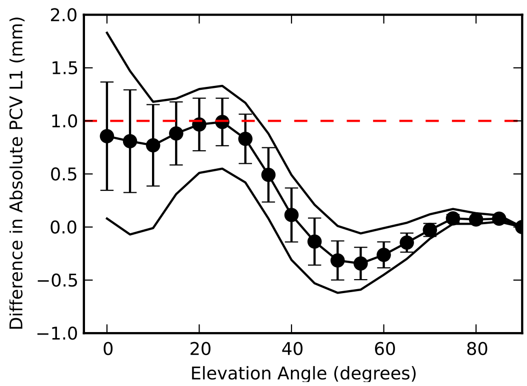

(d) elevation dependent difference ranges (antdpcv)

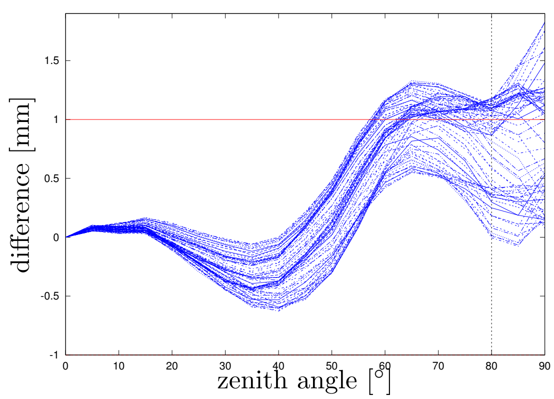

(e) overlay for all azimuth angles (antexfun)

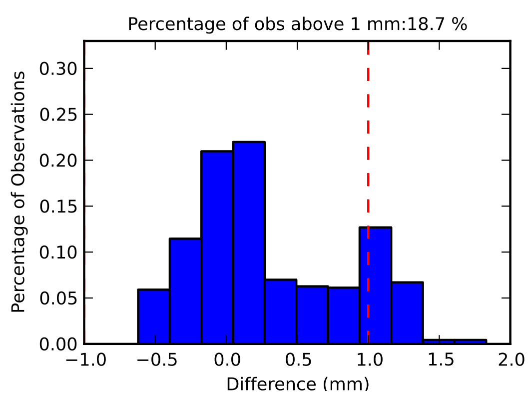

(f) histogram (antdpcv)

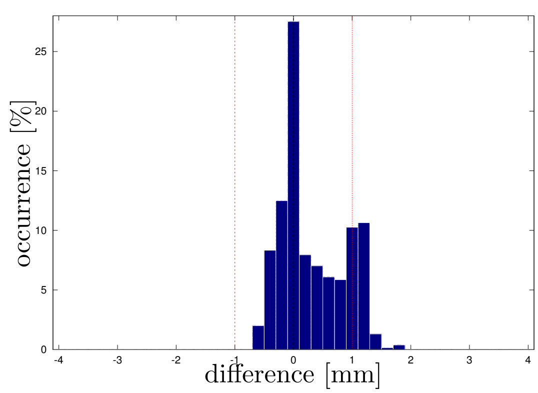

(g) histogram (antexfun)

Figure 15: Calibration differences for $LEIAT504GG\_\_\_\_\_NONE$ on R01.

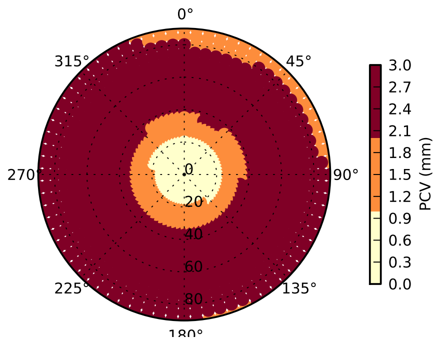

(a) staircase skyplot (antdpcv)

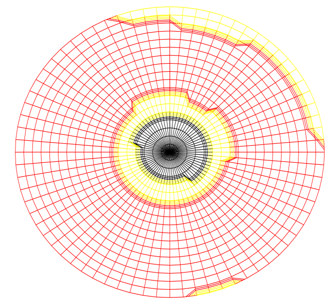

(b) staircase skyplot (antexfun)

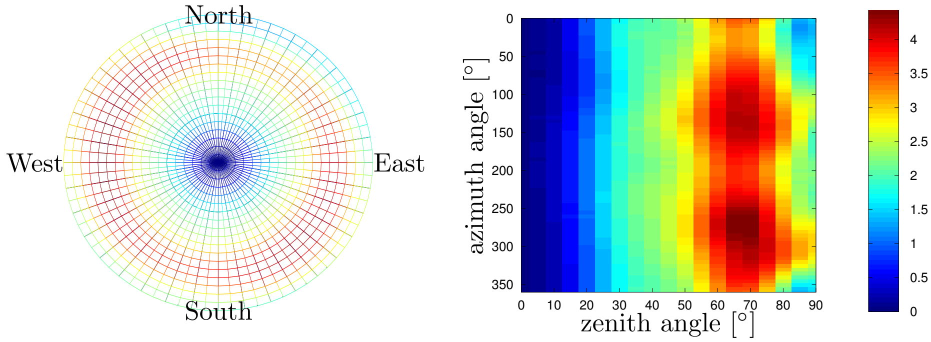

(c) polar (l) and cartesian (r) skyplot (antexfun)

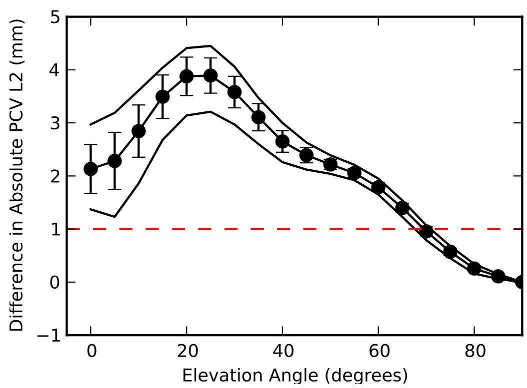

(d) elevation dependent difference ranges (antdpcv)

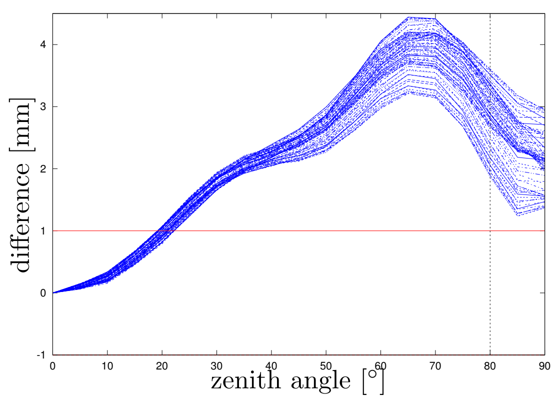

(e) overlay for all azimuth angles (antexfun)

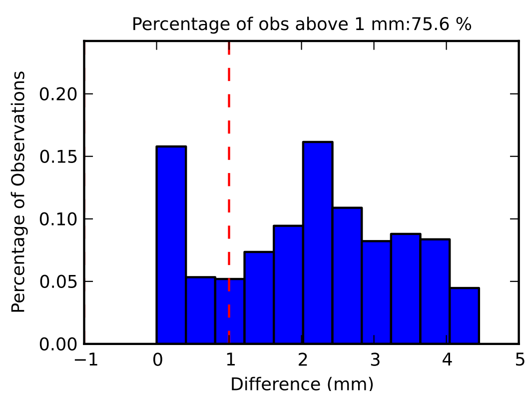

(f) histogram (antdpcv)

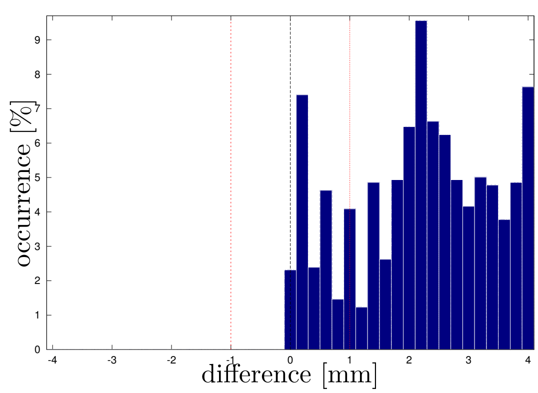

(g) histogram (antexfun)

Figure 16: Calibration differences for $LEIAT504GG\_\_\_\_\_NONE$ on R02.

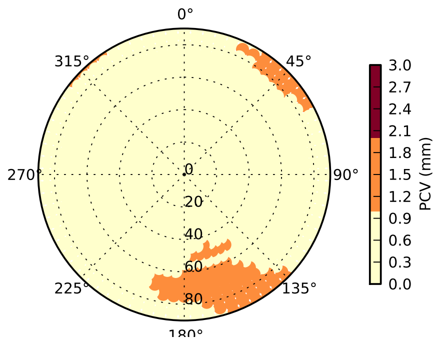

(a) staircase skyplot (antdpcv)

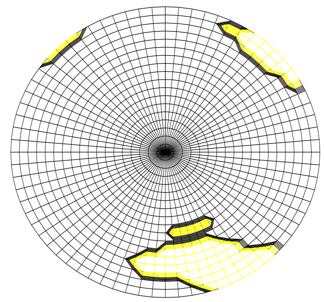

(b) staircase skyplot (antexfun)

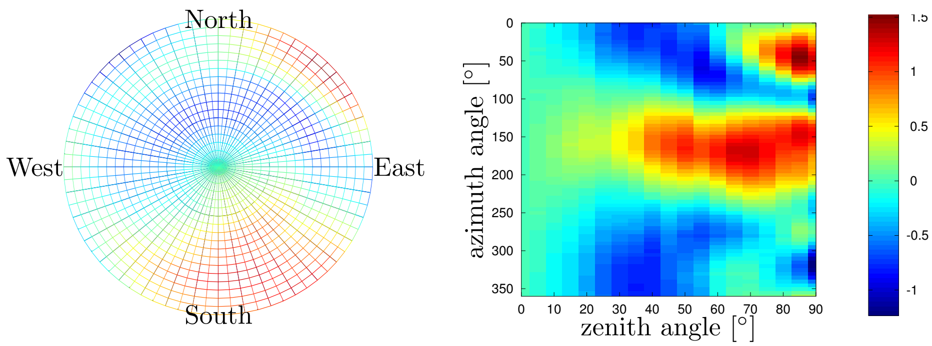

(c) polar (l) and cartesian (r) skyplot (antexfun)

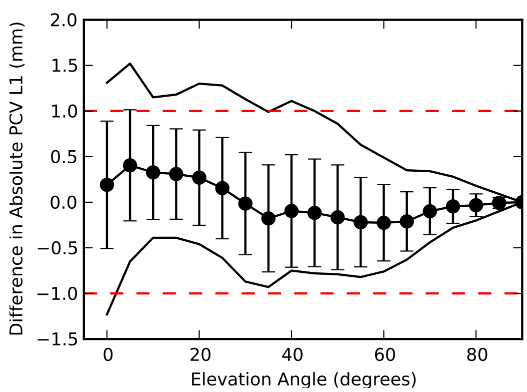

(d) elevation dependent difference ranges (antdpcv)

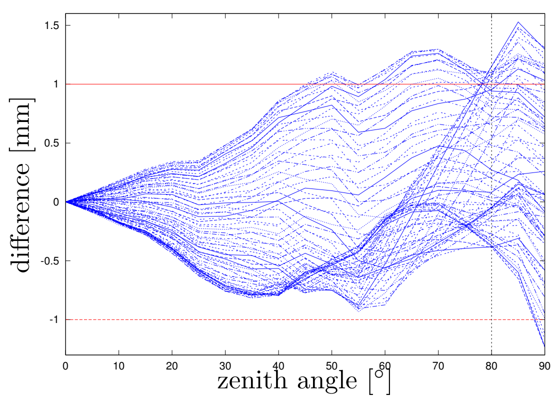

(e) overlay for all azimuth angles (antexfun)

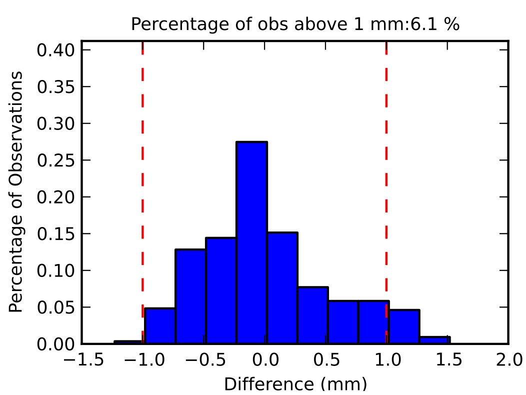

(f) histogram (antdpcv)

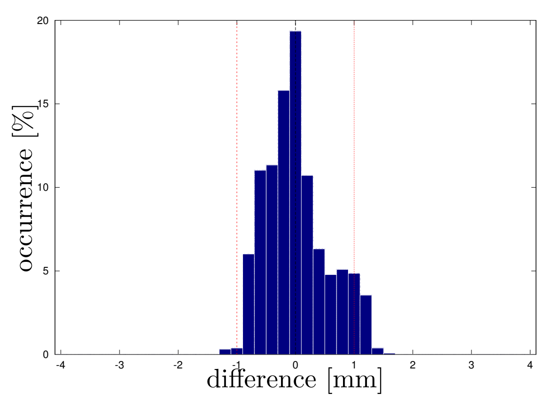

(g) histogram (antexfun)

Figure 17: Calibration differences for $LEIAX1202GG\_\_\_\_\_NONE$ on G01.

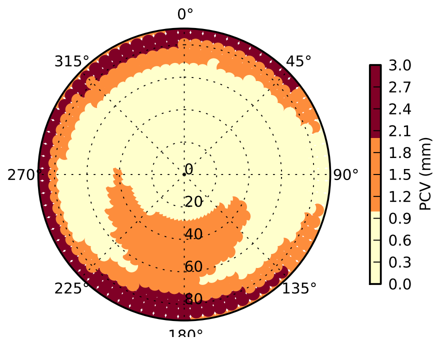

(a) staircase skyplot (antdpcv)

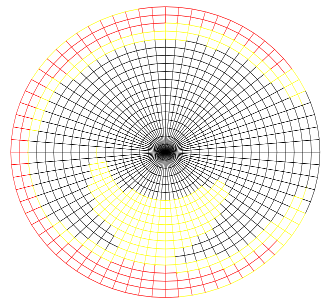

(b) staircase skyplot (antexfun)

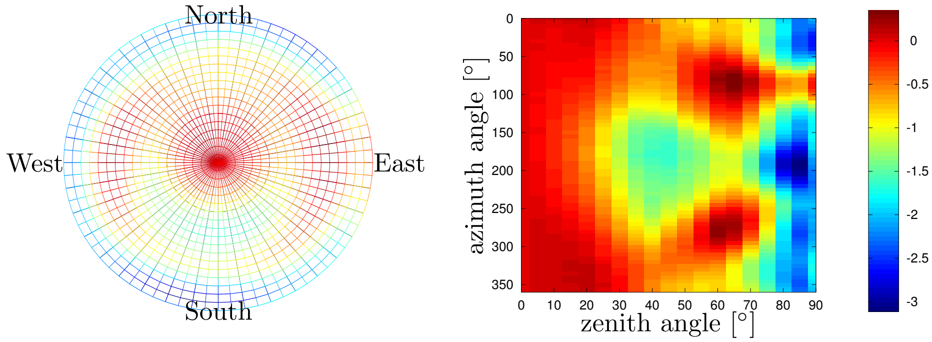

(c) polar (l) and cartesian (r) skyplot (antexfun)

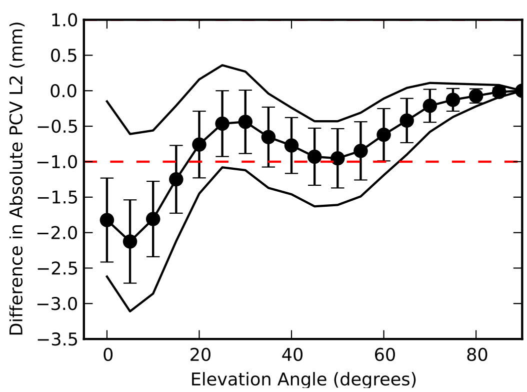

(d) elevation dependent difference ranges (antdpcv)

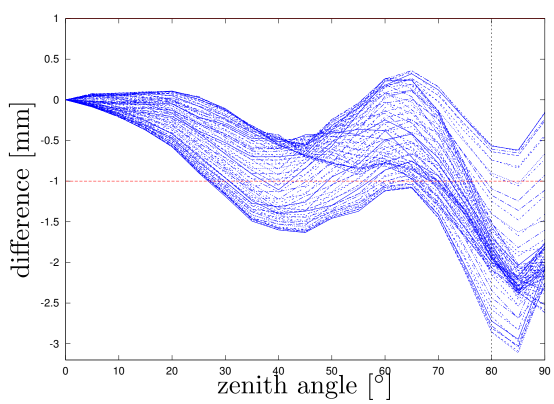

(e) overlay for all azimuth angles (antexfun)

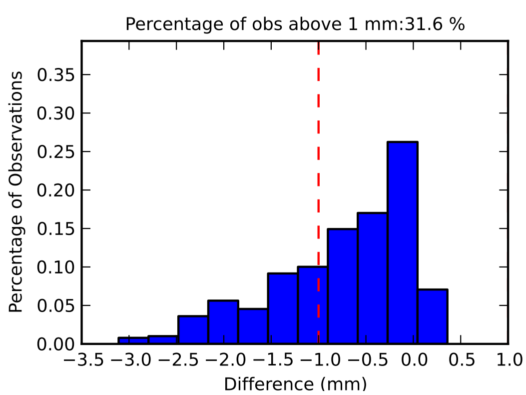

(f) histogram (antdpcv)

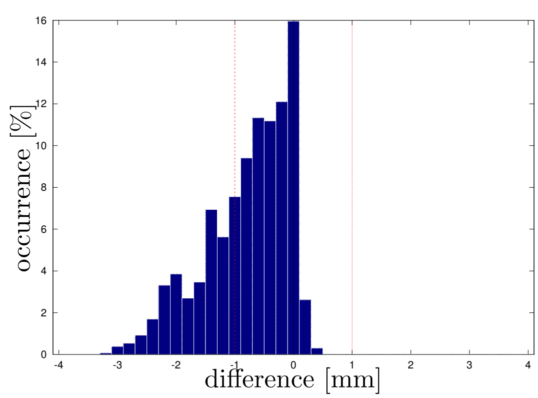

(g) histogram (antexfun)

Figure 18: Calibration differences for $LEIAX1202GG\_\_\_\_\_NONE$ on G02.

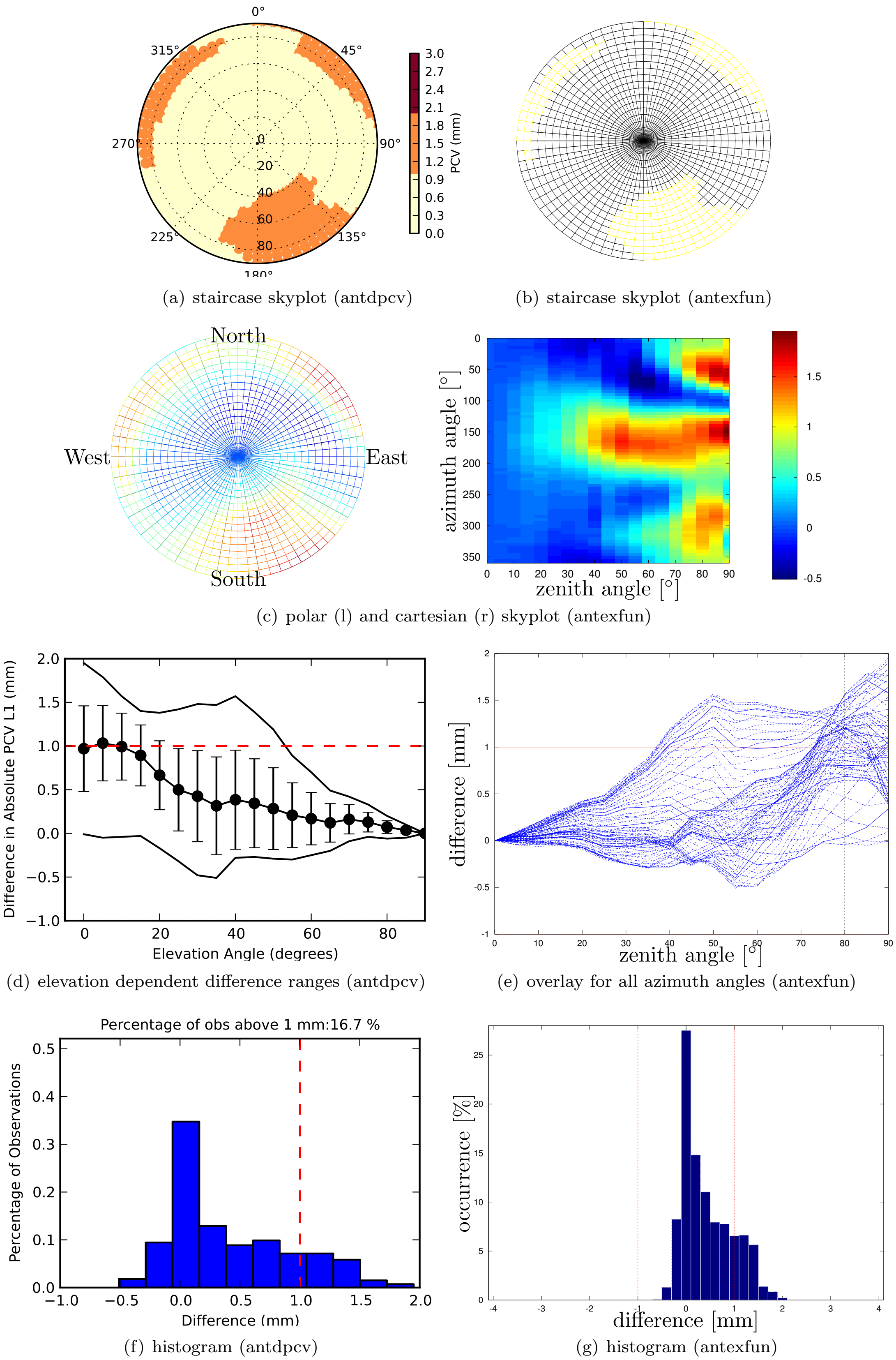

(a) staircase skyplot (antdpcv)

(b) staircase skyplot (antexfun)

(c) polar (l) and cartesian (r) skyplot (antexfun)

(d) elevation dependent difference ranges (antdpcv)

(e) overlay for all azimuth angles (antexfun)

(f) histogram (antdpcv)

(g) histogram (antexfun)

Figure 19: Calibration differences for $LEIAX1202GG\_\_\_\_\_NONE$ on R01.

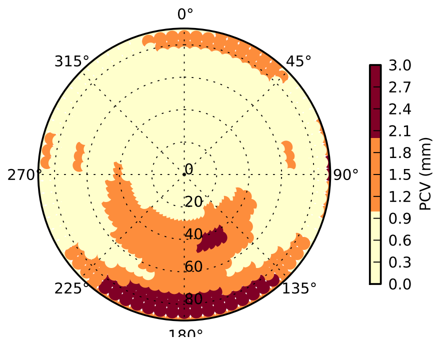

(a) staircase skyplot (antdpcv)

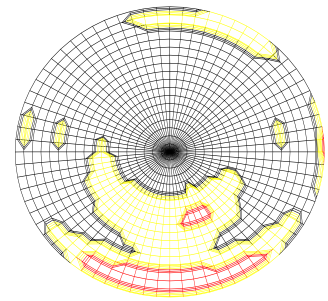

(b) staircase skyplot (antexfun)

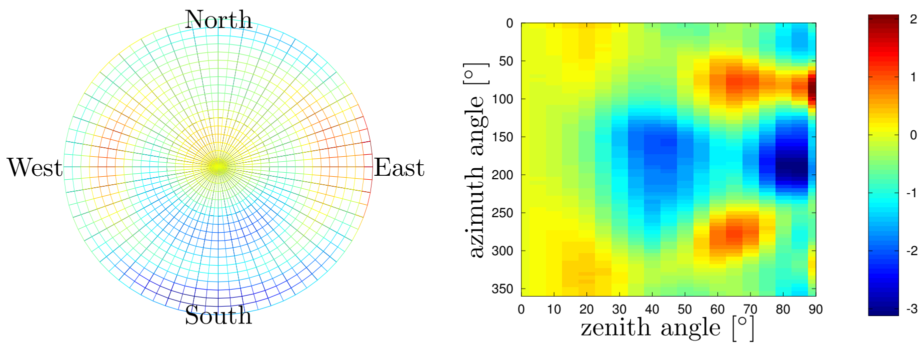

(c) polar (l) and cartesian (r) skyplot (antexfun)

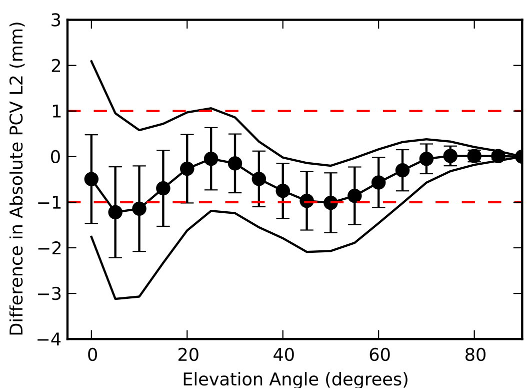

(d) elevation dependent difference ranges (antdpcv)

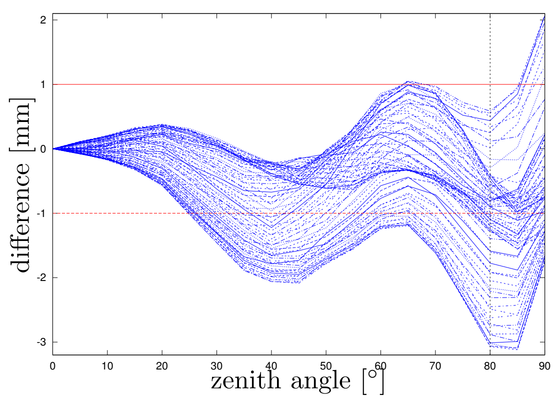

(e) overlay for all azimuth angles (antexfun)

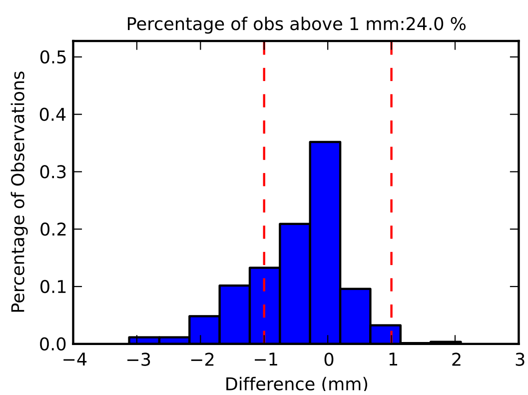

(f) histogram (antdpcv)

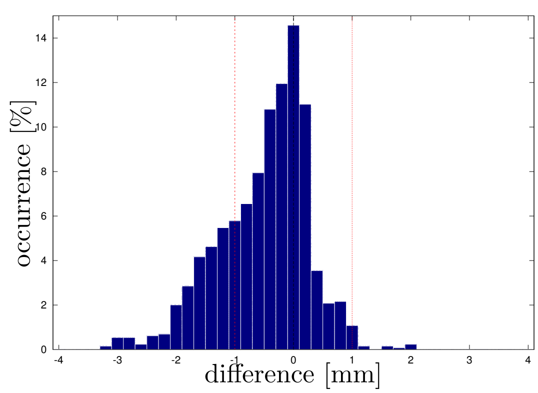

(g) histogram (antexfun)

Figure 20: Calibration differences for $LEIAX1202GG\_\_\_\_\_NONE$ on R02.

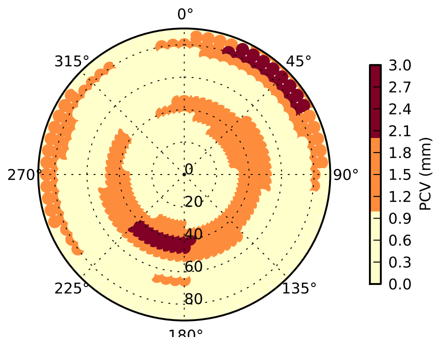

(a) staircase skyplot (antdpcv)

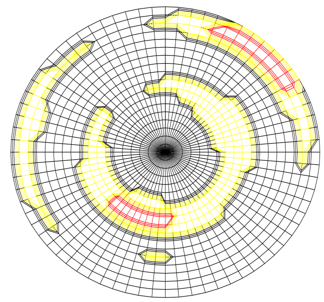

(b) staircase skyplot (antexfun)

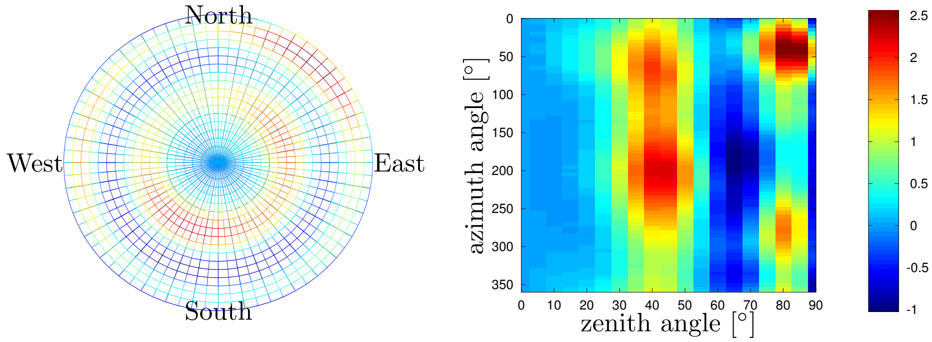

(c) polar (l) and cartesian (r) skyplot (antexfun)

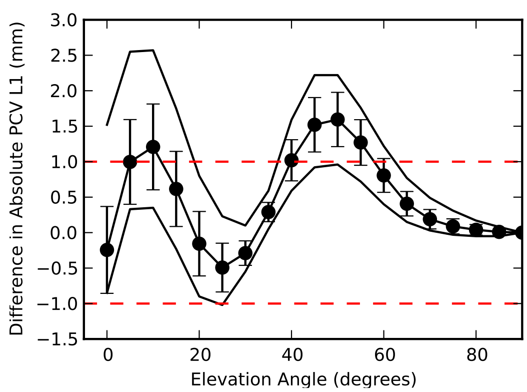

(d) elevation dependent difference ranges (antdpcv)

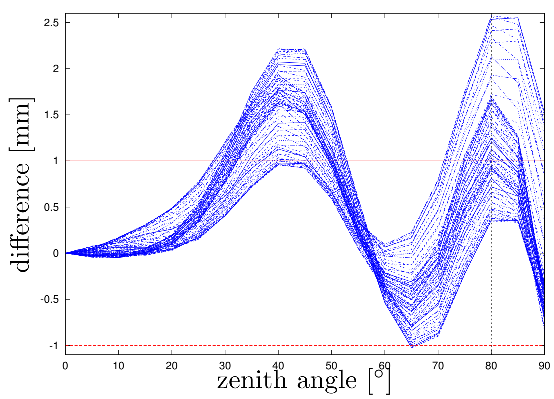

(e) overlay for all azimuth angles (antexfun)

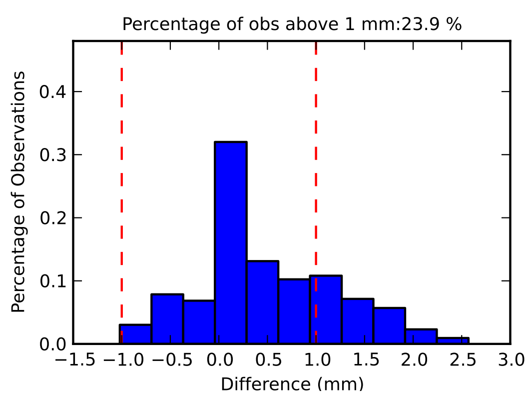

(f) histogram (antdpcv)

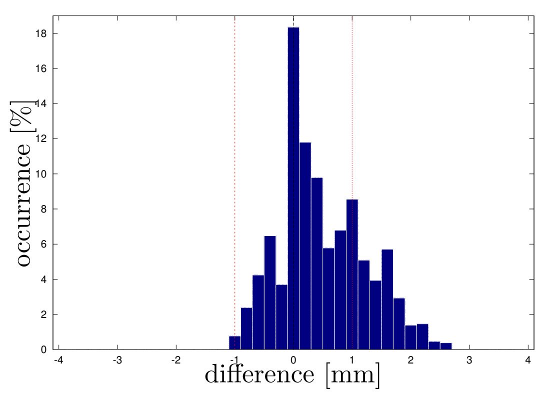

(g) histogram (antexfun)

Figure 21: Calibration differences for $NAX3G+C\_\_\_\_\_\_\_\_\_NONE$ on G01.

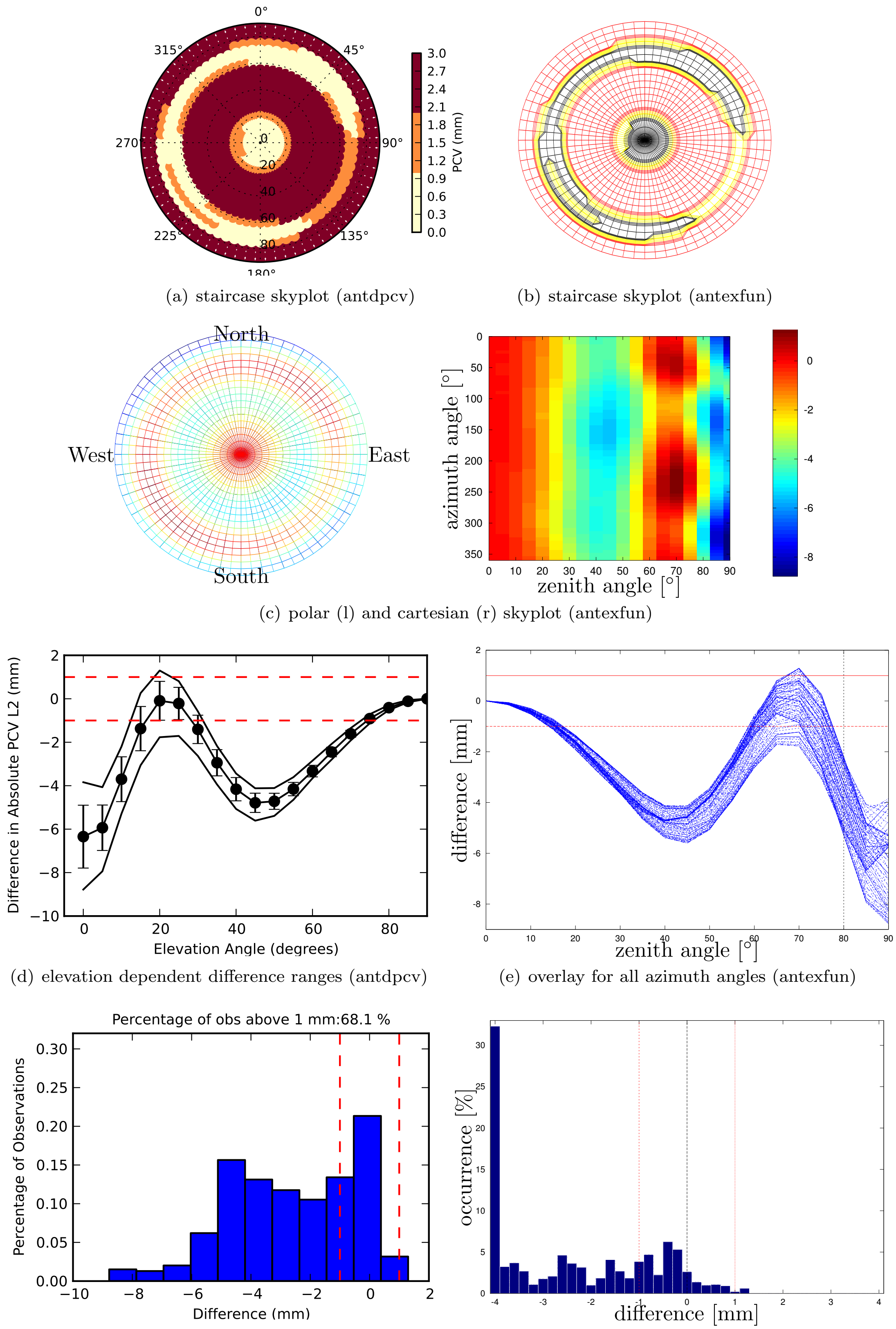

(a) staircase skyplot (antdpcv)

(b) staircase skyplot (antexfun)

(c) polar (l) and cartesian (r) skyplot (antexfun)

(d) elevation dependent difference ranges (antdpcv)

(e) overlay for all azimuth angles (antexfun)

(f) histogram (antdpcv)

(g) histogram (antexfun)

Figure 22: Calibration differences for $NAX3G + C\_\_\_\_\_\_\_\_\_NONE$ on G02.

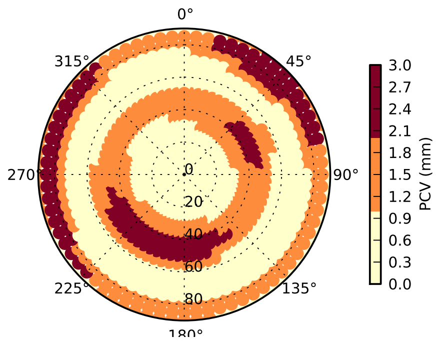

(a) staircase skyplot (antdpcv)

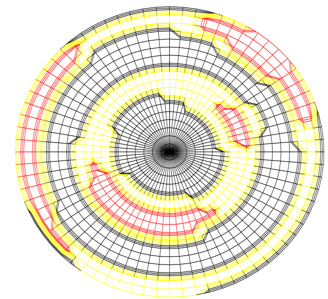

(b) staircase skyplot (antexfun)

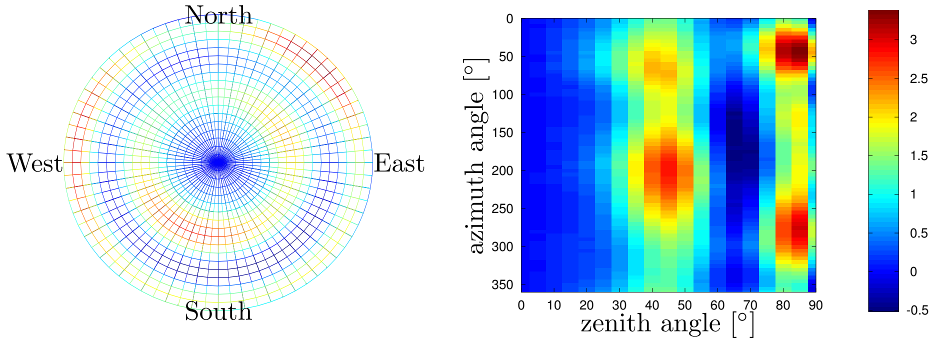

(c) polar (l) and cartesian (r) skyplot (antexfun)

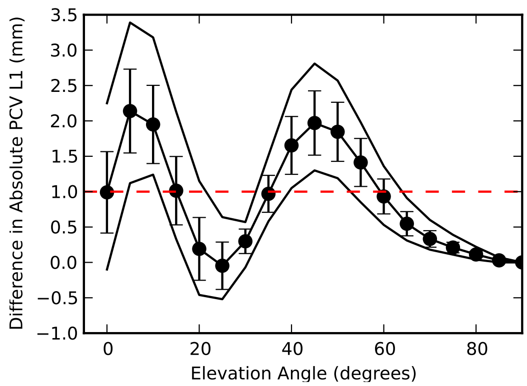

(d) elevation dependent difference ranges (antdpcv)

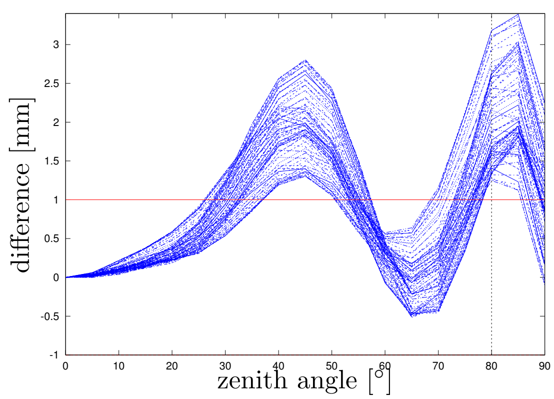

(e) overlay for all azimuth angles (antexfun)

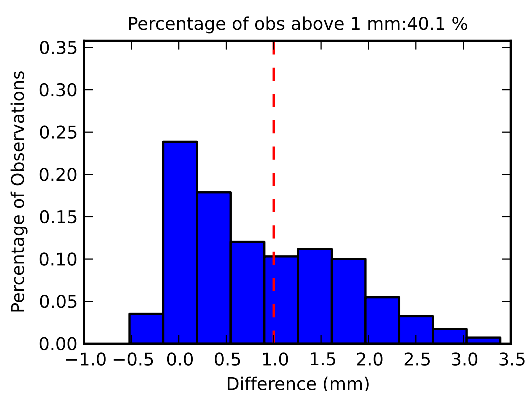

(f) histogram (antdpcv)

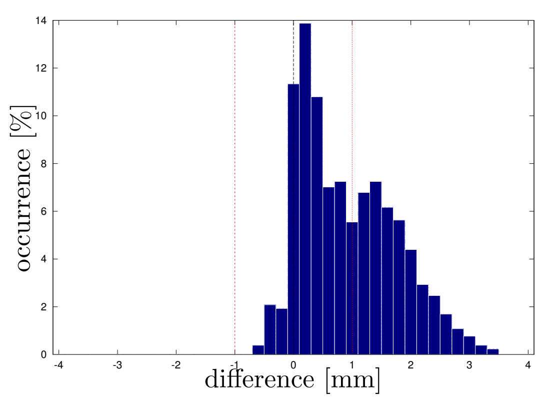

(g) histogram (antexfun)

Figure 23: Calibration differences for $NAX3G+C\_\_\_\_\_\_\_\_NONE$ on R01.

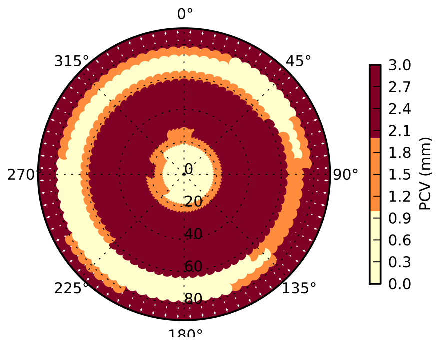

(a) staircase skyplot (antdpcv)

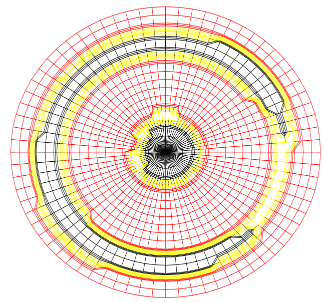

(b) staircase skyplot (antexfun)

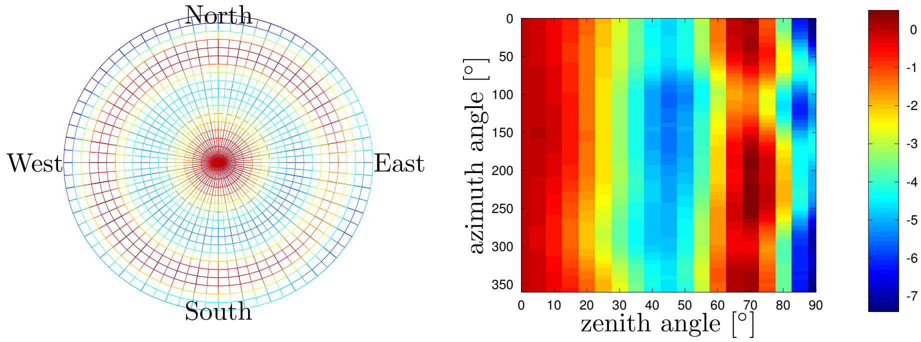

(c) polar (l) and cartesian (r) skyplot (antexfun)

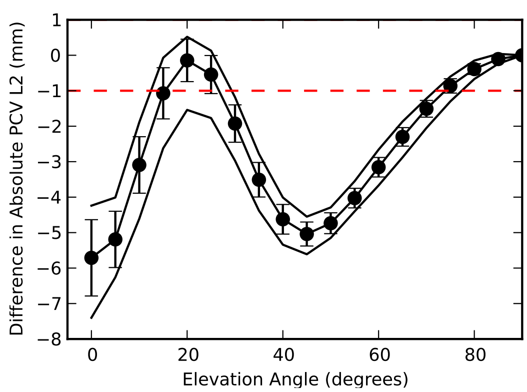

(d) elevation dependent difference ranges (antdpcv)

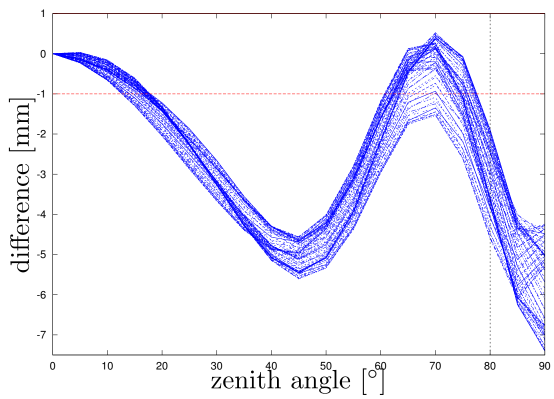

(e) overlay for all azimuth angles (antexfun)

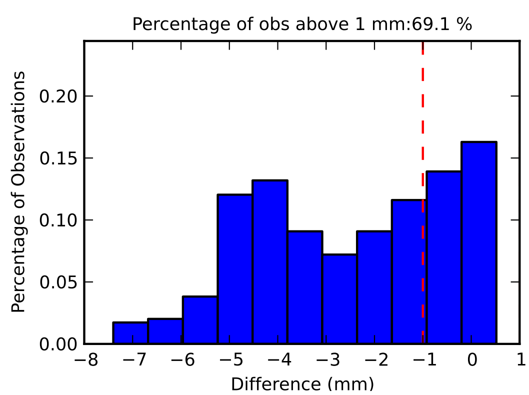

(f) histogram (antdpcv)

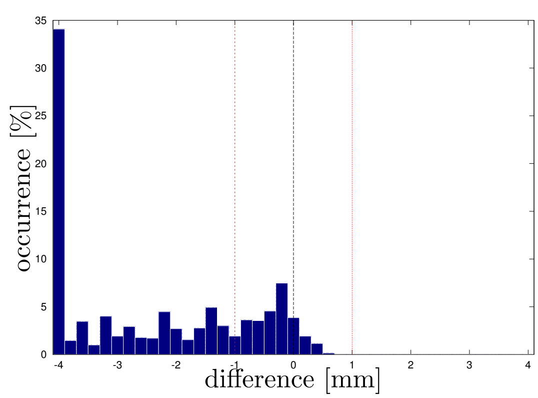

(g) histogram (antexfun)

Figure 24: Calibration differences for $NAX3G+C\_\_\_\_\_\_\_\_NONE$ on R02.

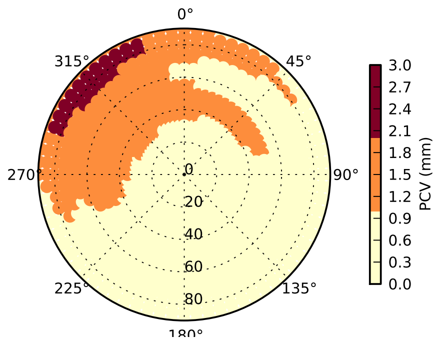

(a) staircase skyplot (antdpcv)

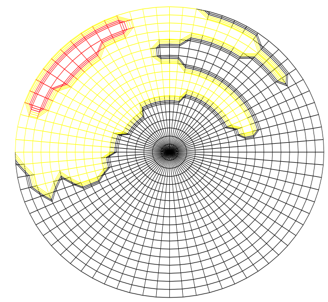

(b) staircase skyplot (antexfun)

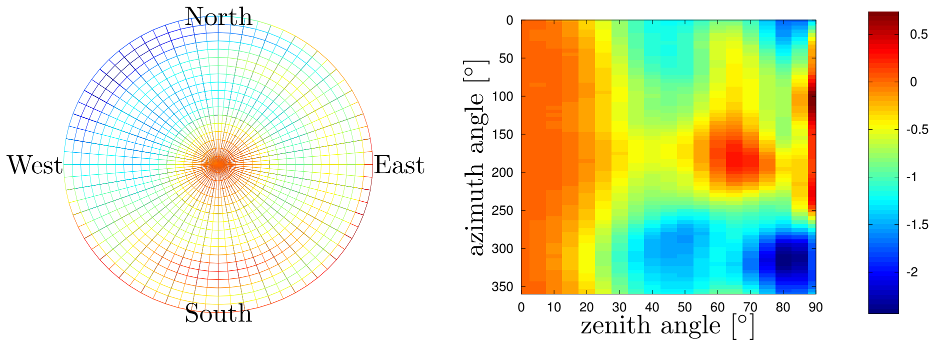

(c) polar (l) and cartesian (r) skyplot (antexfun)

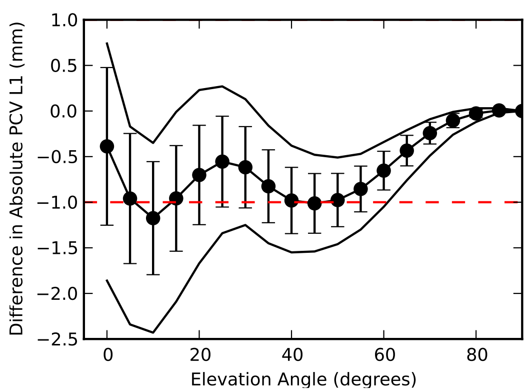

(d) elevation dependent difference ranges (antdpcv)

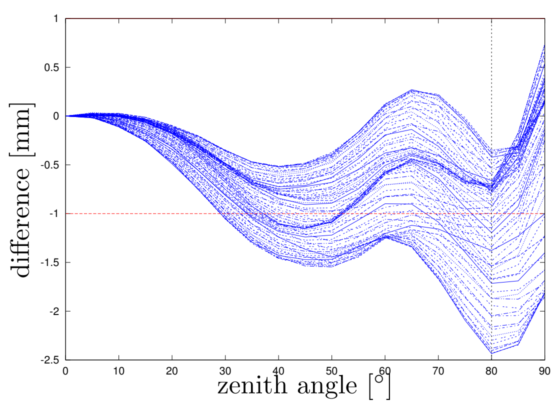

(e) overlay for all azimuth angles (antexfun)

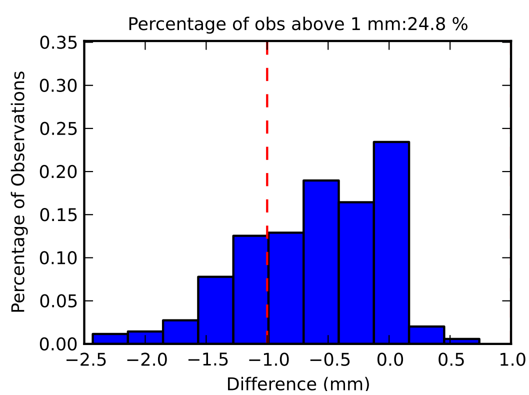

(f) histogram (antdpcv)

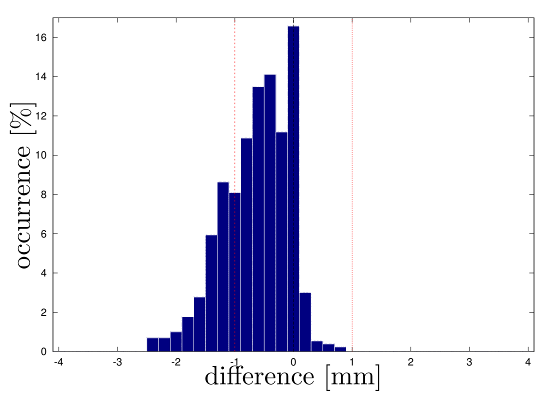

(g) histogram (antexfun)

Figure 25: Calibration differences for $TPSCR.G3\_\_\_\_\_\_\_TPSH$ on G01.

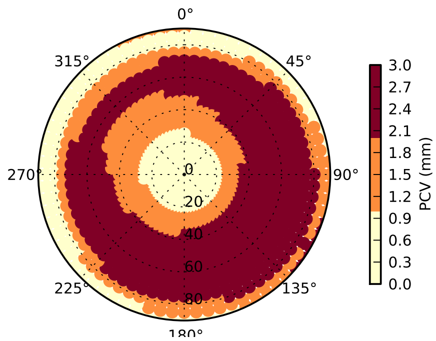

(a) staircase skyplot (antdpcv)

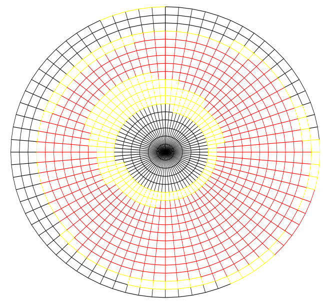

(b) staircase skyplot (antexfun)

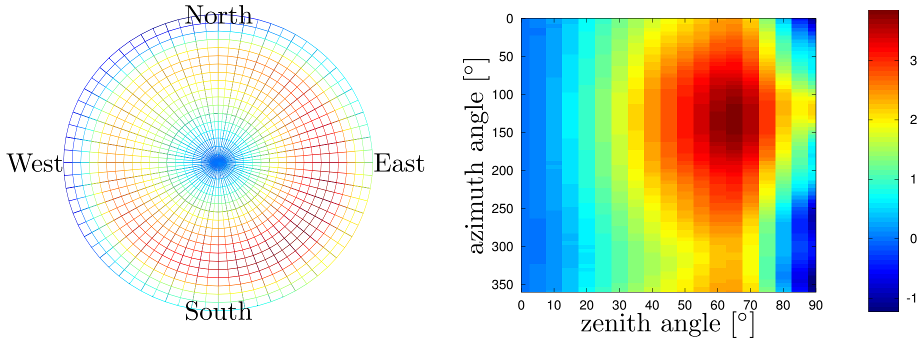

(c) polar (l) and cartesian (r) skyplot (antexfun)

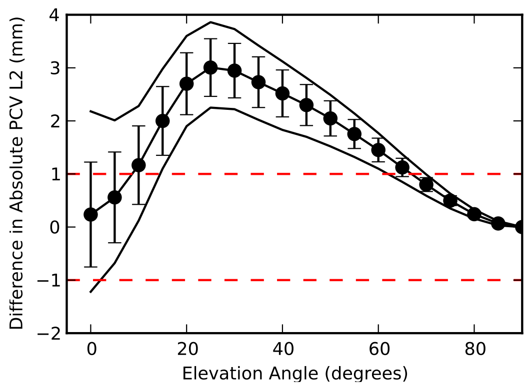

(d) elevation dependent difference ranges (antdpcv)

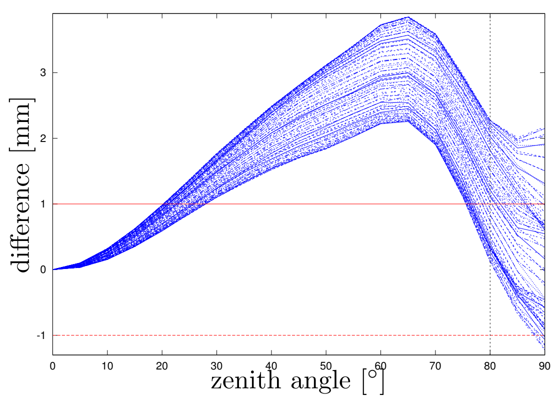

(e) overlay for all azimuth angles (antexfun)

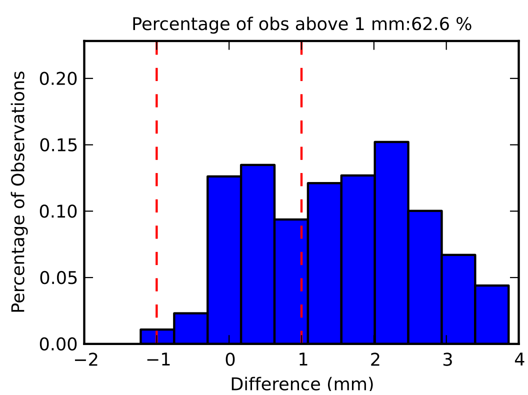

(f) histogram (antdpcv)

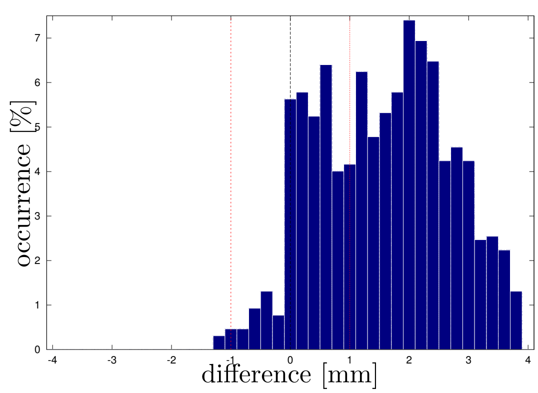

(g) histogram (antexfun)

Figure 26: Calibration differences for $TPSCR.G3\_\_\_\_\_\_\_TPSH$ on G02.

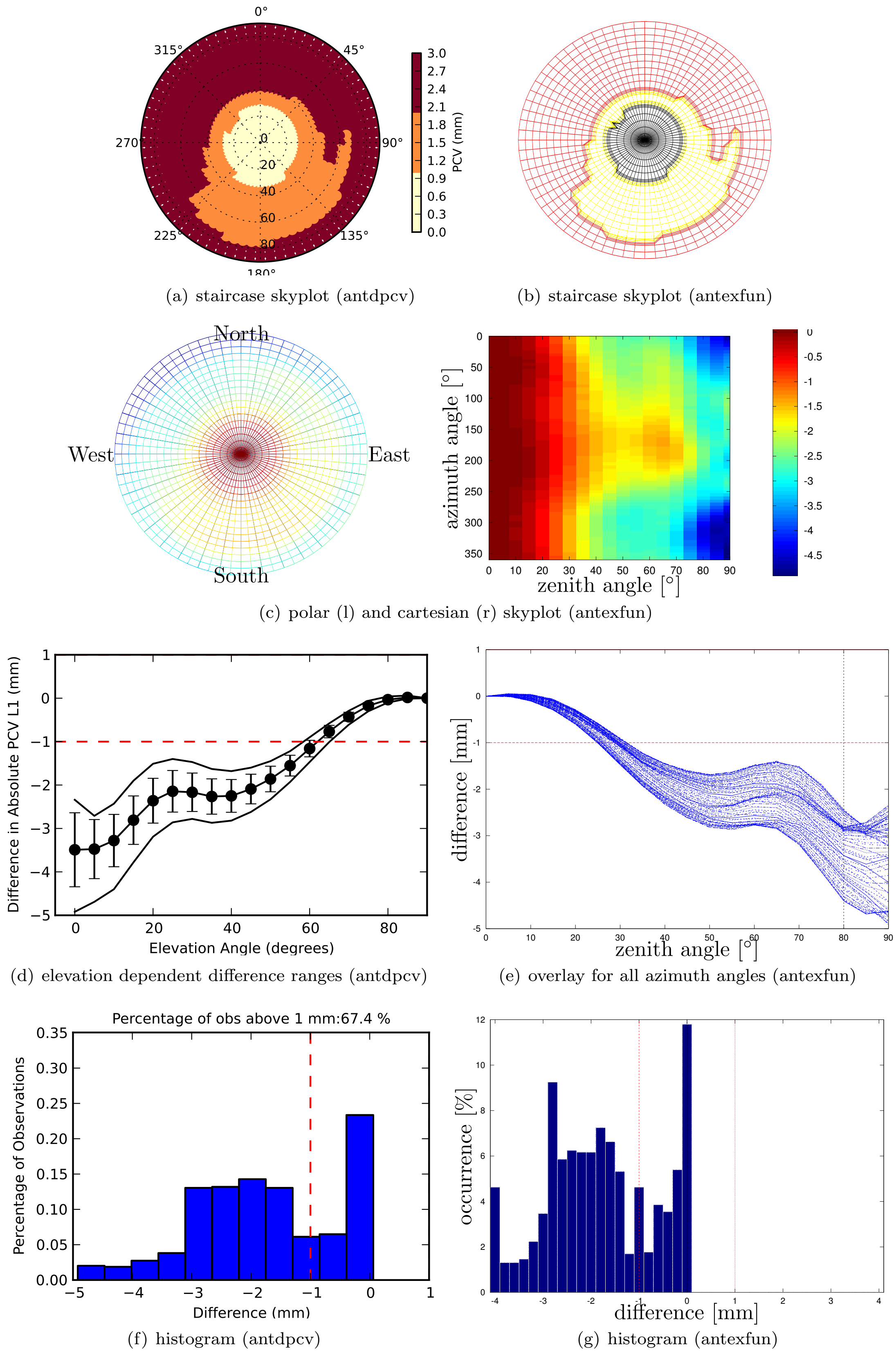

(a) staircase skyplot (antdpcv)

(b) staircase skyplot (antexfun)

(c) polar (l) and cartesian (r) skyplot (antexfun)

(d) elevation dependent difference ranges (antdpcv)

(e) overlay for all azimuth angles (antexfun)

(f) histogram (antdpcv)

(g) histogram (antexfun)

Figure 27: Calibration differences for $TPSCR.G3\_\_\_\_\_\_\_TPSH$ on R01.

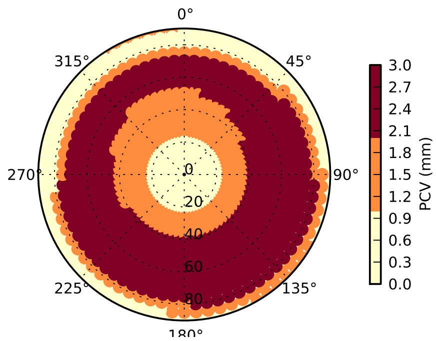

(a) staircase skyplot (antdpcv)

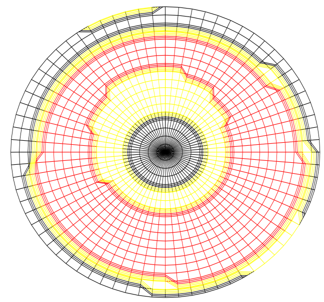

(b) staircase skyplot (antexfun)

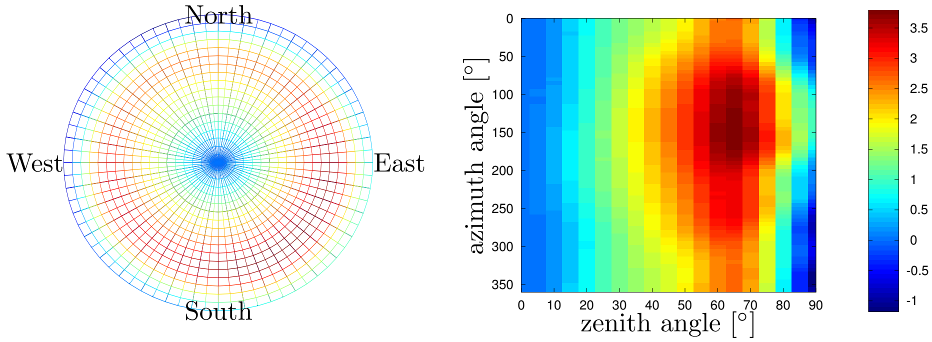

(c) polar (l) and cartesian (r) skyplot (antexfun)

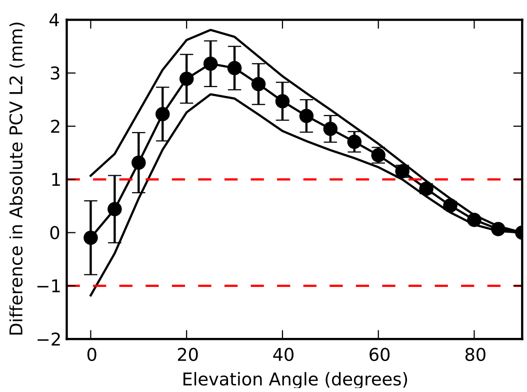

(d) elevation dependent difference ranges (antdpcv)

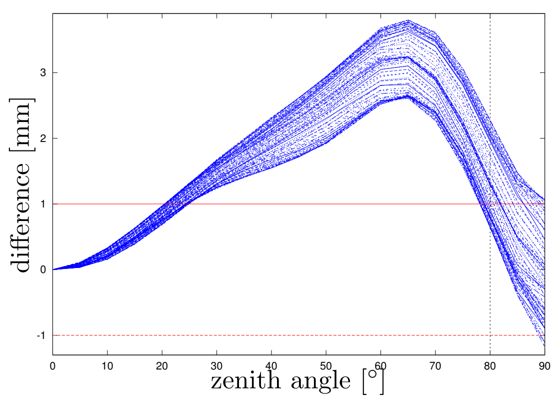

(e) overlay for all azimuth angles (antexfun)

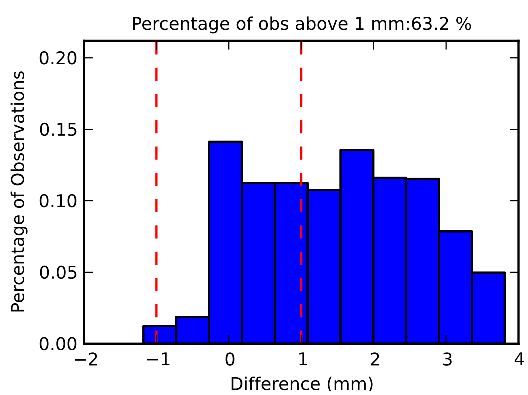

(f) histogram (antdpcv)

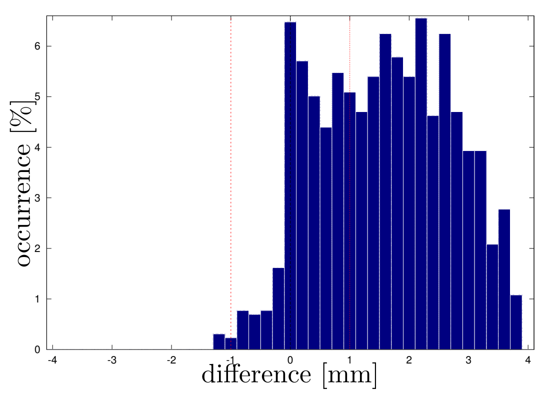

(g) histogram (antexfun)

Figure 28: Calibration differences for $TPSCR.G3\_\_\_\_\_\_\_TPSH$ on R02.

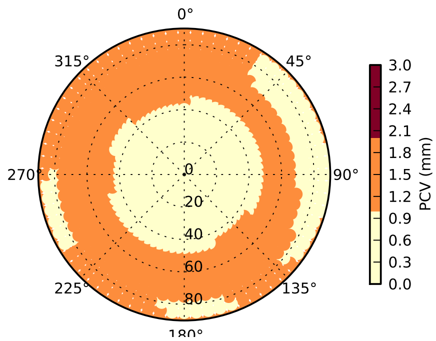

(a) staircase skyplot (antdpcv)

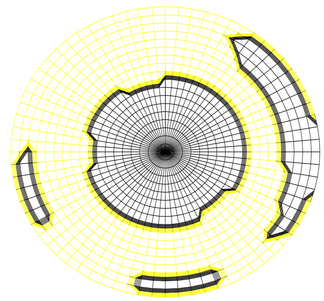

(b) staircase skyplot (antexfun)

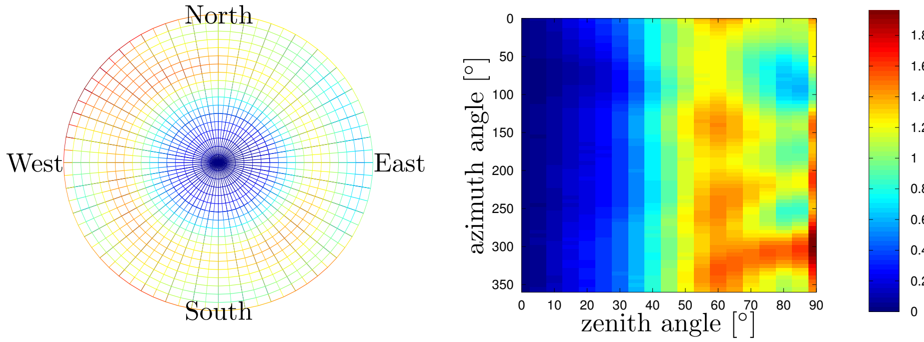

(c) polar (l) and cartesian (r) skyplot (antexfun)

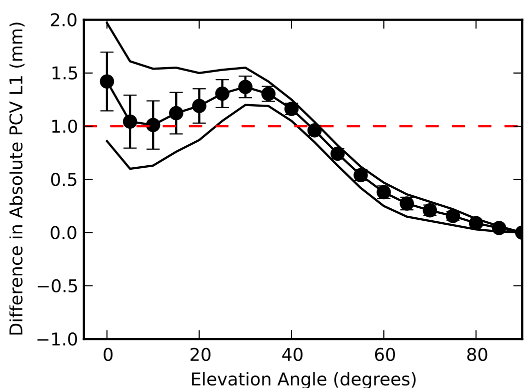

(d) elevation dependent difference ranges (antdpcv)

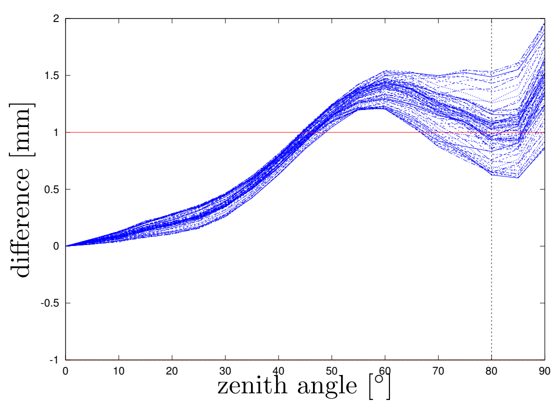

(e) overlay for all azimuth angles (antexfun)

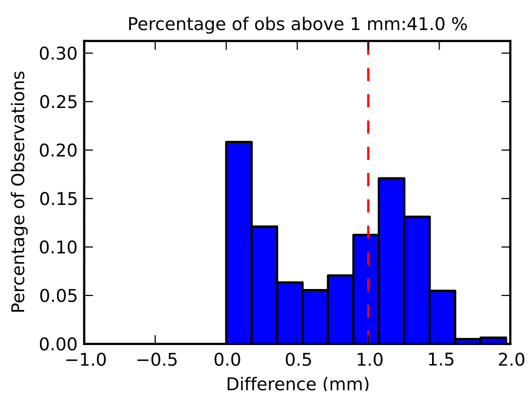

(f) histogram (antdpcv)

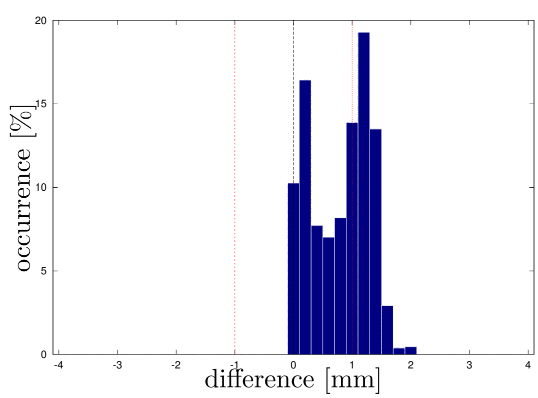

(g) histogram (antexfun)

Figure 29: Calibration differences for $TRM41249.00\_\_\_\_\_NONE$ on G01.

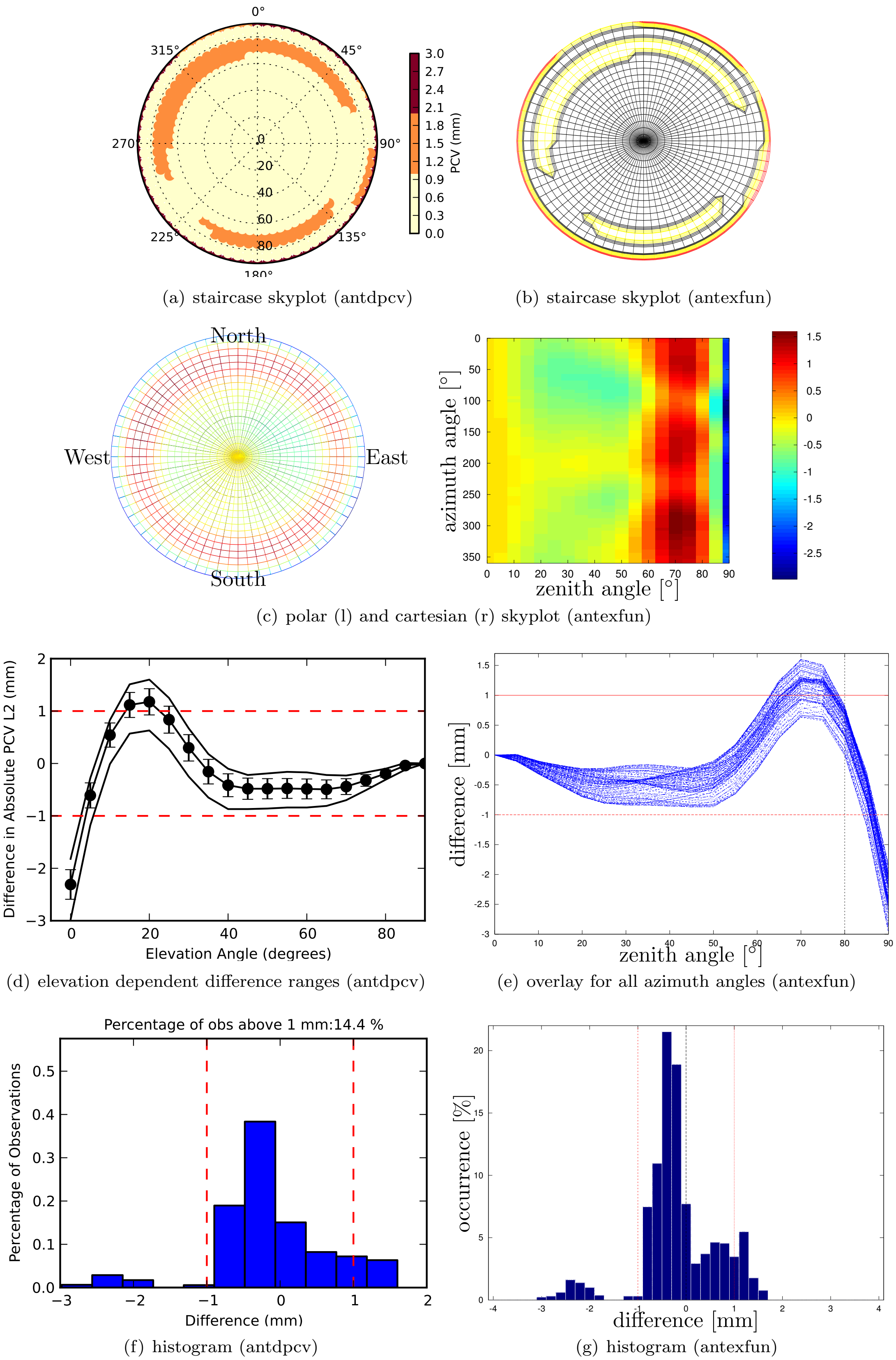

(a) staircase skyplot (antdpcv)

(b) staircase skyplot (antexfun)

(c) polar (l) and cartesian (r) skyplot (antexfun)

(d) elevation dependent difference ranges (antdpcv)

(e) overlay for all azimuth angles (antexfun)

(f) histogram (antdpcv)

(g) histogram (antexfun)

Figure 30: Calibration differences for $TRM41249.00\_\_\_\_\_NONE$ on G02.

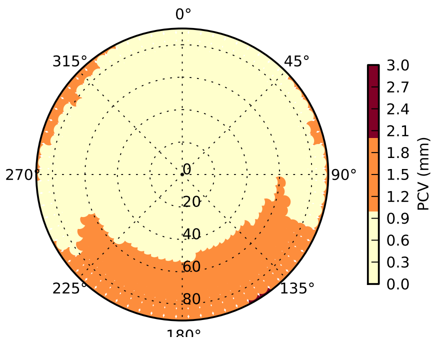

(a) staircase skyplot (antdpcv)

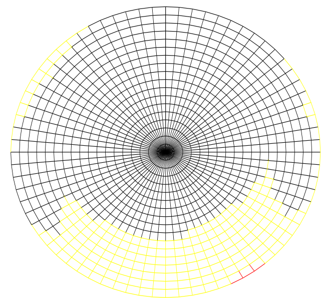

(b) staircase skyplot (antexfun)

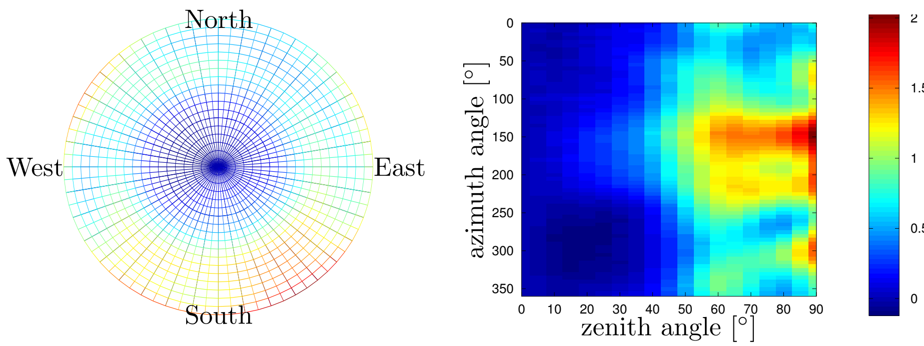

(c) polar (l) and cartesian (r) skyplot (antexfun)

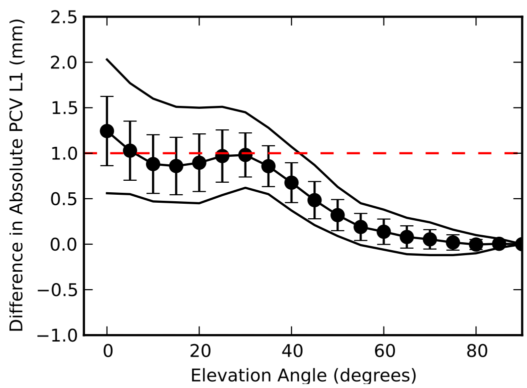

(d) elevation dependent difference ranges (antdpcv)

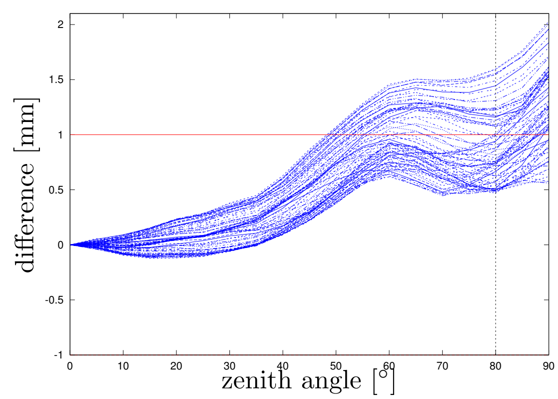

(e) overlay for all azimuth angles (antexfun)

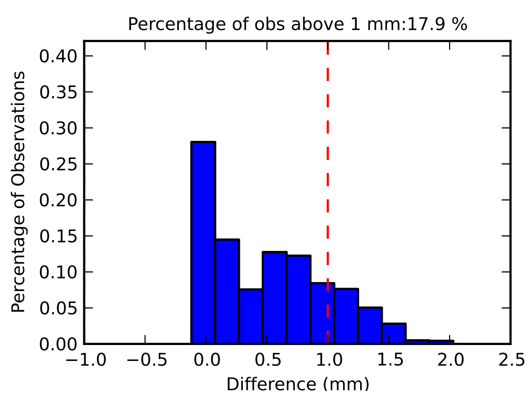

(f) histogram (antdpcv)

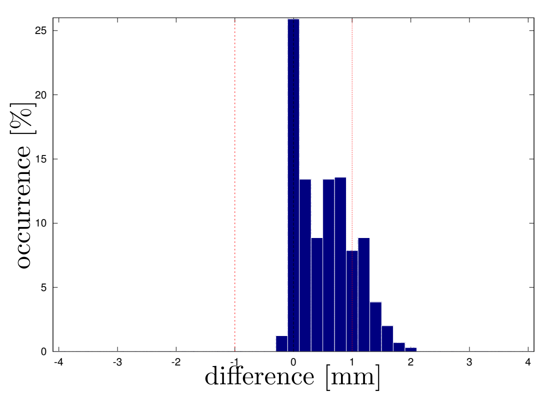

(g) histogram (antexfun)

Figure 31: Calibration differences for $TRM55971.00\_\_\_\_\_NONE$ on G01.

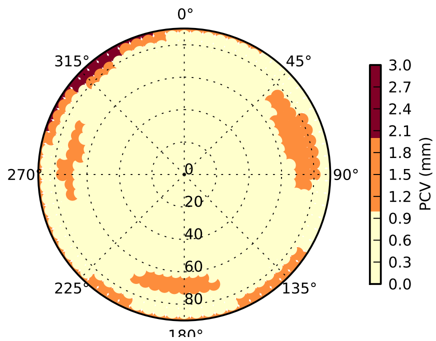

(a) staircase skyplot (antdpcv)

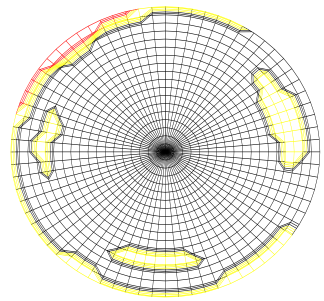

(b) staircase skyplot (antexfun)

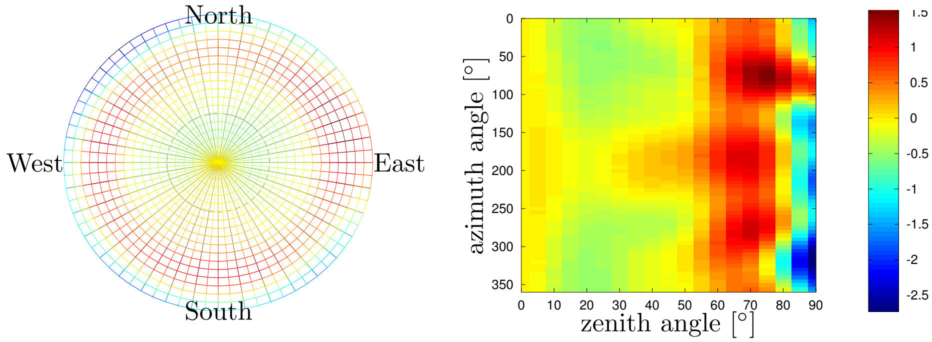

(c) polar (l) and cartesian (r) skyplot (antexfun)

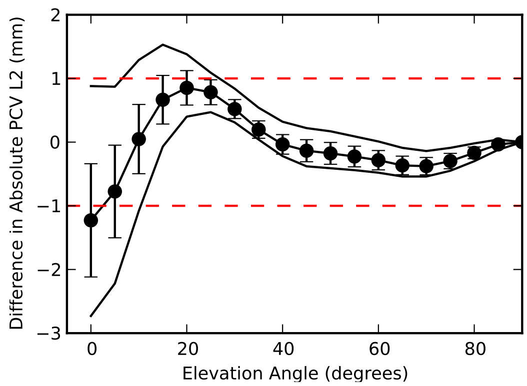

(d) elevation dependent difference ranges (antdpcv)

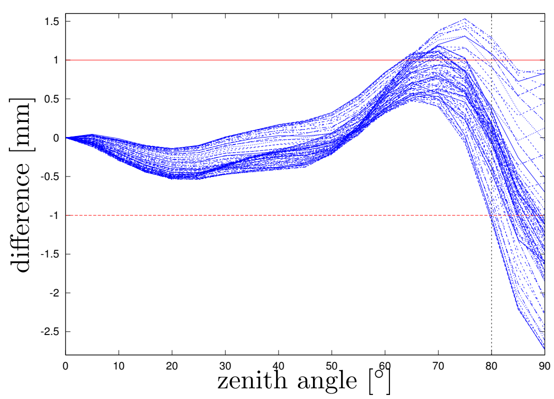

(e) overlay for all azimuth angles (antexfun)

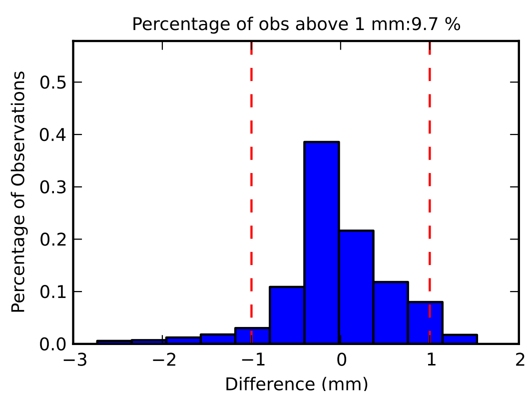

(f) histogram (antdpcv)

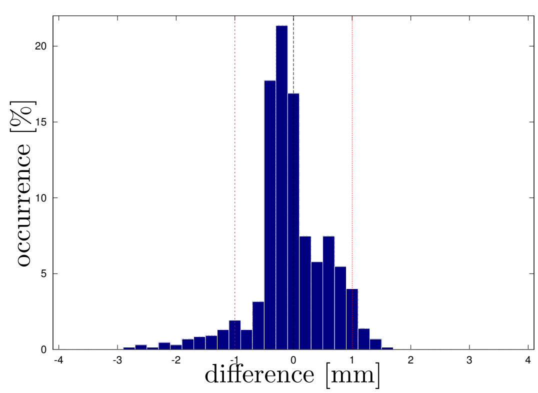

(g) histogram (antexfun)

Figure 32: Calibration differences for $TRM55971.00\_\_\_\_\_NONE$ on G02.

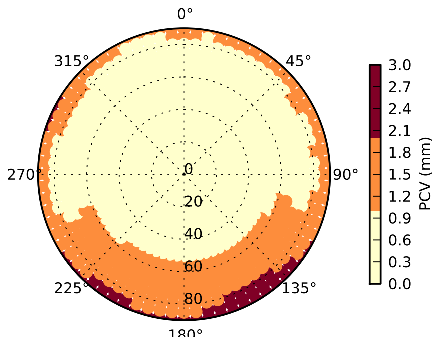

(a) staircase skyplot (antdpcv)

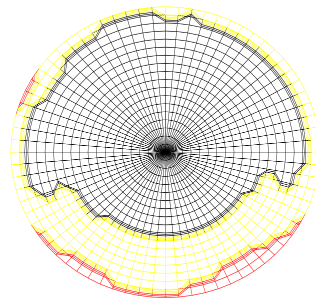

(b) staircase skyplot (antexfun)

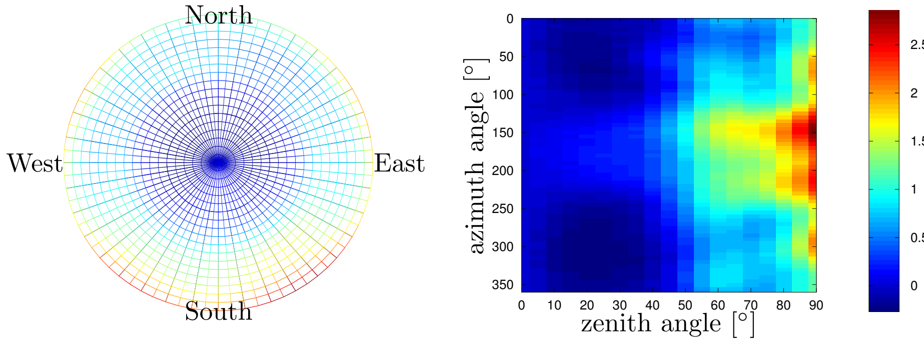

(c) polar (l) and cartesian (r) skyplot (antexfun)

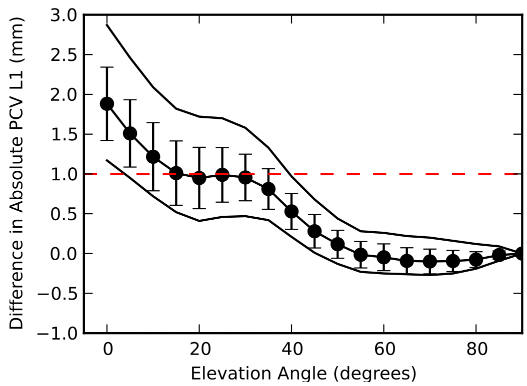

(d) elevation dependent difference ranges (antdpcv)

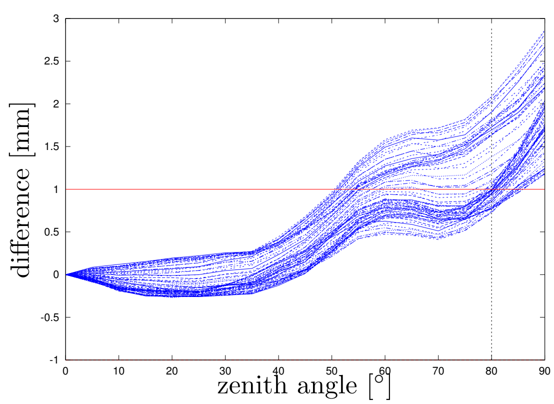

(e) overlay for all azimuth angles (antexfun)

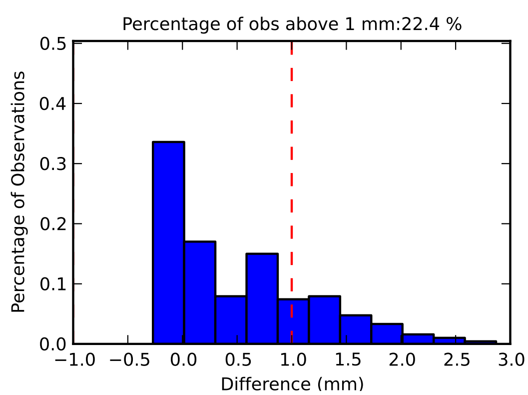

(f) histogram (antdpcv)

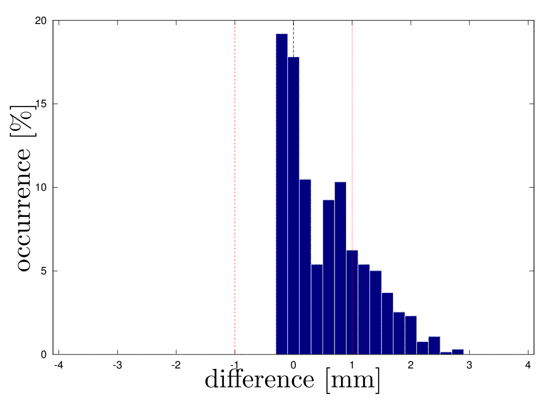

(g) histogram (antexfun)

Figure 33: Calibration differences for $TRM55971.00\_\_\_\_\_NONE$ on R01.

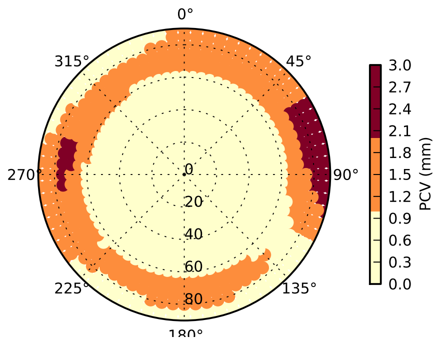

(a) staircase skyplot (antdpcv)

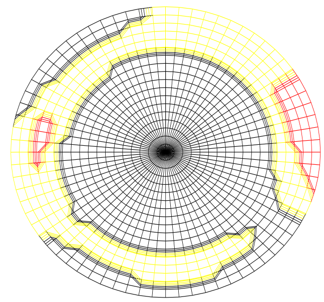

(b) staircase skyplot (antexfun)

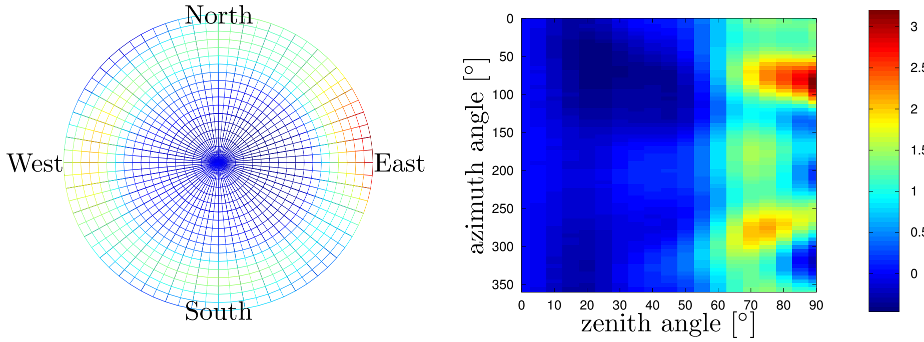

(c) polar (l) and cartesian (r) skyplot (antexfun)

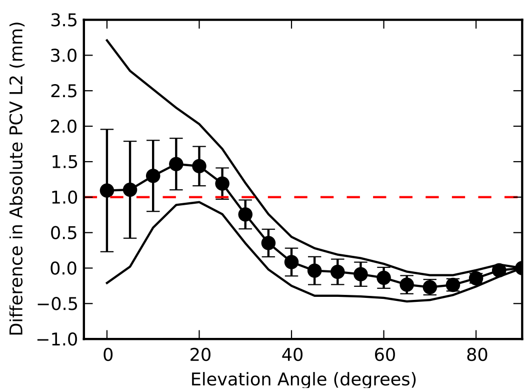

(d) elevation dependent difference ranges (antdpcv)

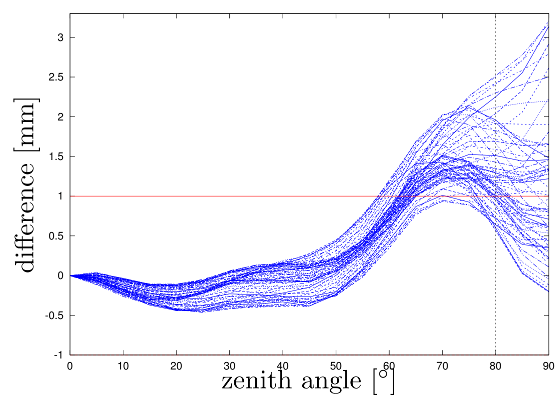

(e) overlay for all azimuth angles (antexfun)

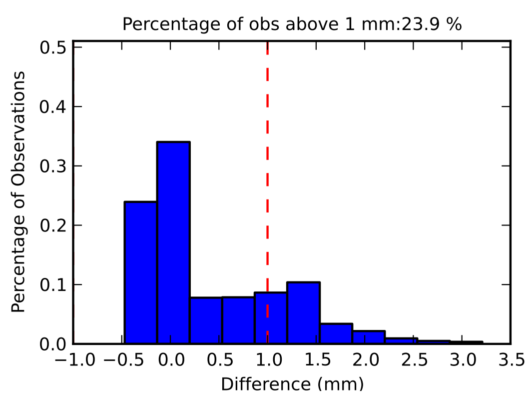

(f) histogram (antdpcv)

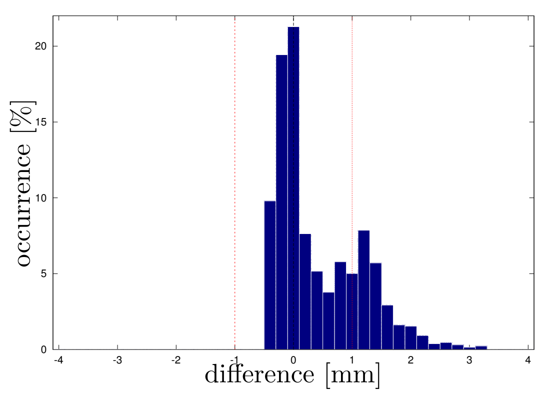

(g) histogram (antexfun)

Figure 34: Calibration differences for $TRM55971.00\_\_\_\_\_NONE$ on R02.

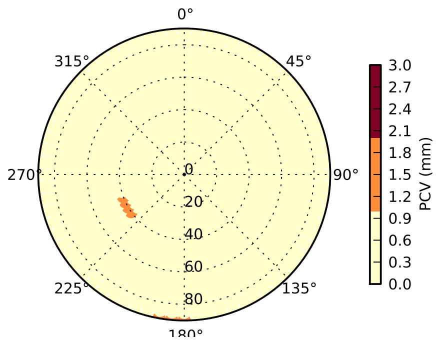

(a) staircase skyplot (antdpcv)

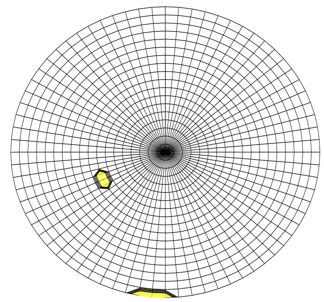

(b) staircase skyplot (antexfun)

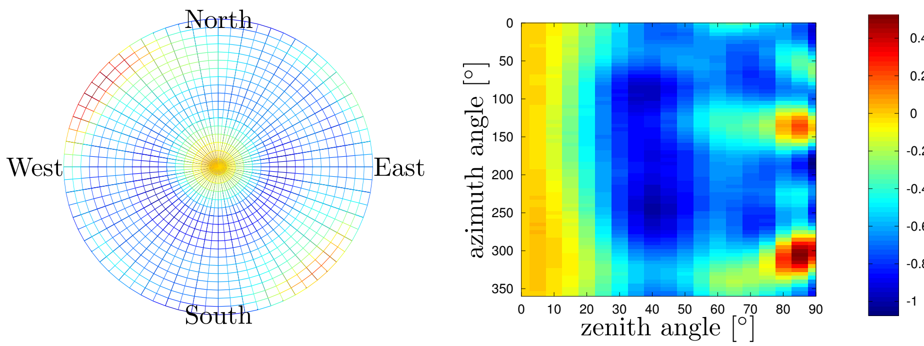

(c) polar (l) and cartesian (r) skyplot (antexfun)

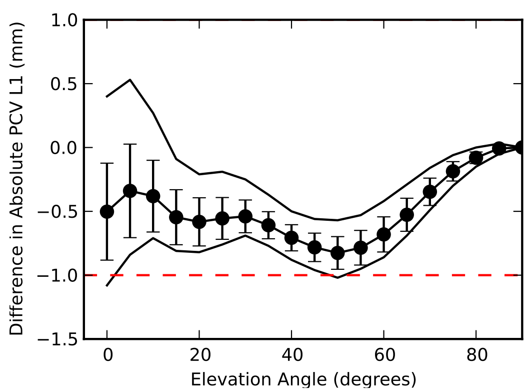

(d) elevation dependent difference ranges (antdpcv)

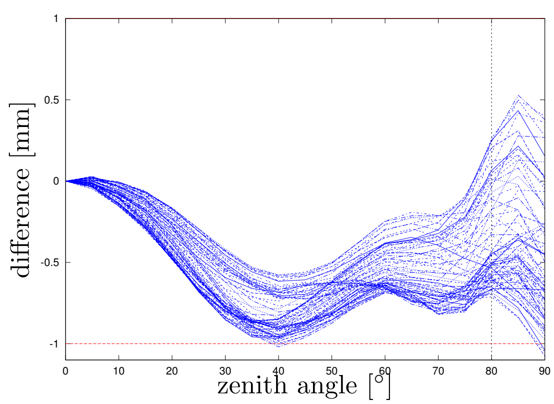

(e) overlay for all azimuth angles (antexfun)

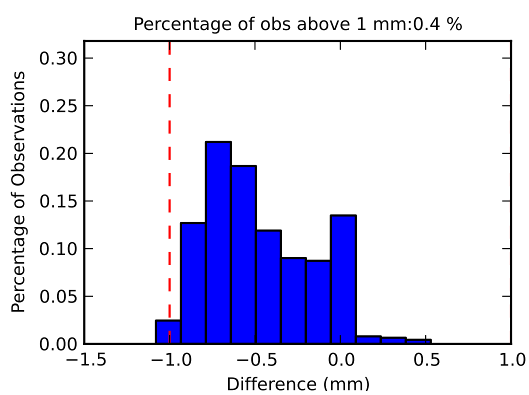

(f) histogram (antdpcv)

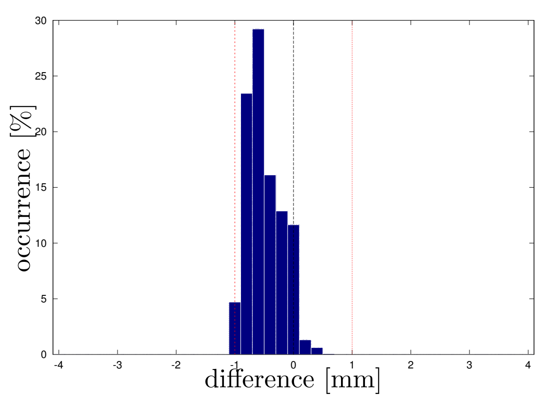

(g) histogram (antexfun)

Figure 35: Calibration differences for $TRM55971.00\_\_\_\_\_TZGD$ on G01.

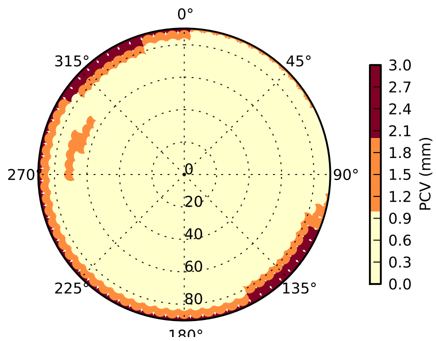

(a) staircase skyplot (antdpcv)

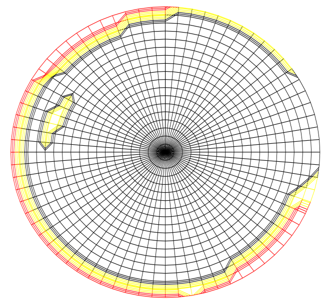

(b) staircase skyplot (antexfun)

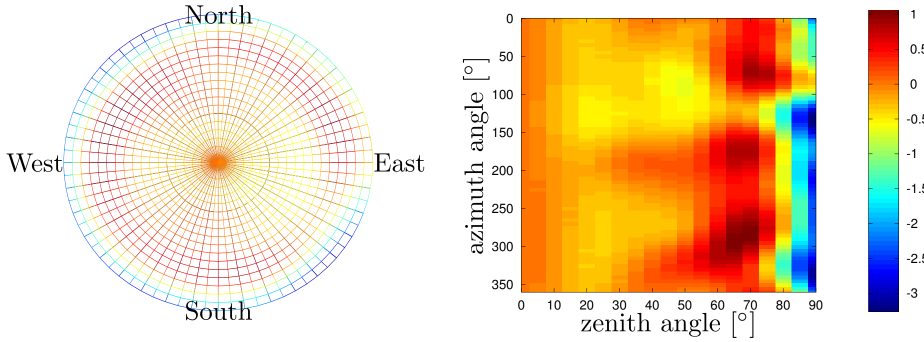

(c) polar (l) and cartesian (r) skyplot (antexfun)

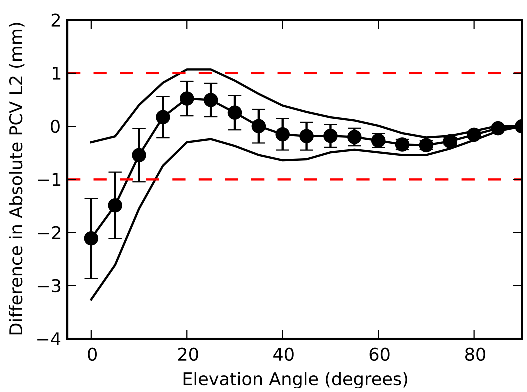

(d) elevation dependent difference ranges (antdpcv)

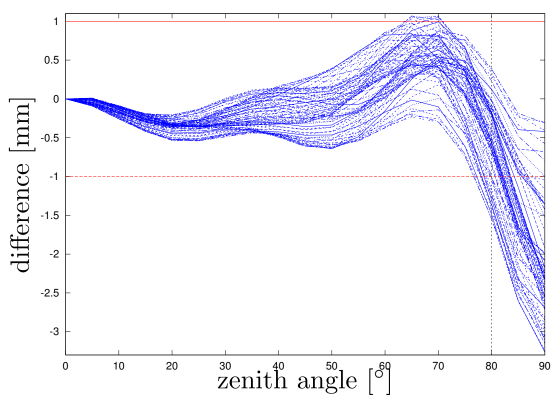

(e) overlay for all azimuth angles (antexfun)

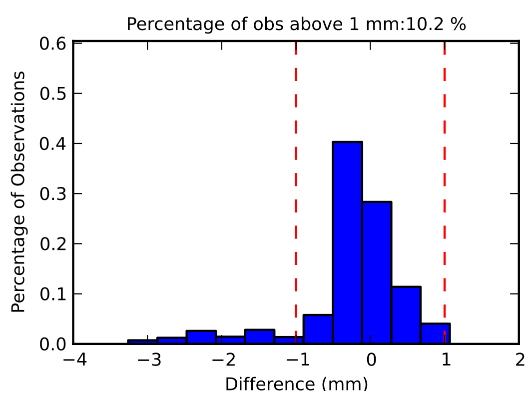

(f) histogram (antdpcv)

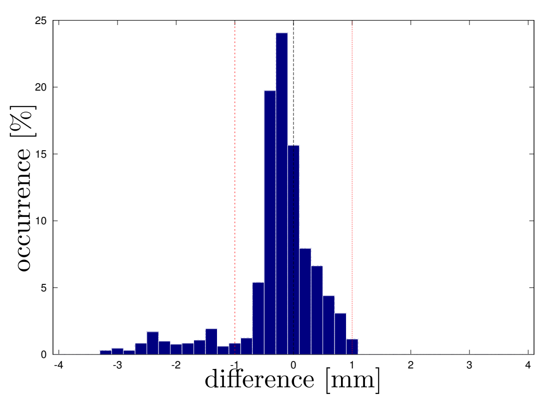

(g) histogram (antexfun)

Figure 36: Calibration differences for $TRM55971.00\_\_\_\_\_TZGD$ on G02.

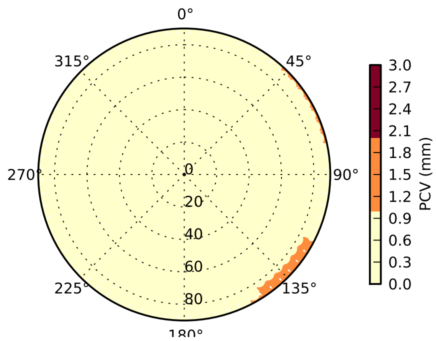

(a) staircase skyplot (antdpcv)

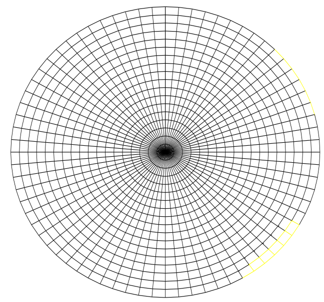

(b) staircase skyplot (antexfun)

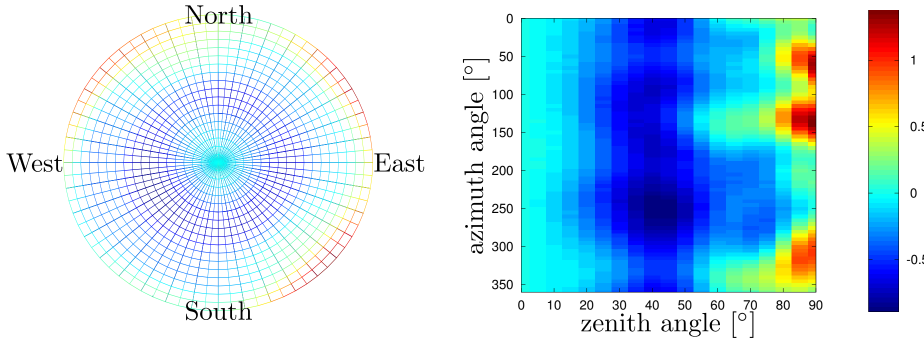

(c) polar (l) and cartesian (r) skyplot (antexfun)

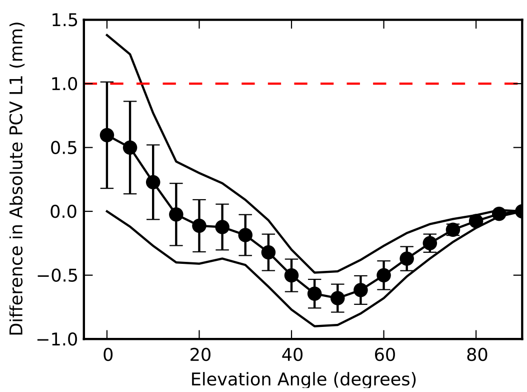

(d) elevation dependent difference ranges (antdpcv)

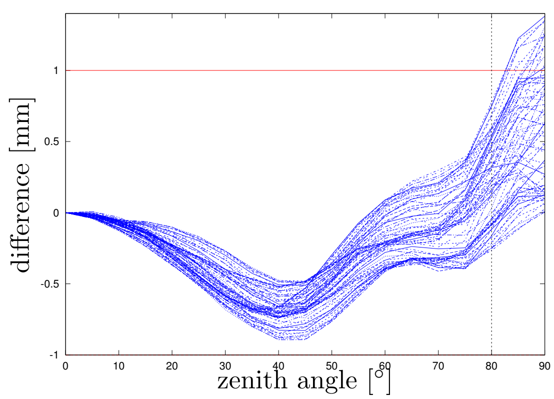

(e) overlay for all azimuth angles (antexfun)

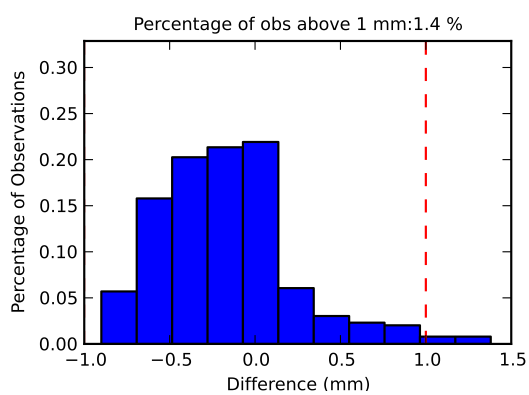

(f) histogram (antdpcv)

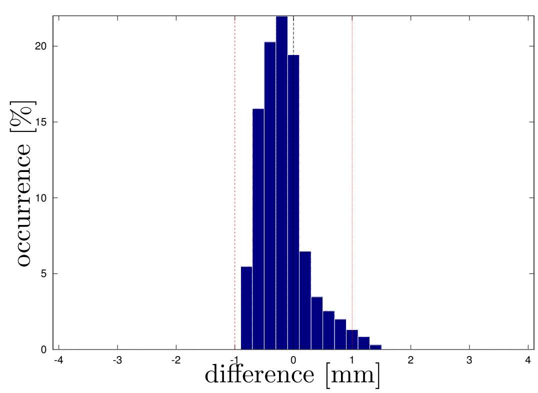

(g) histogram (antexfun)

Figure 37: Calibration differences for $TRM55971.00\_\_\_\_\_TZGD$ on R01.

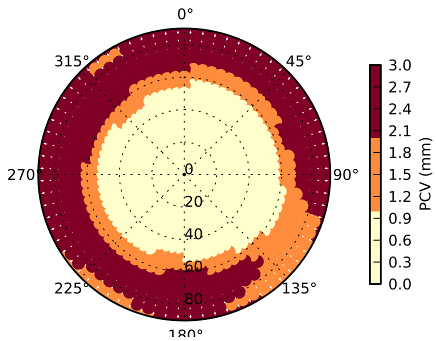

(a) staircase skyplot (antdpcv)

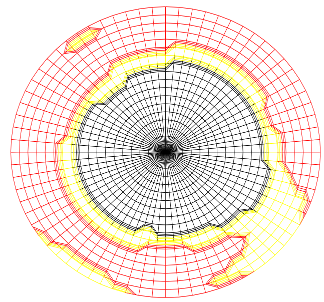

(b) staircase skyplot (antexfun)

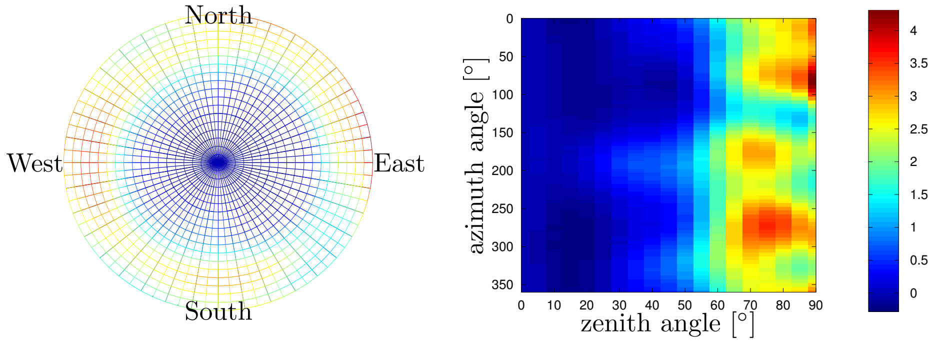

(c) polar (l) and cartesian (r) skyplot (antexfun)

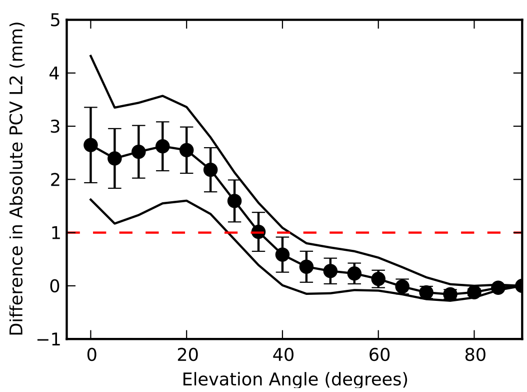

(d) elevation dependent difference ranges (antdpcv)

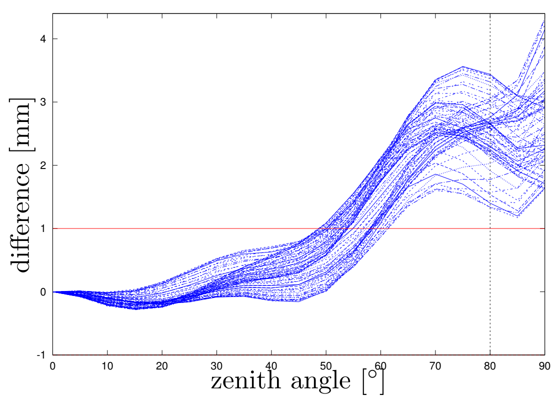

(e) overlay for all azimuth angles (antexfun)

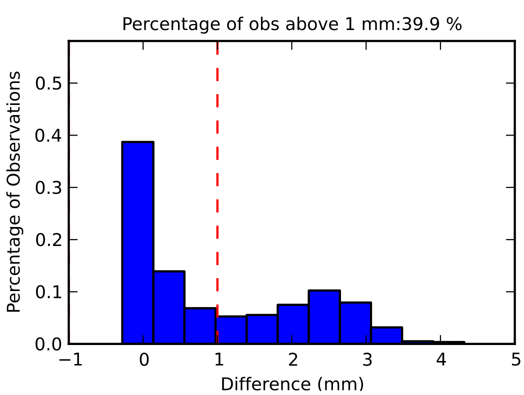

(f) histogram (antdpcv)

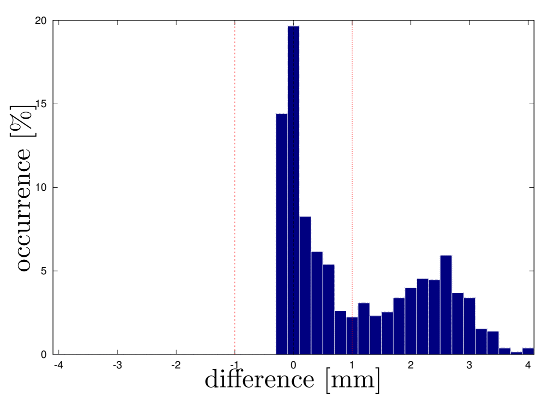

(g) histogram (antexfun)

Figure 38: Calibration differences for $TRM55971.00$_____$TZGD$ on R02.

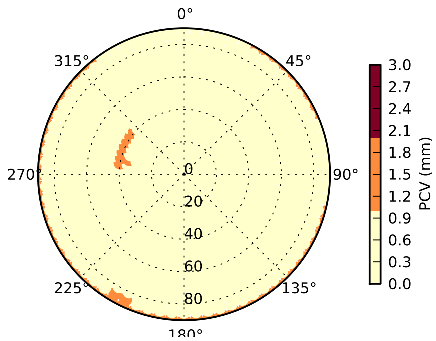

(a) staircase skyplot (antdpcv)

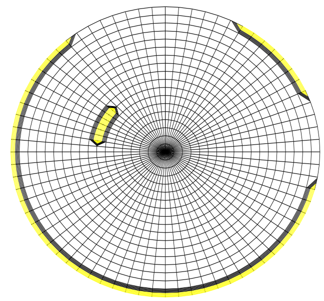

(b) staircase skyplot (antexfun)

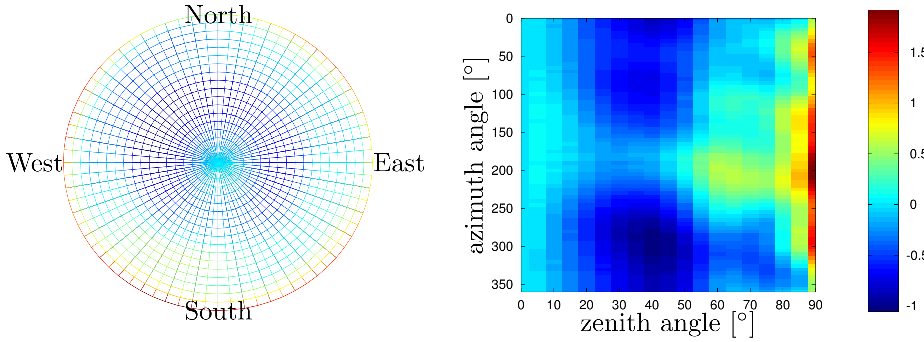

(c) polar (l) and cartesian (r) skyplot (antexfun)

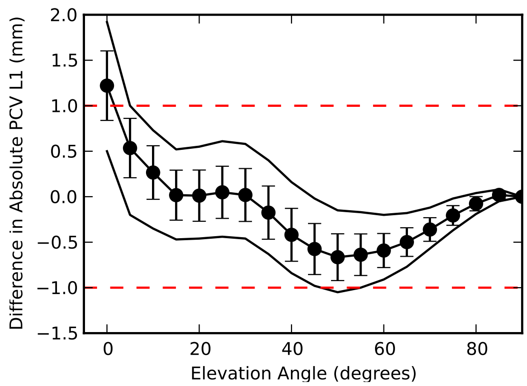

(d) elevation dependent difference ranges (antdpcv)

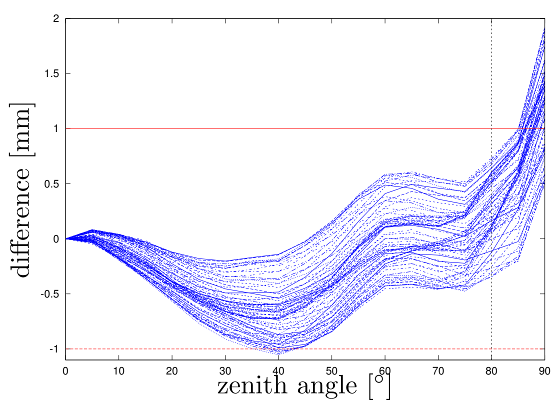

(e) overlay for all azimuth angles (antexfun)

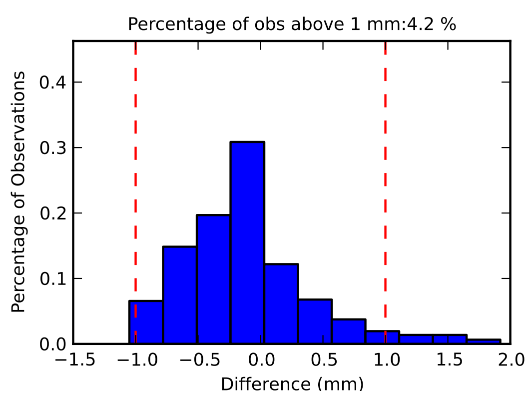

(f) histogram (antdpcv)

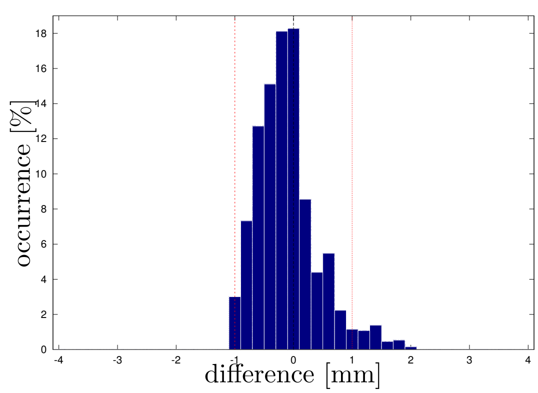

(g) histogram (antexfun)

Figure 39: Calibration differences for $TRM57971.00\_\_\_\_\_NONE$ on G01.

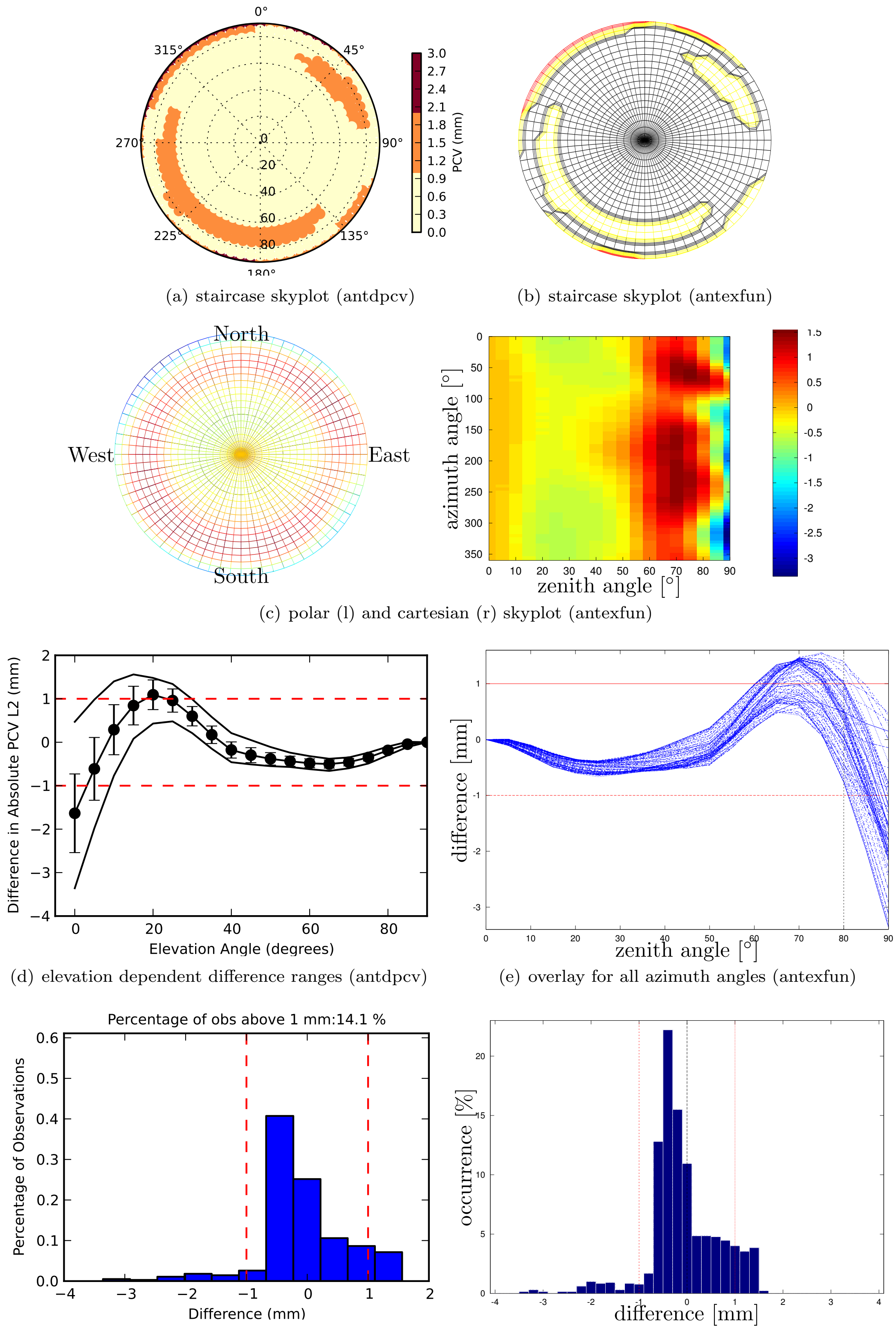

(a) staircase skyplot (antdpcv)

(b) staircase skyplot (antexfun)

(c) polar (l) and cartesian (r) skyplot (antexfun)

(d) elevation dependent difference ranges (antdpcv)

(e) overlay for all azimuth angles (antexfun)

(f) histogram (antdpcv)

(g) histogram (antexfun)

Figure 40: Calibration differences for $TRM57971.00\_\_\_\_\_NONE$ on G02.

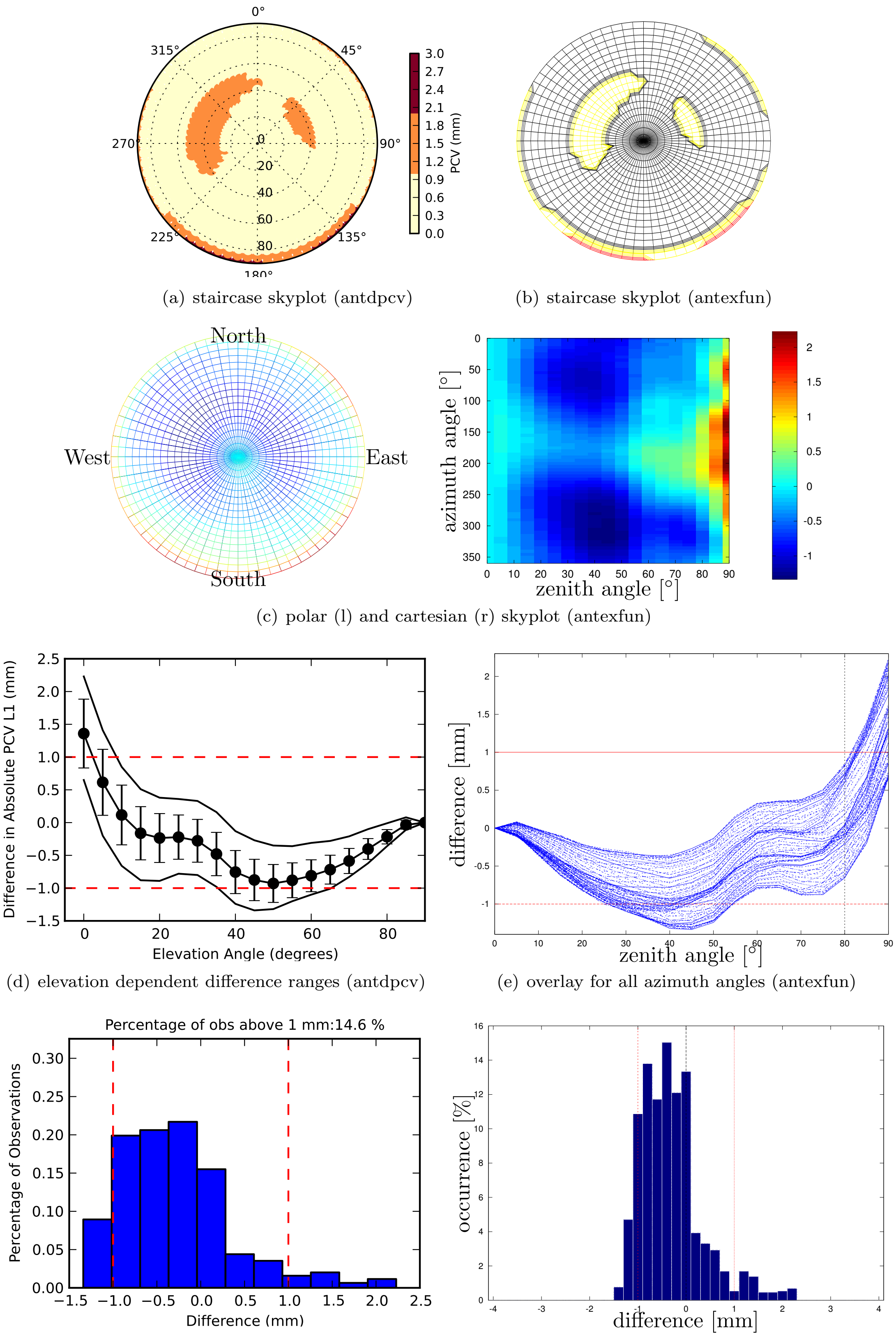

(a) staircase skyplot (antdpcv)

(b) staircase skyplot (antexfun)

(c) polar (l) and cartesian (r) skyplot (antexfun)

(d) elevation dependent difference ranges (antdpcv)

(e) overlay for all azimuth angles (antexfun)

(f) histogram (antdpcv)

(g) histogram (antexfun)

Figure 41: Calibration differences for $TRM57971.00\_\_\_\_\_NONE$ on R01.

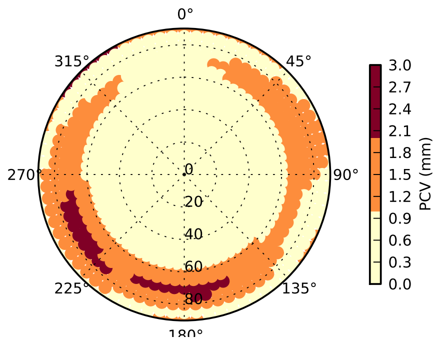

(a) staircase skyplot (antdpcv)

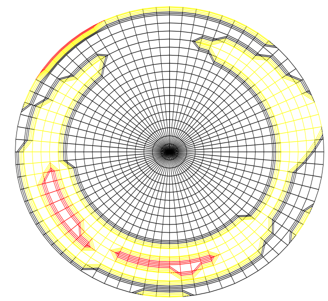

(b) staircase skyplot (antexfun)

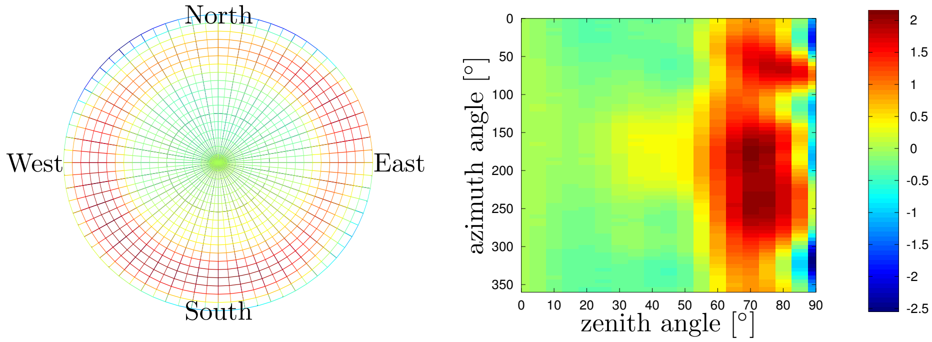

(c) polar (l) and cartesian (r) skyplot (antexfun)

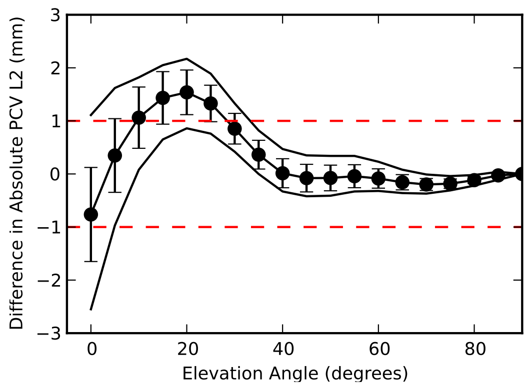

(d) elevation dependent difference ranges (antdpcv)

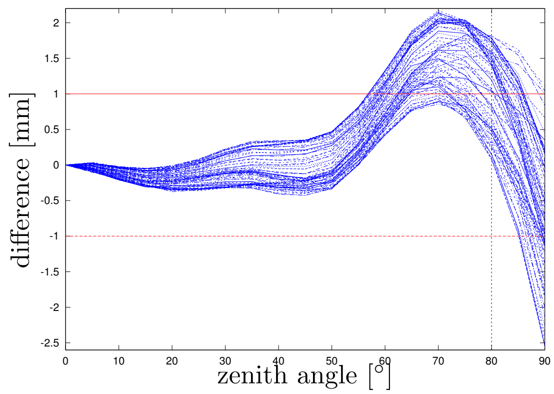

(e) overlay for all azimuth angles (antexfun)

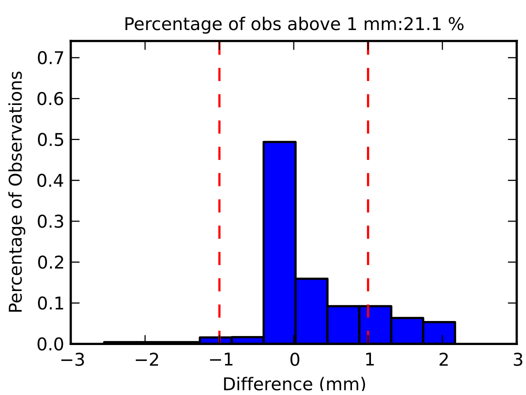

(f) histogram (antdpcv)

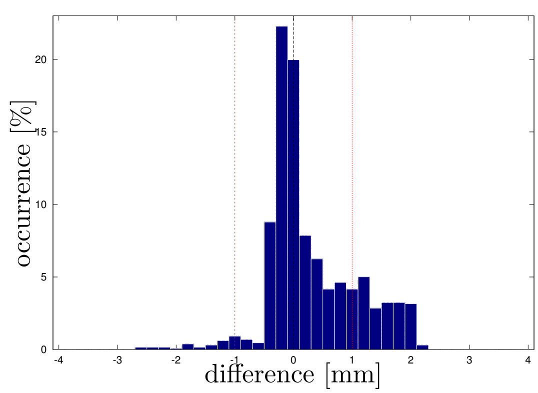

(g) histogram (antexfun)

Figure 42: Calibration differences for $TRM57971.00\_\_\_\_\_NONE$ on R02.

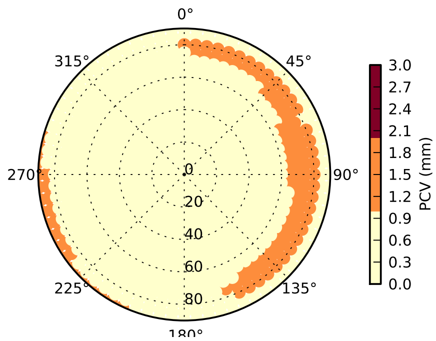

(a) staircase skyplot (antdpcv)

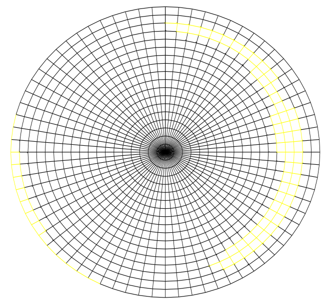

(b) staircase skyplot (antexfun)

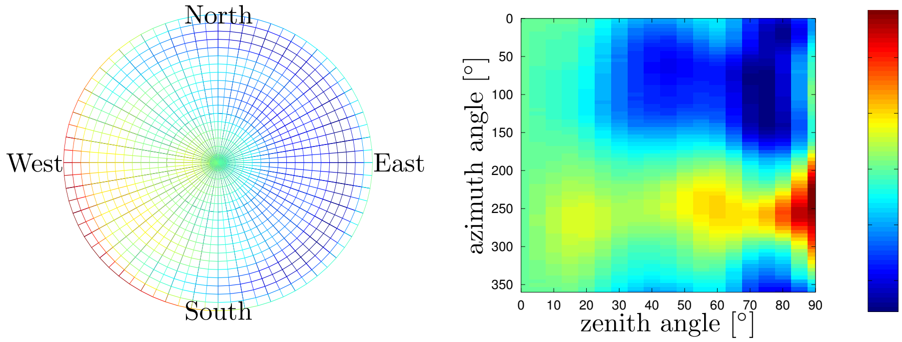

(c) polar (l) and cartesian (r) skyplot (antexfun)

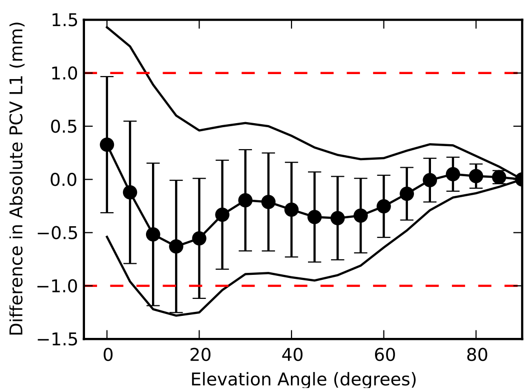

(d) elevation dependent difference ranges (antdpcv)

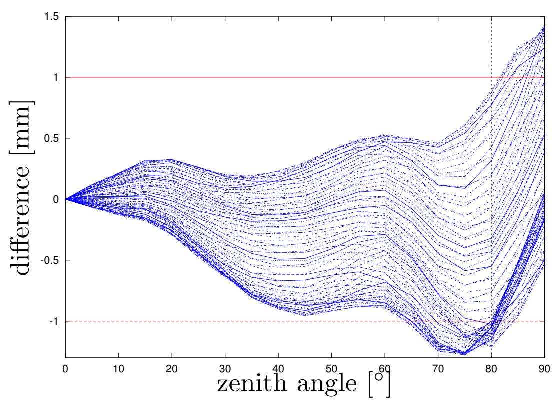

(e) overlay for all azimuth angles (antexfun)

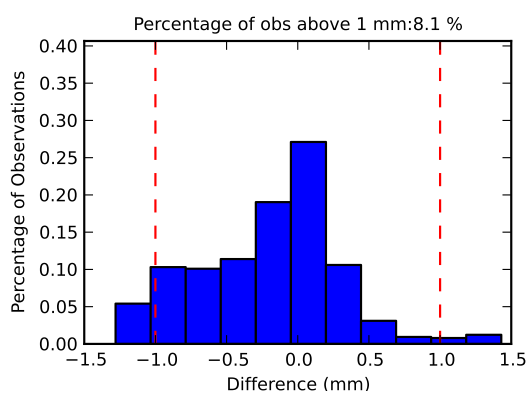

(f) histogram (antdpcv)

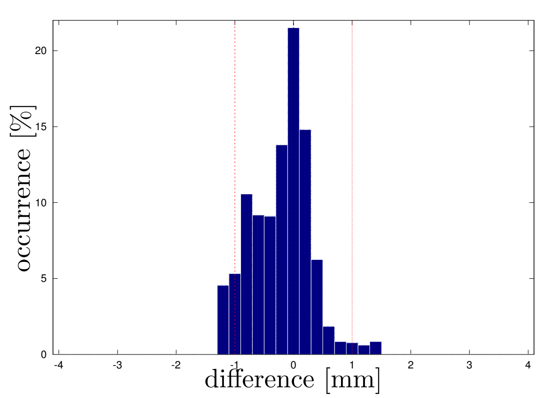

(g) histogram (antexfun)

Figure 43: Calibration differences for $TRM59800.00\_\_\_\_\_NONE$ on G01.

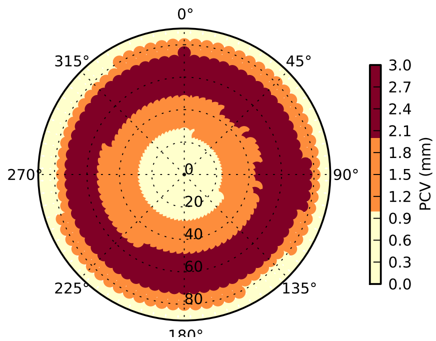

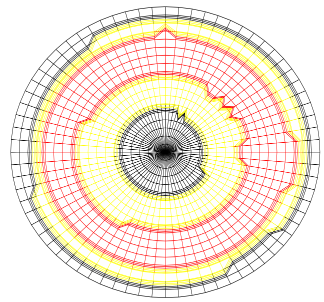

(a) staircase skyplot (antdpcv) (b) staircase skyplot (antexfun)

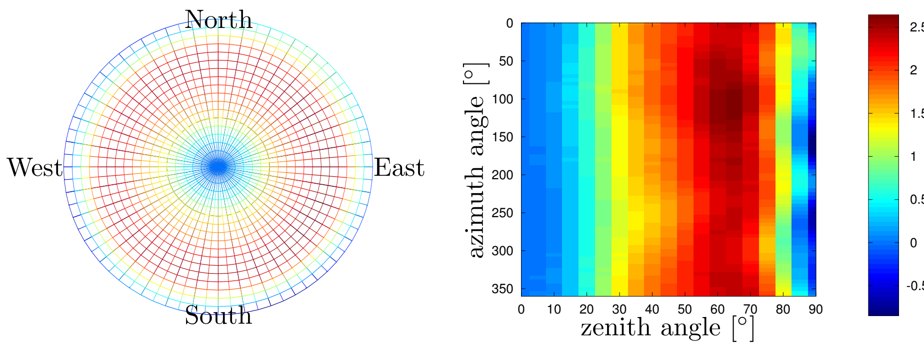

(c) polar (l) and cartesian (r) skyplot (antexfun)

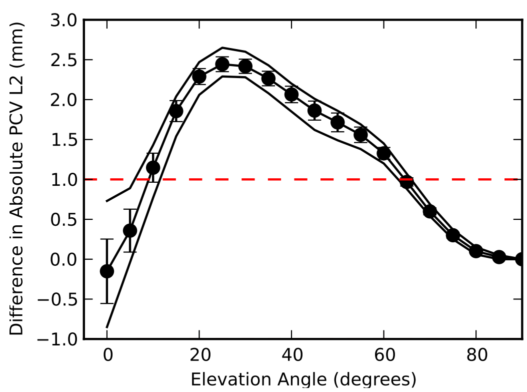

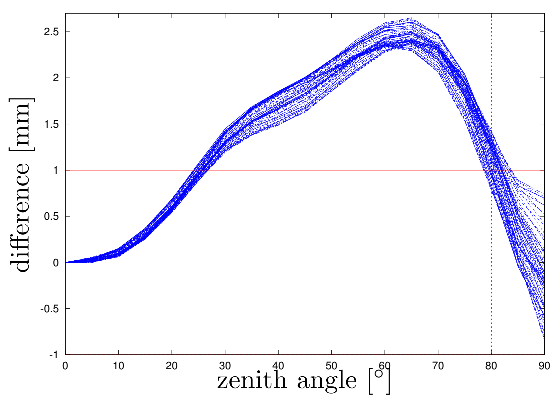

(d) elevation dependent difference ranges (antdpcv) (e) overlay for all azimuth angles (antexfun)

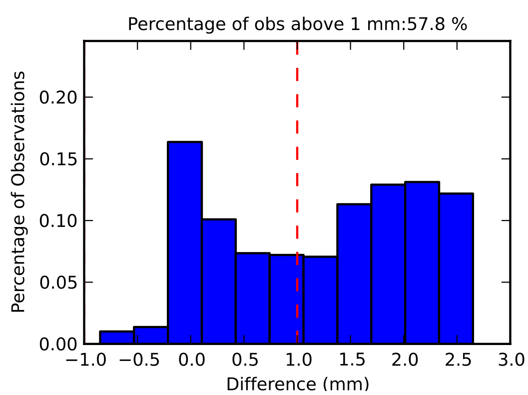

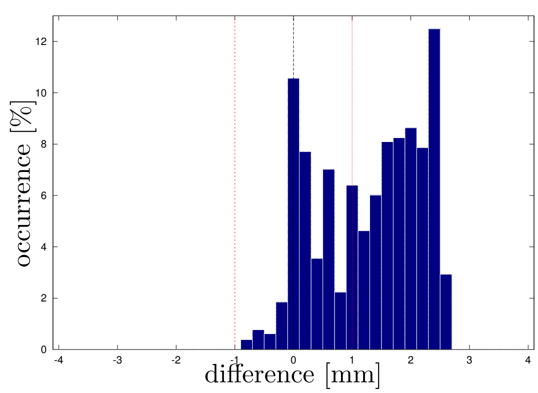

(f) histogram (antdpcv) (g) histogram (antexfun)

Figure 44: Calibration differences for $TRM59800.00\_\_\_\_\_NONE$ on G02.

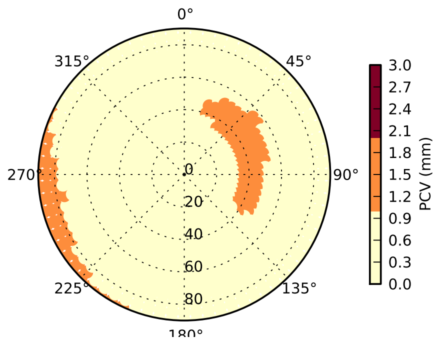

(a) staircase skyplot (antdpcv)

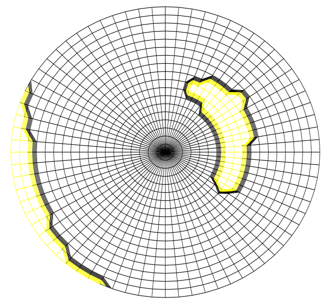

(b) staircase skyplot (antexfun)

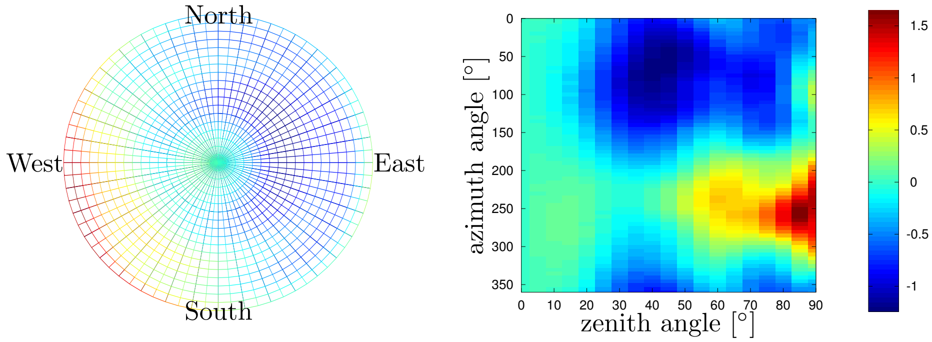

(c) polar (l) and cartesian (r) skyplot (antexfun)

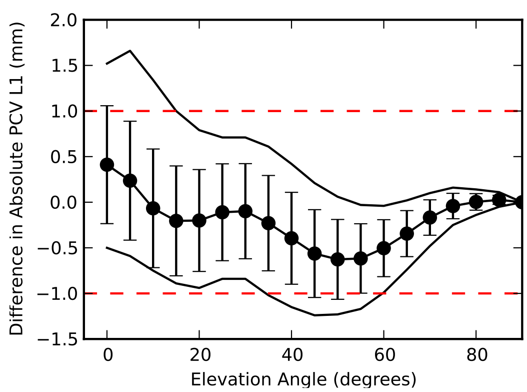

(d) elevation dependent difference ranges (antdpcv)

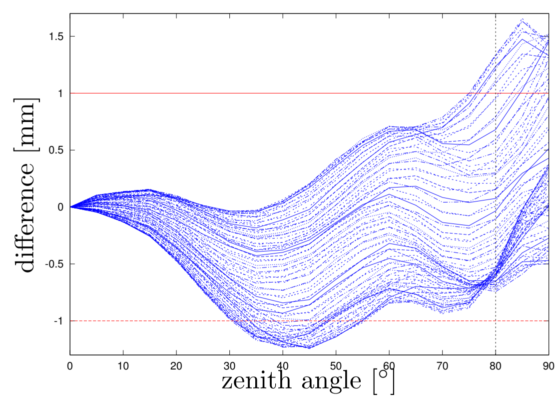

(e) overlay for all azimuth angles (antexfun)

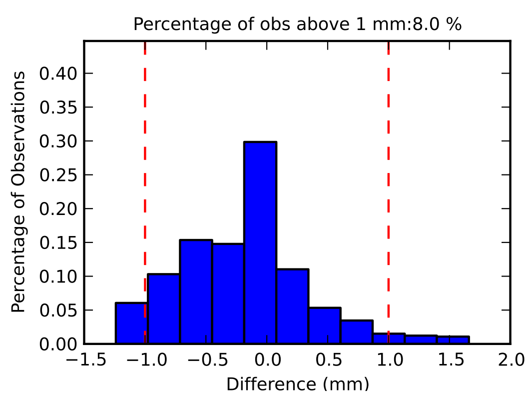

(f) histogram (antdpcv)

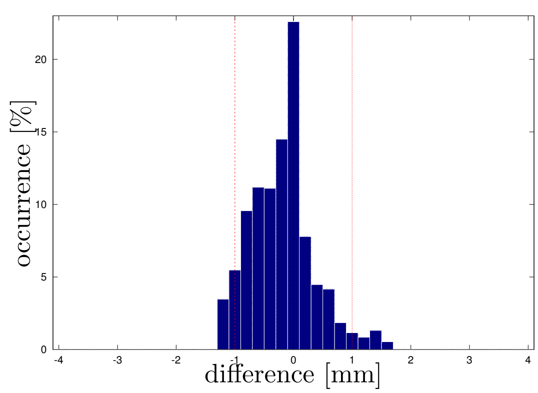

(g) histogram (antexfun)

Figure 45: Calibration differences for $TRM59800.00\_\_\_\_\_NONE$ on R01.

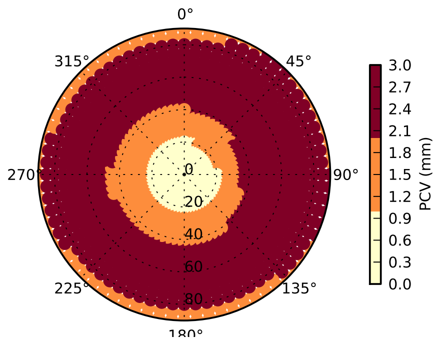

(a) staircase skyplot (antdpcv)

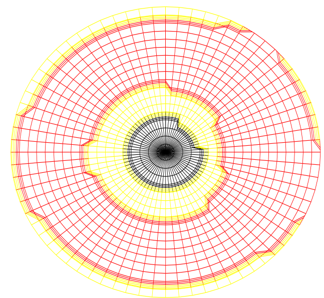

(b) staircase skyplot (antexfun)

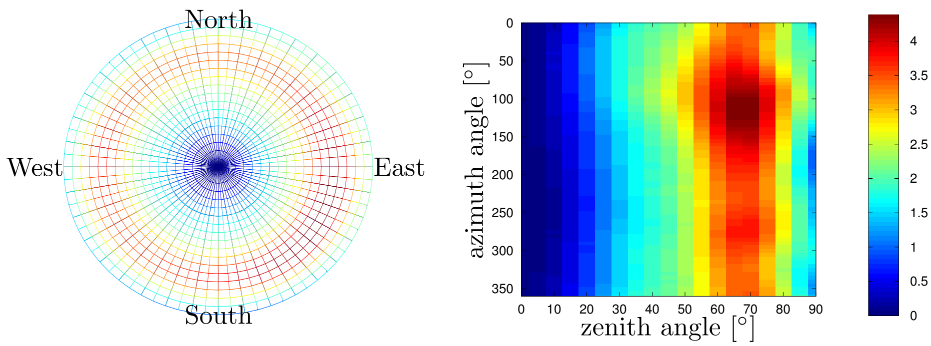

(c) polar (l) and cartesian (r) skyplot (antexfun)

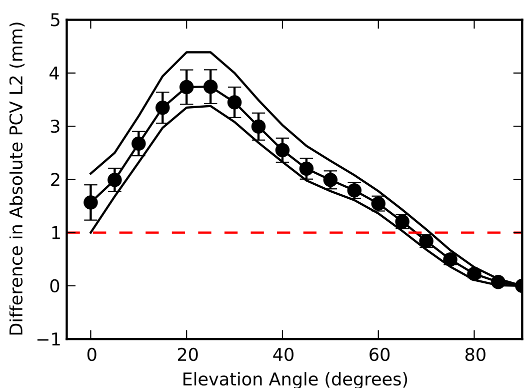

(d) elevation dependent difference ranges (antdpcv)

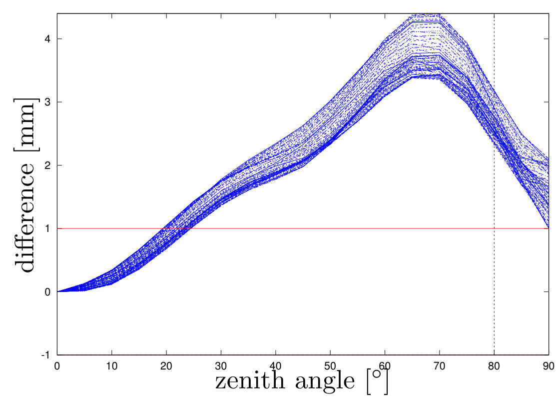

(e) overlay for all azimuth angles (antexfun)

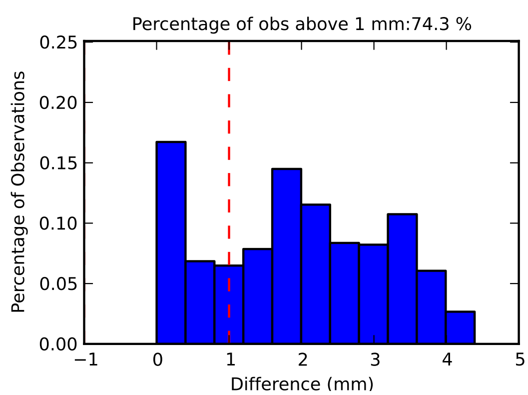

(f) histogram (antdpcv)

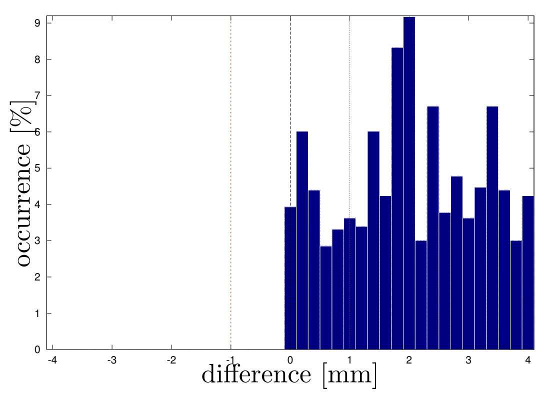

(g) histogram (antexfun)

Figure 46: Calibration differences for $TRM59800.00\_\_\_\_\_NONE$ on R02.

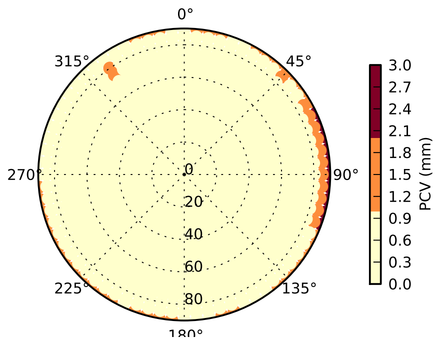

(a) staircase skyplot (antdpcv)

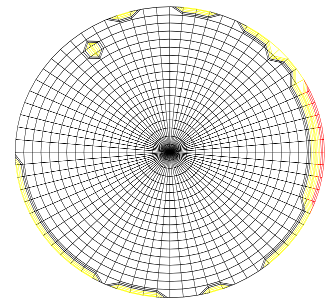

(b) staircase skyplot (antexfun)

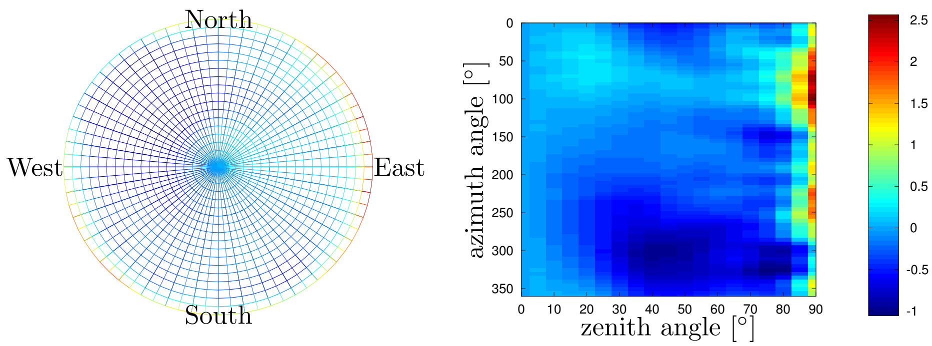

(c) polar (l) and cartesian (r) skyplot (antexfun)

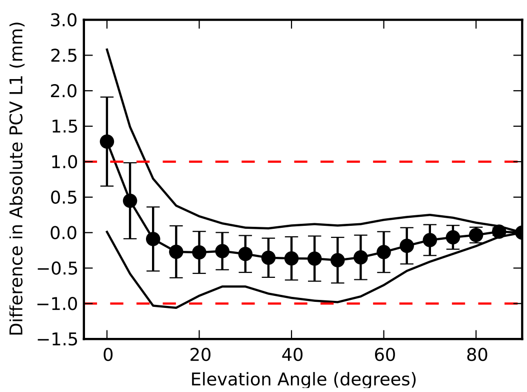

(d) elevation dependent difference ranges (antdpcv)

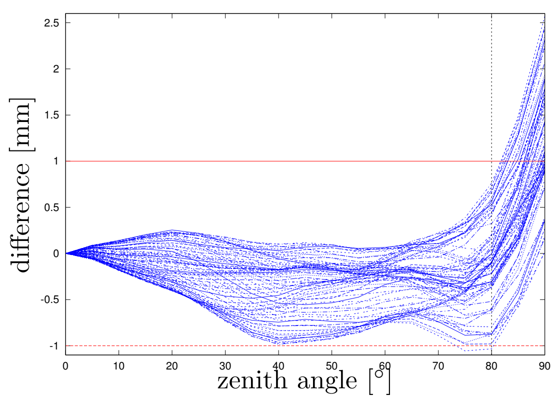

(e) overlay for all azimuth angles (antexfun)

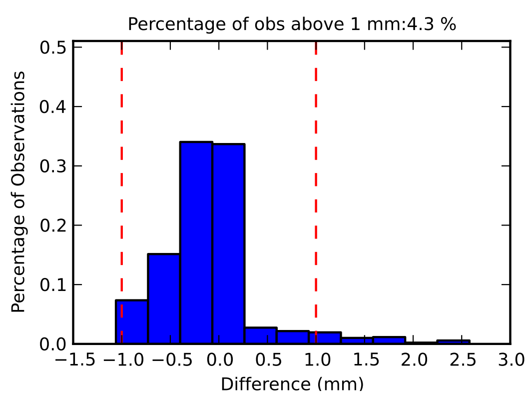

(f) histogram (antdpcv)

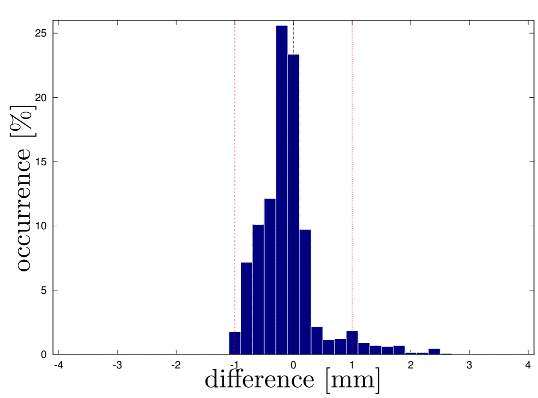

(g) histogram (antexfun)

Figure 47: Calibration differences for $TRM59800.00\_\_\_\_\_SCIS$ on G01.

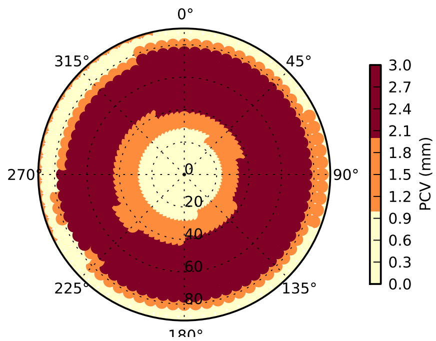

(a) staircase skyplot (antdpcv)

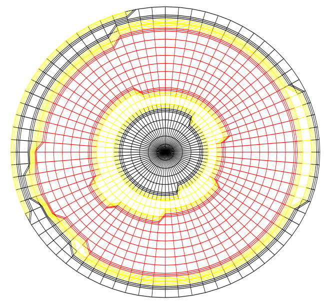

(b) staircase skyplot (antexfun)

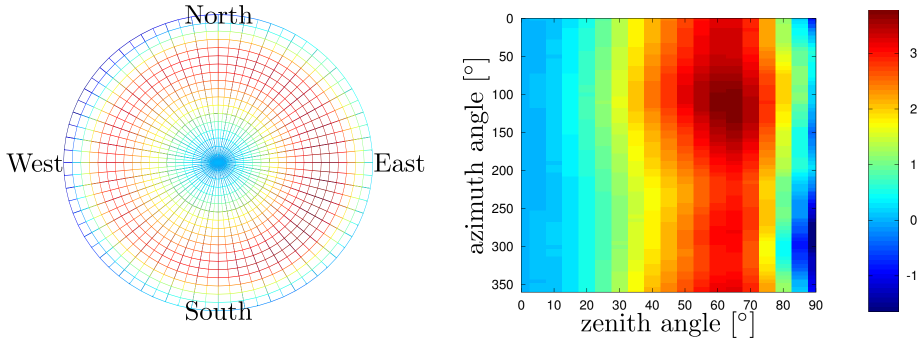

(c) polar (l) and cartesian (r) skyplot (antexfun)

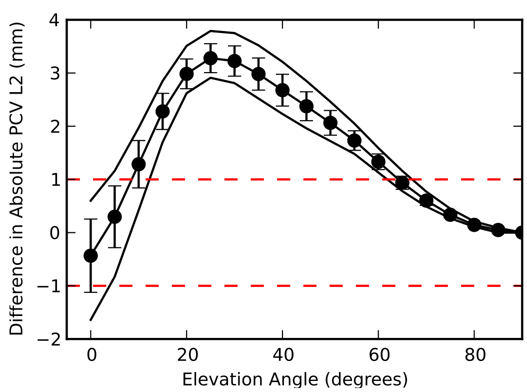

(d) elevation dependent difference ranges (antdpcv)

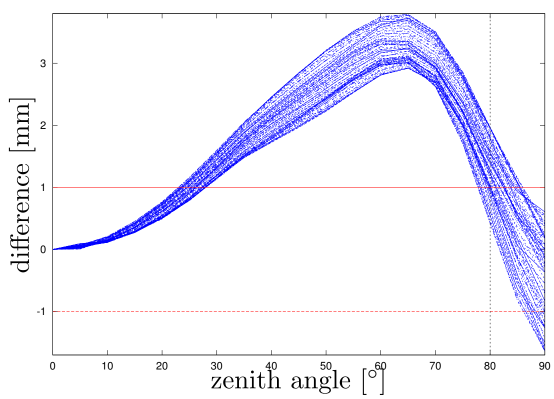

(e) overlay for all azimuth angles (antexfun)

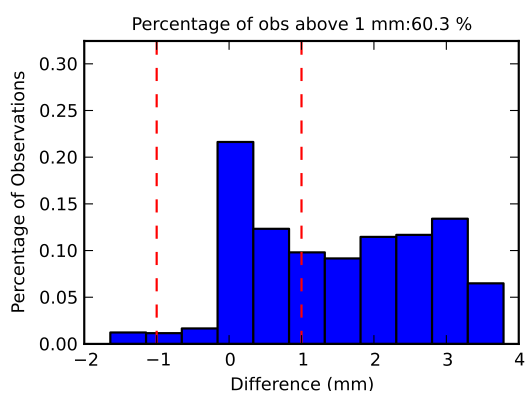

(f) histogram (antdpcv)

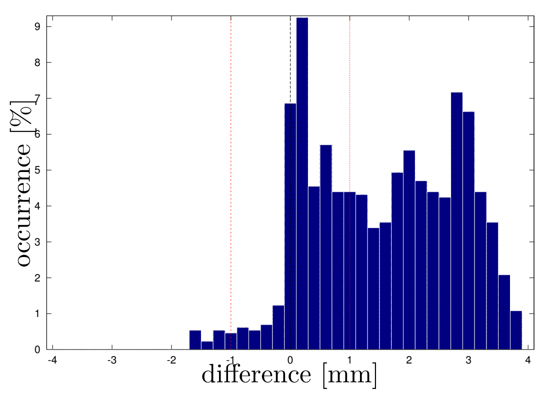

(g) histogram (antexfun)

Figure 48: Calibration differences for $TRM59800.00\_\_\_\_\_SCIS$ on G02.

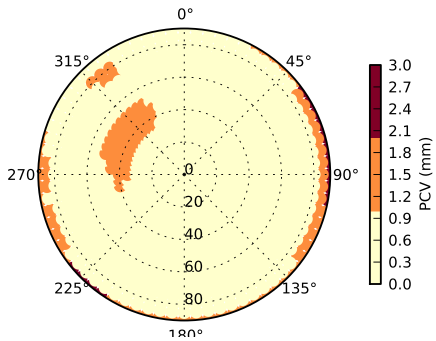

(a) staircase skyplot (antdpcv)

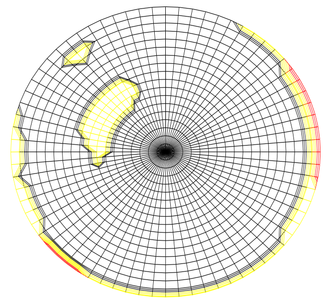

(b) staircase skyplot (antexfun)

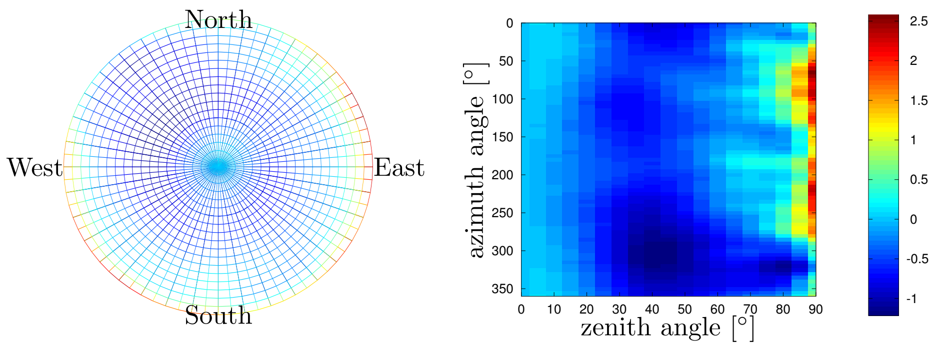

(c) polar (l) and cartesian (r) skyplot (antexfun)

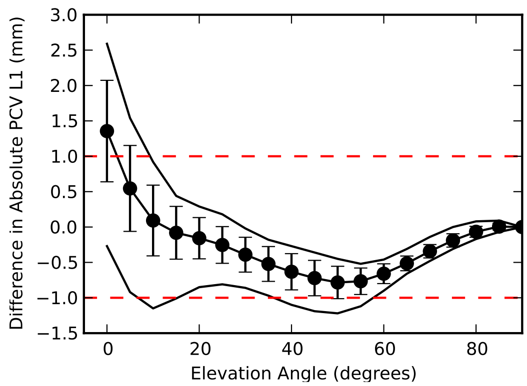

(d) elevation dependent difference ranges (antdpcv)

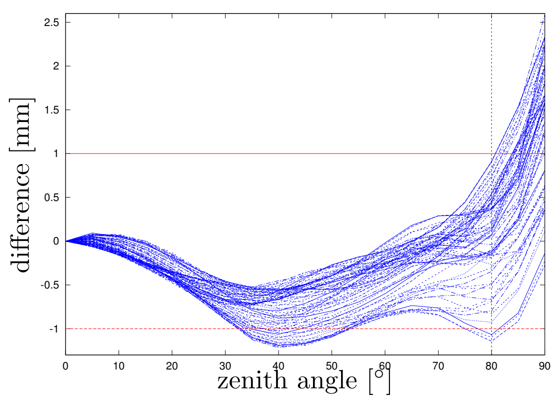

(e) overlay for all azimuth angles (antexfun)

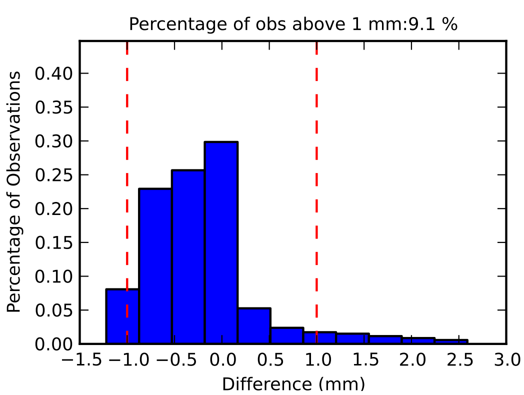

(f) histogram (antdpcv)

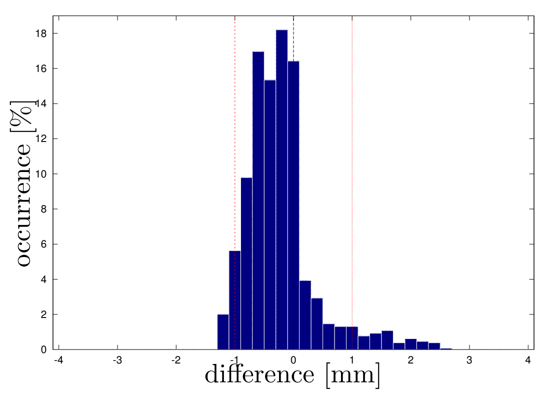

(g) histogram (antexfun)

Figure 49: Calibration differences for $TRM59800.00\_\_\_\_\_SCIS$ on R01.

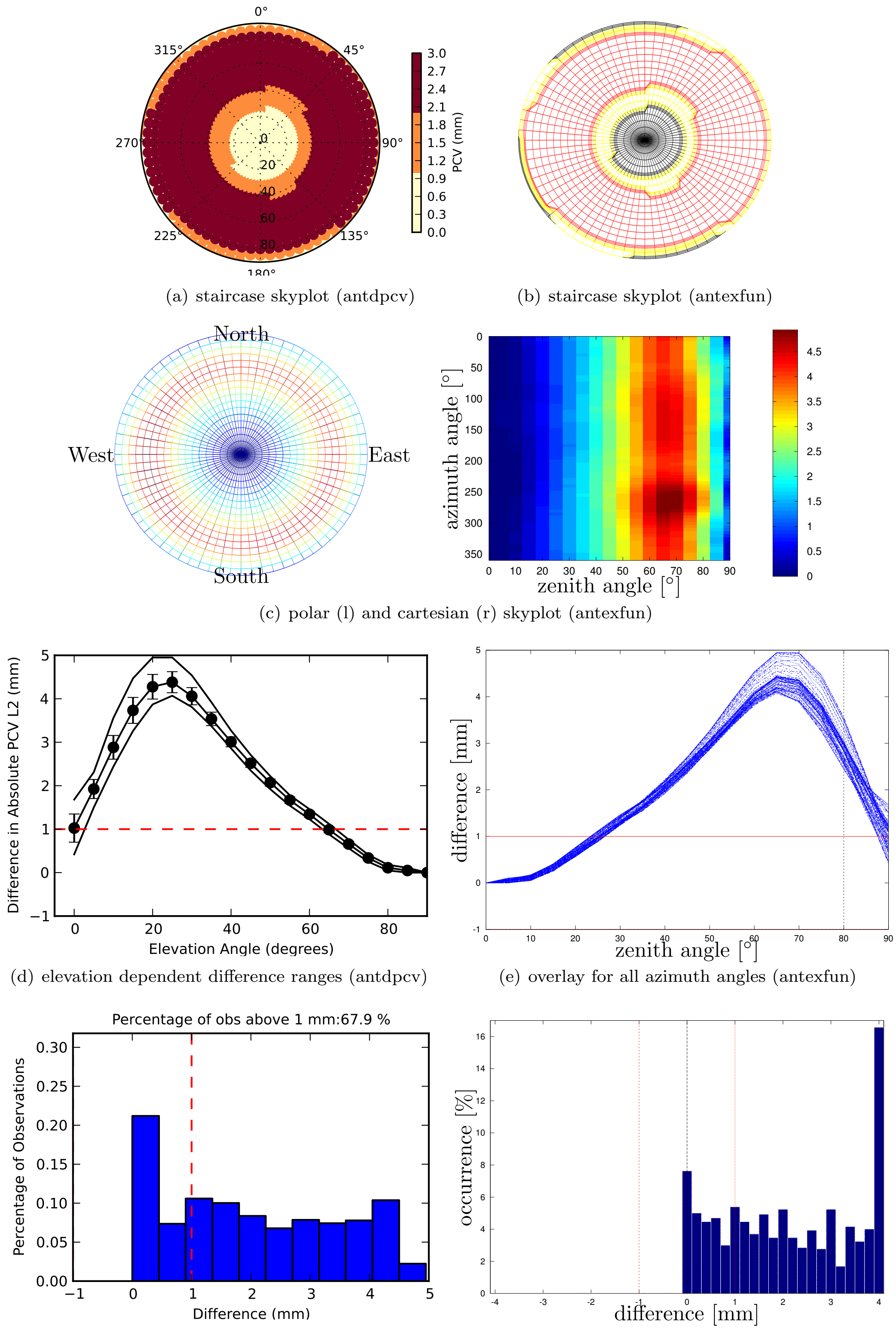

(a) staircase skyplot (antdpcv)

(b) staircase skyplot (antexfun)

(c) polar (l) and cartesian (r) skyplot (antexfun)

(d) elevation dependent difference ranges (antdpcv)

(e) overlay for all azimuth angles (antexfun)

(f) histogram (antdpcv)

(g) histogram (antexfun)

Figure 50: Calibration differences for $TRM59800.00\_\_\_\_\_SCIS$ on R02.